NIST-GCR-93-623

Transient Cooling of a Hot Surface by Droplets Evaporation

P. Tartarini
Y. Liao
C. Kidder
M. di Marzo

Grant 70NANB8H0840

NIST

Notice

This report was prepared for the Building and Fire Research Laboratory of the National Institute of Standards and Technology under grant number 70NANB8H0840. The statements and conclusions contained in this report are those of the authors and do not necessarily reflect the views of the National Institute of Standards and Technology or the Building and Fire Research Laboratory.

TRANSIENT COOLING OF A HOT SURFACE BY DROPLETS EVAPORATION

Final Report

P. Tartarini, Y. Liao, C. Kidder, M. di Marzo

Prepared for the

Center for Fire Research

National Institute of Standards and Technology

Gaithersburg, MD 20899

Mechanical Engineering Department

University of Maryland

College Park, Md 20742

November 1991

FOREWORD

This report describes the research performed during the period July 1990 - July 1991 under a joint research program between the Mechanical Engineering Department of the University of Maryland and the Buildings and Fire Research Laboratory of the National Institute of Standards and Technology. The research is conducted by Graduate Research Assistants of the ME Department under the joint supervision of Dr. di Marzo (UMCP) and Dr. Evans (CFR - NIST). This joint research program was initiated in January 1985.

The long term objective of the study of droplet-solid interaction is to obtain information applicable to the extinguishment of fire through a droplet array (e.g. spray). The solids of concern include low thermal conductivity materials, typical of fire applications.

Several important results were obtained in the first years of research. In particular, the modelling of the boundary condition at the liquid-vapor interface (at the droplet exposed surface) was validated with the data collected for water droplets evaporating on an aluminum block (diMarzo 1986a, 1986b, 1988). The simple model that describes the cooling effect induced in the aluminum by the evaporating droplet (diMarzo and Evans 1986, diMarzo *et al.* 1987) provided the input for the formulation of a preliminary multi-droplet model (diMarzo *et al.* 1987). An extensive experimental data base was also collected for water droplet evaporating on Macor (a glass like material able to withstand strong thermal stresses). An infrared thermographic technique has been developed to monitor the

predicts the total evaporation time and it is further validated with transient surface temperature measurements obtained by infrared thermography. The predictions are in excellent agreement with the experimental data. The spatial and temporal heat flux distribution under the evaporating droplet is studied. The extent of the droplet evaporative cooling is quantified by introducing a novel concept defining the droplet radius of influence. A closed form solution predicting the radius of influence is derived and tested against the experimental data and the model predictions. An empirical correlation for the prediction of the evaporation time is also presented. Insight into the evaporative cooling phenomena is provided for materials with various thermal conductivity. The relevant parameters are identified and their influence on the phenomena is assessed.

In Part B the experimental program conducted with radiant heat input for single droplets evaporating on Macor is described. A new experimental set-up for the study of dropwise evaporation in a radiant heat transfer field has been designed, constructed and tested. The various issues of concern (steady state solid temperature distribution, radiant heater design and configuration, infrared background noise and post test data manipulation) are outlined.

In Part C a novel model is presented, which extends the single droplet results to a multi-droplet system. Numerical results are obtained for different values of the impingement area, mass flow rate of the spray and initial solid surface temperature. However, this portion of the research is still in progress and it will constitute an essential portion of the next grant period.

PART A

SINGLE-DROPLET MODEL

A1. INTRODUCTION

The cooling of hot surfaces by droplet sprays has been studied extensively. Multi-droplet systems were investigated by Bonacina et al. (1979). He reinforced Toda's (1972) conclusion that conduction in the liquid is the relevant heat transfer mode in absence of nucleate boiling. Convective heat transfer within the liquid droplet could be due to Rayleigh instabilities or more likely to surface tension. The Rayleigh instability driven motion should be ruled out due to the large response time which exceeds the droplet evaporation time. The surface tension induced convective motion is more plausible (see Ostrach and Pradhan, 1978). However, the velocities that would results from this driving mechanism are very small (order of 10^{-4} meters-per-second). The temperature profiles in the liquid are linear for such small internal motions. Flow visualization experiments were conducted by the authors with small ink tracers and no significant convective motion was detected even for large droplets under large thermal gradients. Sadhal and Plesset (1979) investigated the effect of solid properties. Grissom and Wierum (1981) further developed these ideas to define a range of conditions for spray evaporative cooling. Rizza (1981) formulated a thermal model for a semi-infinite solid subjected to droplet evaporation on its exposed surface. His main assumption of uniform and constant solid-liquid interfacial temperature is corroborated by Seki et al. (1978), and by the extensive experimental observations of Makino and Michiyoshi, see for example Makino and Michiyoshi (1979,1984). A simple model for single droplet evaporation was introduced by diMarzo and Evans (1989). This model is limited to evaporation at the liquid-vapor interface in complete suppression

of nucleate boiling. Photographic inspection of evaporating droplets (diMarzo and Evans, 1987) revealed that the droplet shape can be approximated by a segment of a sphere. Zhang and Yang (1982) confirmed this assumption along with the more general behavior of droplet-surface interactions described by Simon and Hsu (1971) and by the extensive work of Wayner (see as an example Wayner, 1973).

These studies focused mostly on water droplet deposited on high thermal conductivity materials. Thus, the assumption of uniform and constant solid-liquid interfacial temperature is reasonable and the modeling of the liquid region can be de-coupled from the treatment of the solid. *This is not the case for dropwise evaporative cooling taking place on low conductivity materials.* Abu-Zaid and Atreya (1989) measured the interfacial temperature at various locations and confirmed that the temperature changes during the transient. The thermal behavior of the surface during the evaporation, monitored by infrared thermography (Klassen et al., 1990), also reveals that a sharp change in the interfacial conditions is taking place in the later part of the droplet evaporation transient.

The objective of this study is to provide a basis for the modeling of solid fuel fire extinguishment process and for the modeling of the cooling mechanism by sprinkler generated sprays in a fire environment. The thermal behavior of different materials subjected to dropwise evaporative cooling is studied. In particular, the effect of their different thermal conductivity (the range considered spans more than two orders of magnitude) is assessed. A model which describes the coupled thermal behavior of solid and

liquid during the evaporative transient has been formulated. This model is fully described by Tartarini et al. (1990) and will be the subject of a paper currently in preparation. The predictions of the model are presented and compared with the experimental results. Further analysis of numerical and experimental results is carried out to provide more insight into the evaporative cooling mechanism. A novel correlation for the prediction of the total evaporation time is proposed. An approximate, closed-form solution is used to deduce the relevant normalized governing parameters.

A2. PHENOMENOLOGY

A droplet gently deposited on a hot surface wets a circular area of radius R which remains constant throughout all the evaporation. The water-solid contact angle decreases without reaching its minimum regressive value (see Simon and Hsu, 1971). Therefore, the shape is described by a segment of a sphere of constant base. The heat is conducted through the droplet from the solid surface to the liquid vapor interface where it evaporates the liquid and is convected and radiated into the ambient. The thermal conductivity of the solid determines the extent of the cooling and the magnitude of the local the temperature drop. As the evaporation progresses the thickness of the liquid layer, that constituted the droplet, decreases thus the heat transfer increases due to the reduced resistance. This fact implies that the heat flux at the droplet base increases as time elapses and the portion of the liquid-vapor interface where most of the evaporation takes places extends gradually from the droplet edge to all the interfacial area as also the central portion of the droplet (at small radii) thins. Detailed description of phenomenology of the droplet evaporation and of the solid surface temperature behavior is provided by diMarzo and Evans (1987) and by Klassen et al. (1990). Experiments were conducted on aluminum and on Macor (a glass-like material). Some important physical properties of aluminum and Macor are reported in Table 1. The thermal conductivity of aluminum is about 180 W/m°C while Macor exhibits a thermal conductivity of 1.3 W/m°C. This difference of more than two orders of magnitude spans over most of the non-porous, solid materials range. The thermal conductivity more than the thermal diffusivity of the materials is the main parameter characterizing the

evaporative cooling behavior.

Figure A1 illustrates the differences between the aluminum and Macor behaviors. The temperature profiles on the surface of the two materials are compared (at different times during the transient $t/\tau = 0.3$ and $t/\tau = 0.9$) for an identical heat sink (30 μl water droplet evaporating in 95 seconds). Note that all the aluminum cooling is bounded within half degree Centigrade while the Macor cools over 30 degrees Centigrade. This huge difference in behavior explains why a constant and uniform interfacial temperature can be assumed for high conductivity materials and leads to meaningless results for a low thermal conductivity solid.

The region of the solid surface affected by the droplet presence is confined to few droplet diameters for Macor while its effects extend on a large portion of the aluminum surface. The actual temperature drop at the solid surface is significant for Macor although it is very small for aluminum. These observations will be quantified in the following and provide insight on the cooling strategies to be used for different materials.

The results obtained for high thermal conductivity solids are valid over a range of materials (copper, aluminum, steel). In all these cases, uniform and constant interfacial temperature can be assumed. De-coupling the liquid from the solid means that the liquid droplet behaves independently of the substrate as long as the interfacial temperature is close to the initial solid surface temperature. The interfacial temperature at the initial liquid-solid

contact can be obtained considering the exact solution available for two semi-infinite solids. Seki et al. (1978) bases his analysis on this consideration and suggests that the interfacial temperature should be:

$$T_c = \frac{T_l\sqrt{\rho_l c_l k_l} + T_s\sqrt{\rho_s c_s k_s}}{\sqrt{\rho_l c_l k_l} + \sqrt{\rho_s c_s k_s}} \qquad \text{(A1)}$$

The relation between this interfacial temperature and the actual computed value will be discussed in the following and its use in the analysis will also be outlined.

A3. THEORETICAL MODEL

A3.1. Model description

The modeling of the coupled solid and liquid thermal behavior is described by the transient conduction equation for both domains with the appropriate boundary conditions. The governing equations, with respect to the coordinate system depicted in Fig. A2, are:

$$\frac{\partial T}{\partial t} = \alpha_s \nabla^2 T \qquad \text{(A2)}$$

$$\frac{\partial T}{\partial t} = \alpha_l \nabla^2 T \qquad \text{(A3)}$$

A linear temperature distribution in the solid is required as initial condition. The far-field temperature distribution must be unaffected by the droplet evaporation. Initially, the liquid droplet is in thermal equilibrium with the ambient. By introducing an overall heat transfer coefficient h at the exposed solid surface, the boundary conditions at the liquid-vapor interface and at the exposed solid surface can be written as:

$$\text{at } 0 \le r \le R,\ z = 0:$$

$$T = T_o$$

$$k_s \frac{\partial T}{\partial z} = k_l \frac{\partial T}{\partial z} \qquad \text{(A4, A5, A6)}$$

$$\text{at } r > R,\ z = 0:$$

$$k_s \frac{\partial T}{\partial z} = h\,(T_o - T_a)$$

At the liquid-vapor interface a small portion of the heat conducted from below through the liquid is convected and radiated into the ambient. Most of the heat evaporates the liquid. To account for the evaporation, the vapor diffusion in the air is considered. The mass transfer coefficient is obtained with the Chilton-Colburn analogy (Chilton and Colburn, 1934). Details of the derivation of this liquid-vapor interfacial condition are given by diMarzo and Evans (1987). Note that the overall heat transfer coefficient h account for all the heat transferred to the ambient while the mass transfer coefficient is related to the convective heat transfer h_{conv}. The final formulation can be written as:

$$-k_l \nabla T - h\,(T_i - T_a) = 0.624\, h_{conv} \left(\frac{D}{\alpha_a}\right)^{\frac{2}{3}} \frac{\Lambda}{c_a} \frac{x_i - x_a}{1 - x_a} \tag{A7}$$

Extremely strong local thermal gradients at the drop initial contact preclude the solution of this problem with conventional finite difference schemes. The solution is obtained by using a Boundary Element Method (BEM) for the solid region and a Control Volume Method (CVM) for the liquid region. The BEM is described in detail by Kavoosi et al. (1989). The adjoint equation to Eq. (A2) (see Wrobel and Brebbia, 1981) is satisfied by the following Green's function:

$$G(r, z, t; r^*, z^*, t^*) = (4\pi\alpha_g t^*)^{-3/2} \times \left[e^{-\frac{(r-r^*)^2 + (z-z^*)^2}{4\pi t^*}} + e^{-\frac{(r-r^*)^2 + (z+z^*)^2}{4\pi t^*}} \right] \tag{A8}$$

A linear combination of Eq. (A2) and of its adjoint equation, is integrated over the solid

and temporal domain. The transient terms are reduced to two spatial integrals at the initial time and at the present time. The integral at the initial time is eliminated with a proper choice of a transformed temperature as shown in Eq. (A9). The spatial integral at the present time is simply the integrand since the Green's function reduces to a Dirac function. After defining:

$$u(r, t) = T - T_s - \frac{qz}{k_s} \tag{A9}$$

and by using the Gauss theorem on the right hand side one obtains:

$$u(r, t) = \int_0^t \int_0^\infty \nabla u(r*, t*)\, r*\, t*^{-3/2}\, L_0\left(\frac{2 r r*}{4 \alpha_s t*}\right) e^{-\frac{(r - r*)^2}{4 \alpha_s t*}}\, dr*\, dt* \tag{A10}$$

Details on the CVM are given by Tartarini et al. (1990).

The governing equation for the liquid is cast in the following form:

$$\int_v \frac{\partial T}{\partial t}\, dv = \alpha_1 \int_s \nabla T \bullet \hat{n}\, ds \tag{A11}$$

which is integrated for each elementary volume of the discretized liquid domain. These two equations, Eq. (A10) and Eq. (A11), are then combined in matricial form. By inverting the matrix, one obtains the transient temperature and heat flux distribution in the liquid and over the solid surface. The description of this complex numerical solution is the subject of a paper currently in preparation.

The input to the code must prescribe: a) the droplet initial volume; b) the droplet shape parameter β as defined by Bonacina et al. (1979); c) the initial surface temperature; d) the

overall heat transfer coefficient and e) the convective heat transfer coefficient. The shape parameter and the two heat transfer coefficients are provided by correlations based on experimental data. The code predicts: a) the transient temperature profiles on the solid surface and at all liquid locations; b) the heat fluxes at all points of the liquid domain and on the solid surface; c) the total evaporation time and d) the transient liquid inventory.

A3.2. Model validation

The validation of the model predictions is obtained by comparing them with experimental results obtained by Klassen et al. (1990). These experiments provide the temperature distribution during the evaporative transient of a water droplet deposited on Macor. Figure A3 illustrates some of these comparisons for various initial surface temperatures and droplet volumes at a time corresponding to 90 per cent of the total evaporation time. A comparison toward the end of the evaporation time is selected to maximize the discrepancies between predictions and data due to the parabolic nature of the problem. These local temperature profile comparisons (for $r/R > 1$) illustrate the typical model capabilities which are deemed satisfactory. A comprehensive comparison of the model with the data is obtained by looking at the overall predicted evaporation time for aluminum and Macor and at the experimental results obtained by Klassen et al. (1990) and by diMarzo and Evans (1989). Figure A4 shows the calculated and measured evaporation time for both materials at various initial solid surface temperatures and droplet sizes. The agreement is remarkable in light of the fact that the experimental data are repeatable within ten per cent of the indicated value.

A4. RESULTS AND DISCUSSION

A4.1. Approximate, closed-form solution

In an effort to normalize the relevant parameters, an approximate, closed-form solution is sought. Carslaw and Jaeger (1959) show that, for a semi-infinite solid with a surface heat flux constant and uniform applied over a disk of radius R and no heat transfer on the remainder of the surface, the transient temperature profile on the solid surface is given by

$$T_s - T = \frac{qR}{k_s} \int_0^\infty J_0(\lambda r)\, J_1(\lambda R)\, erf\left(\lambda \sqrt{\alpha_s t}\right) \frac{d\lambda}{\lambda} \qquad \text{(A12)}$$

By introducing the normalized radius η = r/R and the normalized time $\delta = (\alpha_s t)^{1/2}/R$ and by setting q equal to the spatial and temporal average heat flux due to evaporation, one can express the dimensionless temperature θ as follows:

$$\theta = JA\left(\frac{\rho_s}{\rho_l}\right) \delta^2 \beta^3 = \frac{4}{3} \int_0^\infty J_0(\zeta \eta)\, J_1(\zeta)\, erf\,(\zeta \delta)\, \frac{d\zeta}{\zeta} \qquad \text{(A13,A14)}$$

where β is the shape parameter defined by Bonacina et al. (1979) and JA is the Jakob number. These two parameters can be written as:

$$\beta = R\left(\frac{4\pi}{3V}\right)^{1/3} \qquad \text{(A15)}$$

$$JA = \frac{c_s (T_s - T)}{\Lambda} \qquad \text{(A16)}$$

Figure A5 shows a comparison of the approximate solution with the data. The approximate solution under-predicts the temperature profile (for $\eta > 1$). However, the general trends are preserved and substantial advantage is gained with this normalization. This closed-form solution will also be used in the following to assess the droplet cooling effect.

A4.2. Results

The validated model is used to investigate the interfacial temperatures and heat fluxes under the droplet where direct measurements are unavailable. Figure A6 shows the liquid-solid interfacial fluxes for a typical case. It is important to note that the heat flux is not uniform nor constant during the evaporative process. The spatial distribution indicates that most of the evaporation takes place at the outer edge of the droplet. This results confirms the findings of diMarzo and Evans (1989). Therefore it is not surprising that the approximate solution, based on constant and uniform flux, fails to match the surface temperature profiles for $\eta = 1$.

Figure A7 illustrates the behavior of the spatial averaged heat flux for different materials. The onset of nucleate boiling temperature for these five cases is calculated by setting the contact temperature in Eq. (A1) to 100 °C. The resulting initial solid surface temperature for an initial water temperature of 20 °C is the maximum value for which evaporation is still possible and beyond which nucleate boiling is observed. By setting the temperature ratio in the figure to a common value (= 0.8), similar interfacial conditions are expected for the various materials. Recall the temperature profiles of Fig. A1 which clearly indicate the

different local temperature drop for aluminum and Macor. This explains why similar local temperatures at the droplet outer edge are observed for bakelite with an initial surface temperature of 230 °C and for aluminum with an initial surface temperature of 88 °C. Note the temporal behavior of the spatial averaged heat flux which in all cases tends to sharply rise toward the end of the process due to the thinning of the water layer and to the subsequent sharp increase in heat transfer.

Figure A8 shows the corresponding temperature profiles toward the end of the evaporation transient ($t/\tau = 0.9$). Note the dip in the temperature near the edge of the droplet for the bakelite which, due to its very low conductivity, enhances the local temperature gradients. In all cases note that the temperature at the edge of the droplet is higher than the spatial averaged value. Also note the different behavior of the surface temperature distributions outside the wetted area and in particular the radial distance where the effect of the droplet cooling becomes negligible.

Solid-liquid interfacial temperature profiles for Macor and aluminum are shown in Fig. A9. The high thermal conductivity of aluminum results in uniform and constant interfacial temperatures while the lower thermal conductivity of Macor is reflected in non-uniform and variable temperatures. The Macor interfacial temperatures confirm the discrepancies observed in Fig. A5 and demonstrate the limits of the assumptions used by diMarzo and Evans (1989), by Seki et al. (1978) and by Rizza (1981) in their simplified evaporative cooling analyses.

A4.3. Evaporation time correlation

One of the most significant parameters in the analysis of the results is the total evaporation time. The lack of approximate solutions requires the formulation of a correlation. A simple form for the normalized evaporation time is fitted with the experimental data for aluminum and Macor yielding the following result:

$$\delta = \frac{\sqrt{\alpha_s \tau}}{R} = \left(\frac{1.17}{\beta}\right)^{3.69} \left(\frac{\alpha_s}{\alpha_l}\right) \times \exp\left[-2.45 \left(\frac{k_s}{k_l}\right)^{0.640} \frac{T_s - T_a}{T_b - T_a} + 1.99 \left(\frac{k_s}{k_l}\right)^{0.0858}\right] \qquad \text{(A17,A18)}$$

The comparison between the total evaporation times provided by this correlation and those predicted by the model for various materials and for various conditions is shown in Fig. A10. The correlation is in excellent agreement with the model for evaporation times below 100 seconds. For higher evaporation time it tends to over-predict within 20 per cent of the model results. It is notable that the correlation is able to reasonably describe the evaporation time with the normalized parameters identified by the approximate solution.

A4.4. Radius of influence

In order to quantify the extent of the solid surface region affected by the droplet cooling, a significant parameter is the radial heat flux at the surface at any given location. The presence of the droplet is felt when this radial heat flux is greater than a reference value based on the spatial and temporal averaged heat flux, that is:

$$-k_s \frac{\partial T}{\partial r} \geq \phi \frac{\Lambda \rho_l V}{\pi R^2 \tau} \qquad \text{(A19)}$$

By using Eq. (A13) and Eq. (A14), this condition becomes in terms of normalized quantities:

$$\frac{\partial \theta}{\partial \eta} \geq -\frac{4}{3}\phi$$

$$\int_0^\infty J_1(\zeta\eta)\, J_1(\zeta)\, erf(\zeta\delta)\, d\zeta \geq \psi \qquad \text{(A20,A21)}$$

where ϕ and ψ are arbitrary constants. Equations (A20) and (A21) define the radius of influence η_ϕ (= r_ϕ/R) as the minimum value of η that satisfies these inequalities. Two different constants are used because the approximate closed-form solution, which yields Eq. (A21), is able to capture the trends of the radius of influence but not the actual value as clearly seen in Fig. A11. The radius of influence can be defined for ϕ = 0.1 which relates the radial heat flux to ten per cent of the spatial and temporal averaged heat flux [see Eq. (A19)]. The approximate, closed-form solution for ψ = ϕ = 0.1 is shown in the figure. Values of ψ between 0.045 and 0.065 provide a good representation of the model predictions for a wide variety of conditions.

The combination of Eq. (A18) and of Fig. A11 provides a rapid estimate of the radius of influence. Both the evaporation time correlation and the radius of influence plots are excellent predictive tools at low values of the normalized time δ. The usual values of this parameter for most materials and conditions is found to be below five.

A5. CONCLUSIONS

This study briefly reviews the formulation of a model for the prediction of the thermal behavior of the droplet-solid interaction during evaporative cooling. The model is validated over a wide range of parameters. Model predictions for a variety of conditions are used to gain insight into the evaporative process mechanism.

A correlation for the prediction of the total droplet evaporation time is proposed and checked against the model predictions. An approximate, closed-form solution is used to normalize the relevant parameters and to provide estimates of a newly defined radius of influence.

A6. NOMENCLATURE

a	thickness of the droplet
c	specific heat
D	steam water mass diffusivity - diameter
erf	error function
$\vec{f}$	forcing and unknown vector
G	Green's function
h	overall heat transfer coefficient
h_{conv}	convective heat transfer coefficient
h_{fg}	latent heat of vaporization
J_0, J_1, I_0	Bessel's functions
JA	Jakob number
k	thermal conductivity
L_0	modified Bessel's function: $e^{-\zeta} I_o(\zeta)$
Le	Lewis number: $(D/\alpha)^{2/3}$
$\hat{n}$	unit vector normal to the surface
q	reference heat flux: $\Lambda \rho V / (\pi R^2 \tau)$
$\bar{q}$	spatial averaged heat flux
r	radial coordinate
R	radius of the wetted area
s,S	surface
t	time
t_o	recollection time
T	temperature
T_b	onset of nucleate boiling temperature
T_c	contact temperature
u	transformed temperature
v,V	volume or drop volume
W	weight matrix
x	molar fraction of steam in air
z	axial coordinate

α	thermal diffusivity
β	shape parameter
δ	normalized time: $(\alpha_s\ t)^{1/2}/R$
ϵ	solid surface emissivity
ζ,λ	dummy variables
η	normalized radius: r/R
η_ϕ	radius of influence associated with the constant ϕ
θ	normalized temperature
Λ	liquid latent heat of vaporization
ρ	density
σ	Stefan-Boltzmann constant
τ	total evaporation time
ϕ,ψ	arbitrary constants

Subscripts

a	ambient, air
i	liquid-vapor interfacial property
l	liquid
o	generic point index
r	in the radial direction
s	solid
z	in the axial direction
*	Green's function argument

A7. REFERENCES

- Abu-Zaid, M., Atreya, A., 1989, *"Effect of Water on Piloted Ignition of Cellulosic Materials"*, NIST Report, NIST-GCR-89-561.

- Bonacina, C., Del Giudice, S., Comini, G., 1979, *"Dropwise Evaporation"*, ASME Journal of Heat Transfer, Vol. 101, pp. 441-446.

- Carslaw, H.S., and Jaeger, J.C., 1959, *Conduction of Heat in Solids*, Clarendon Press, Oxford, pp. 214-217 and 264.

- Chilton, T.H. and Colburn, A.P., 1934, *"Mass Transfer (Absorption) Coefficients Prediction Data on Heat Transfer Fluid Motion"*, Industrial Engineering Chemistry, Vol. 26, pp. 1183-1187.

- diMarzo, M., Trehan, A.K., 1986, *"Transient Cooling of a Hot Surface by Droplet Evaporation"*, National Bureau of Standards Report, NBS-GCR-86-516.

- diMarzo, M., Evans, D., 1986, *"Evaporation of a Water Droplet Deposited on a Hot High Conductivity Solid Surface"*, National Bureau of Standards Interagency/Internal Report, NBSIR 86-3384.

- diMarzo, M., Wang, Z.Y., Meng, W.H., 1987, *"Transient Cooling of a Hot Surface by Droplets Evaporation"*, National Bureau of Standards Report, NBS-GCR-87-534.

- diMarzo, M., Evans, D., Trehan, A.K., 1987, *"The Cooling Effect of a Single Droplet on a Hot Semi-Infinite Metal Body"*, National Bureau of Standards Interagency/Internal Report, NBSIR 87-3517.

- diMarzo, M., Evans, D., 1987, *"Dropwise Evaporative Cooling of High Thermal*

Conductivity Materials", Heat and Technology, Vol. 5, No. 1-2, pp. 126-136.

- diMarzo, M., Evans, D., 1989, *"Evaporation of a Water Droplet Deposited on a Hot Thermal Conductivity Surface"*, ASME Journal of Heat Transfer, Vol. 111, pp. 210-213.

- Grissom, W.M., Wierum, F.A., 1981, *"Liquid Spray Cooling of a Heated Surface"*, International Journal of Heat and Mass Transfer, Vol.24, pp. 261-271.

- Kavoosi, F., diMarzo, M., Baum, H.R. and Evans, D.D., 1989, *"An Application of Boundary Element Methods to a Transient Axisymmetric Heat Conduction Problem"*, ASME HTD, Vol. 110, pp. 79-85.

- Klassen, M., 1989, *"Infrared Thermography of Dropwise Evaporative Cooling"*, MS Thesis, University of Maryland, Dept. of Mechanical Engineering.

- Klassen, M., diMarzo, M. and Sirkis, J., 1990, *"Infrared Thermography of Dropwise Evaporative Cooling"*, ASME HTD, Vol. 141, pp. 117-121.

- Makino, K., Michiyoshi, I., 1978, *"Heat Transfer Characteristics of Evaporation of a Liquid Droplet on Heated Surfaces"*, Int. Journal of Heat Mass Transfer, VOL 21, pg 605.

- Makino, K., Michiyoshi, I., 1979, *"Effects of the Initial Size of Water Droplet on its Evaporation on Heated Surfaces"*, International Journal of Heat and Mass Transfer, Vol. 22, pp. 979-981.

- Makino, K., Michiyoshi, I., 1984, *"The Behavior of a Water Droplet on Heated Surfaces"*, International Journal of Heat and Mass Transfer, Vol. 27, pp. 781-791.

- Makino, K., Michiyoshi, I., 1987, *"Discussion of Transient Heat Transfer to a Water*

Droplet on Heated Surfaces Under Atmospheric Pressure", Int. Journal of Heat Mass Transfer, VOL 30,, No. 9, pg 1895.

- McAdams, W.H., 1957, *Heat Transmission*, 3rd ed., McGraw-Hill, New York.

- Ostrach, S, and Pradhan, A., 1978, *"Surface-Tension Induced Convection at Reduced Gravity"*, AIAA Journal, Vol. 16, No. 5, pp. 419-424.

- Pedersen, C.O., 1970, *"An Experimental Study of the Behavior and Heat transfer Characteristics of Water Droplets Impinging Upon a heated Surface"*, Int. Journal of Heat Mass transfer,VOL 13, pg 369.

- Rizza, J.J., 1981, *"A Numerical Solution to Dropwise Evaporation"*, ASME Journal of Heat Transfer, Vol. 103, pp. 501-507.

- Sadhal, S.S. and Plesset, M.S., 1979, *"Effect of Solid Properties and Contact Angle in Dropwise Condensation and Evaporation"*, ASME Journal of Heat Transfer, Vol. 101, pp. 48-54.

- Seki, M., Kawamura, H., and Sanokawa, K., 1978, *"Transient Temperature Profile of a Hot Wall Due to an Impinging Liquid Droplet"*, ASME Journal of Heat Transfer, Vol. 100, pp. 167-169.

- Siegel, R., Howell, J.R., 1981, *Thermal Radiation Heat Transfer*, 2nd ed. Hemisphere Publishing Corporation, New York.

- Simon, F.F., Hsu, Y.Y., 1971, *"Wetting Dynamics of Evaporating Drops on Various Surfaces"*, NASA Technical Memorandum, NASA TM X-67913.

- Tartarini, P., Liao, Y., and diMarzo, M., 1990, *"Transient Cooling of a Hot Surface by Droplets Evaporation"*, UMCP Mechanical Engineering Report, No. 90-6.

- Toda, S., (1972), *"A Study of Mist Cooling. First Report: Investigation of Mist Cooling"*, Heat Transfer Japanese Research, Vol. 1, No. 3, pp. 39-50.

- Wayner, P.C., 1973, *"Fluid Flow at the Interline Region of an Evaporating Non-Zero Contact Angle Meniscus"*, International Journal of Heat and mass Transfer, Vol. 16, pp. 1777-1783.

- Wrobel, L.C. and Brebbia, C.A., 1981, *"A Formulation of the Boundary Element Method for Axisymmetric Transient Heat Transfer Conduction"*, International Journal of Heat and Mass Transfer, Vol. 24, pp. 843-850.

- Zhang, N., and Yang, W.J., 1982, *"Natural Convection in Evaporating Minute Drops"*, ASME Journal of Heat Transfer, Vol. 104, pp. 656-662.

A8. FIGURES AND TABLE

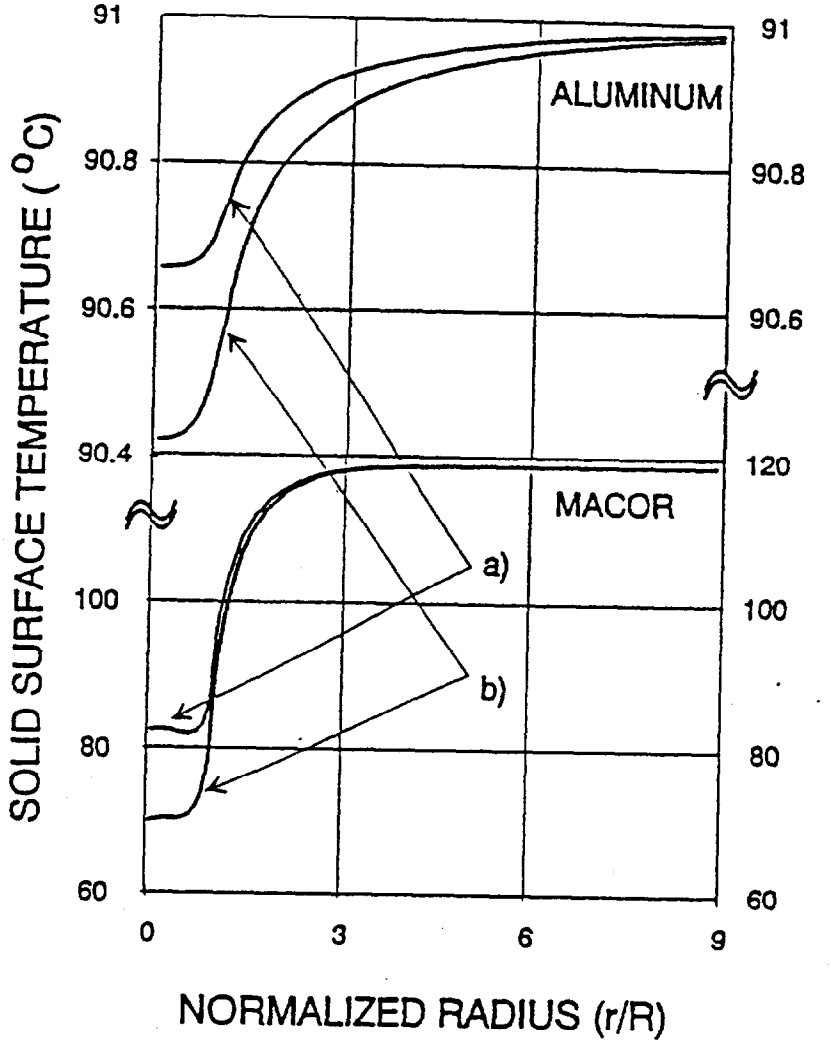

Fig. A1 Typical solid surface temperature profiles for water droplets (V = 30 μl, τ = 95 s) deposited on aluminum (T_s = 91 °C) and Macor (T_s = 119 °C) for a) t/τ = 0.3 and b) t/τ = 0.9

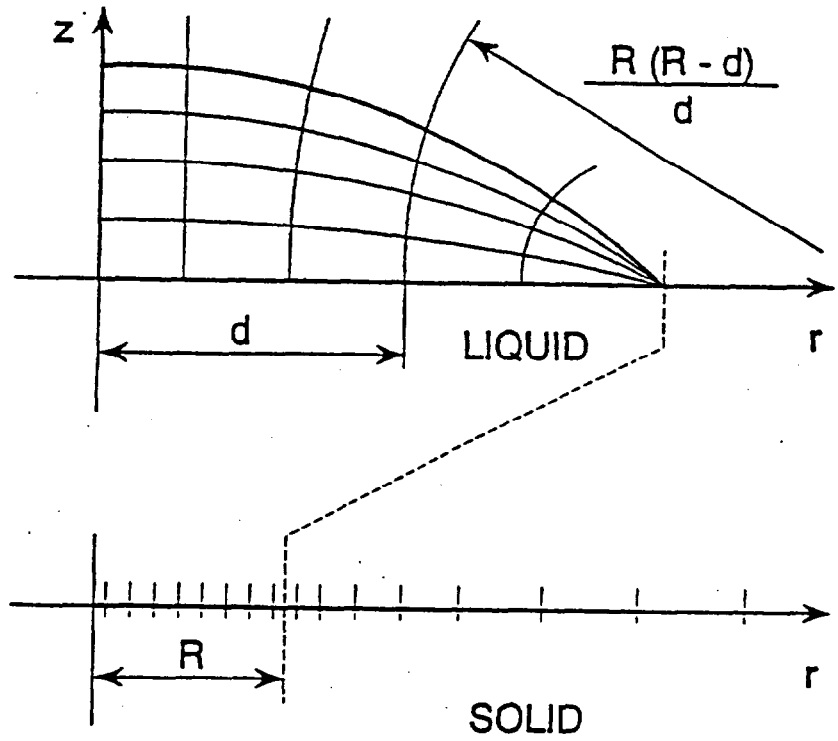

Fig. A2 Coordinate system and nodalization

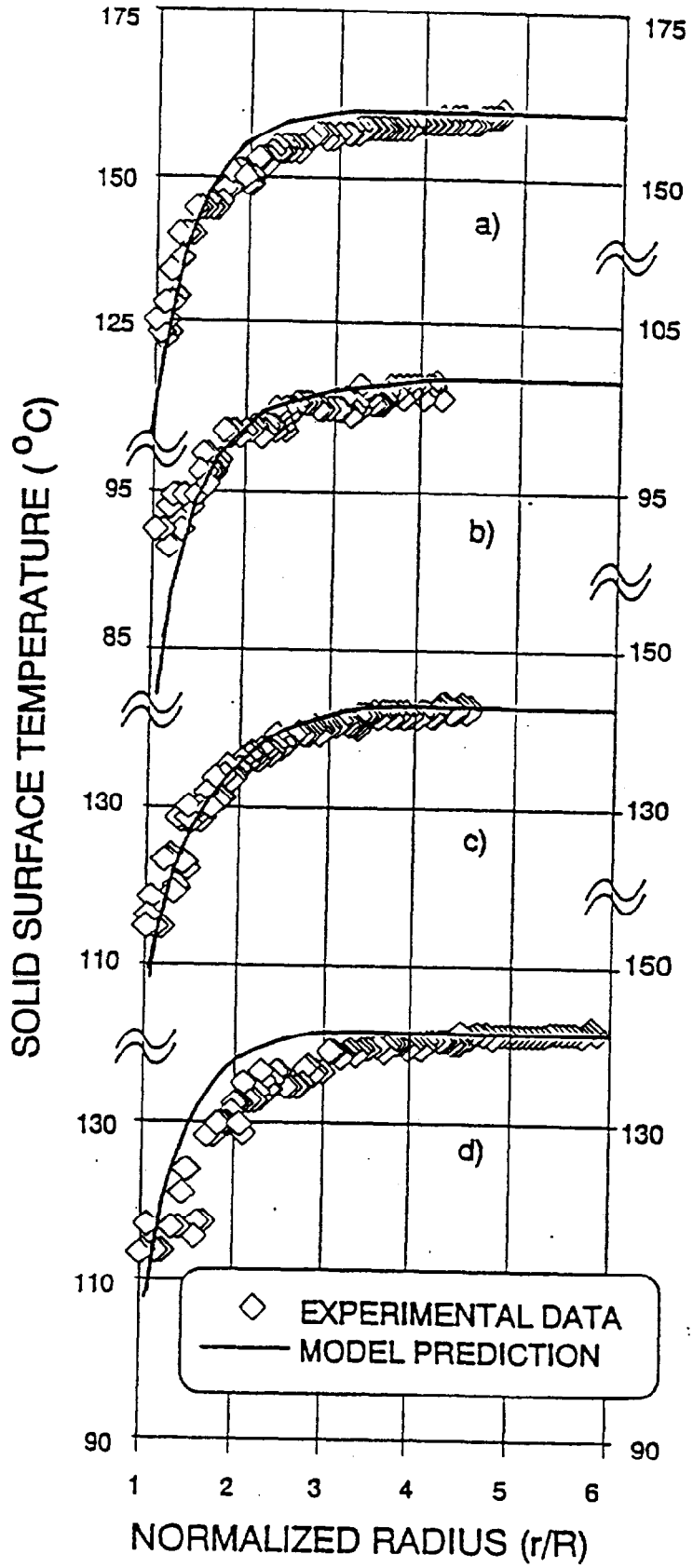

Fig. A3 Model validation: solid surface temperatures for water on Macor at $t/\tau = 0.9$ with a) V = 30 μl, T_s = 160 °C; b) V = 30 μl, T_s = 101 °C; c) V = 10 μl, T_s = 143 °C and d) V = 30 μl, T_s = 143 °C (data from Klassen et al. 1990)

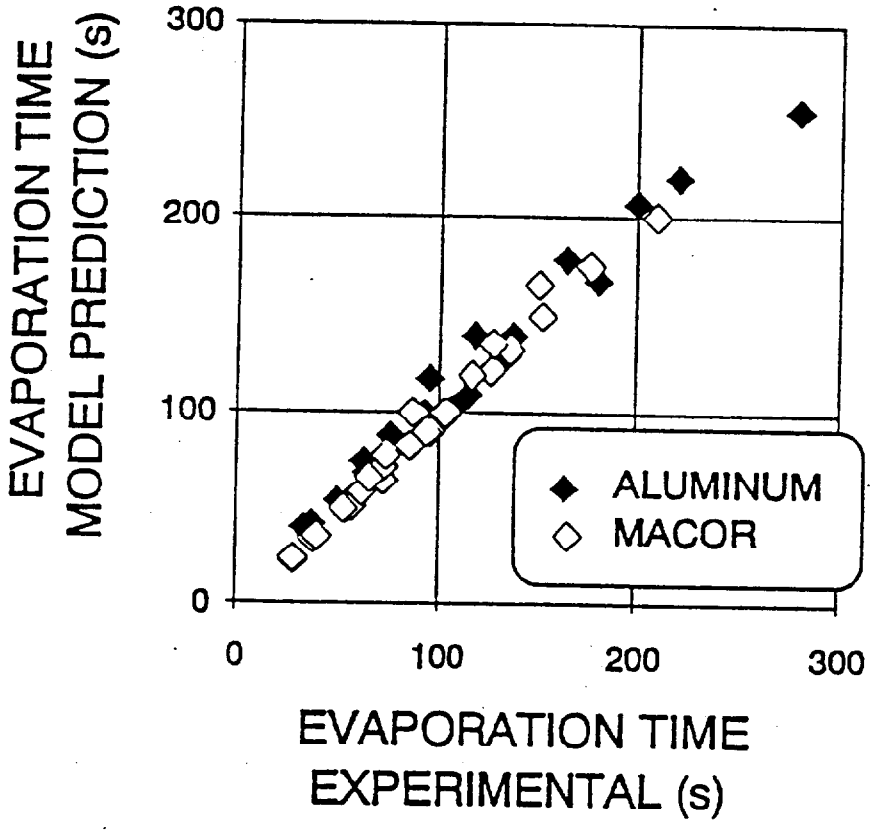

Fig. A4 Model validation: total evaporation time for droplets with V = 10, 30, 50 μl on aluminum with T_s = 75 ÷ 102 °C and on Macor with T_s = 101 ÷ 208 °C (data from Klassen et al. 1990)

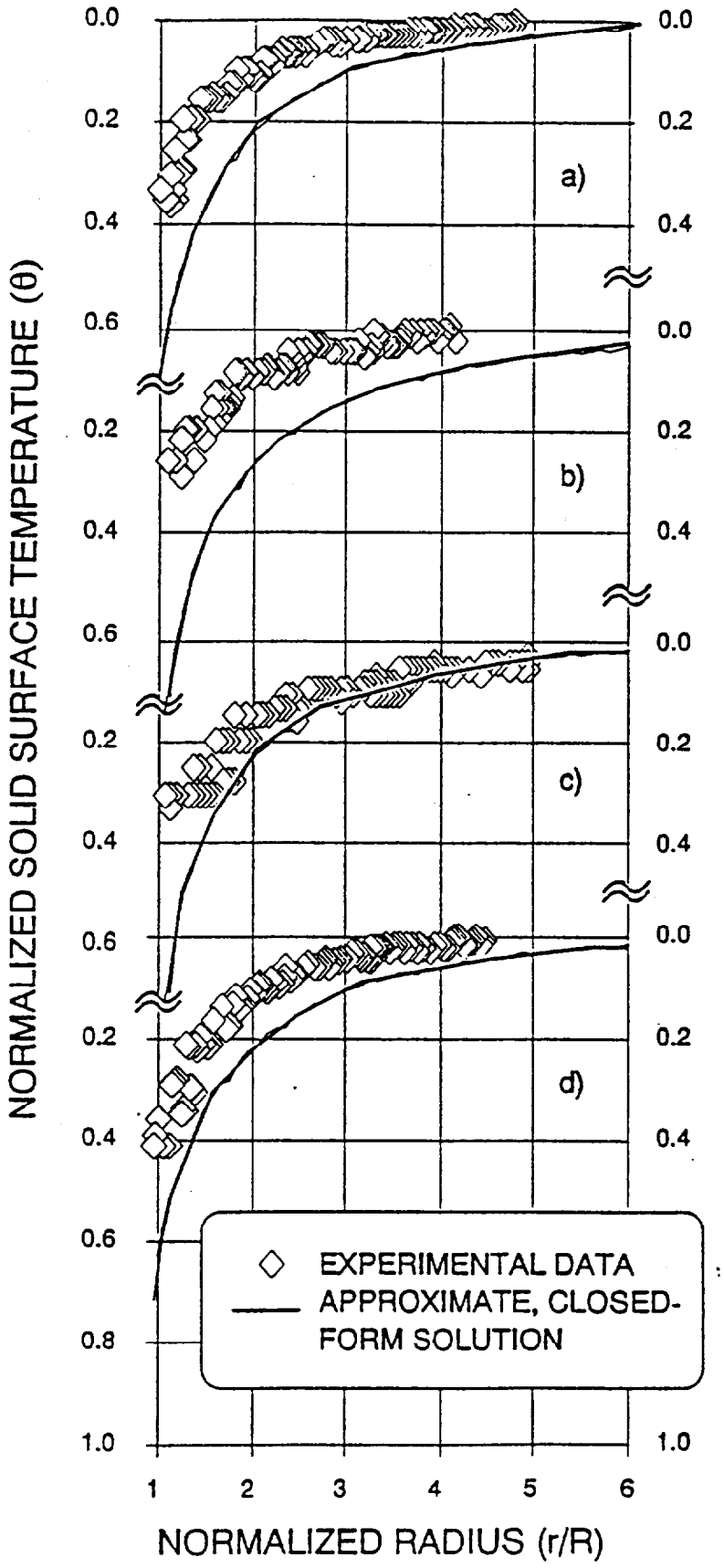

Fig. A5 Approximate, closed-form solution versus experimental data for water droplet on Macor with a) V = 30 μl, T_s = 160 °C; b) V = 30 μl, T_s = 101 °C; c) V = 10 μl, T_s = 143 °C and d) V = 50 μl, T_s = 143 °C (data by Klassen et al., 1990)

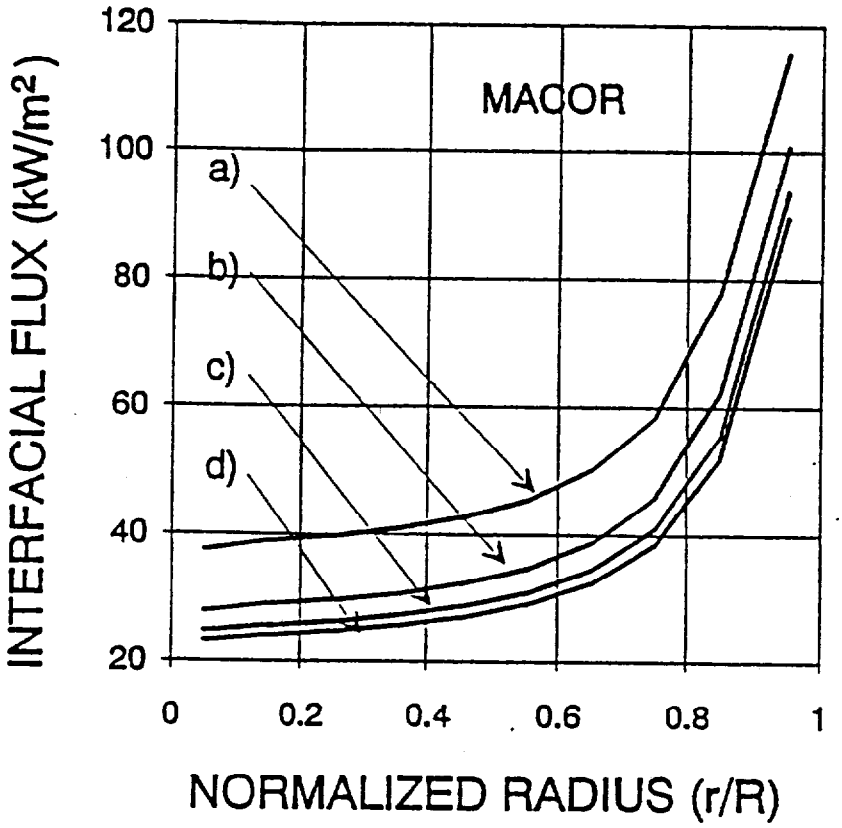

Fig. A6 Liquid-solid interfacial fluxes for water droplet with V = 30 μl on Macor with T_s = 143 °C at d) t/τ = 0.3; c) t/τ = 0.5; b) t/τ = 0.7; a) t/τ = 0.9 and τ = 64 s

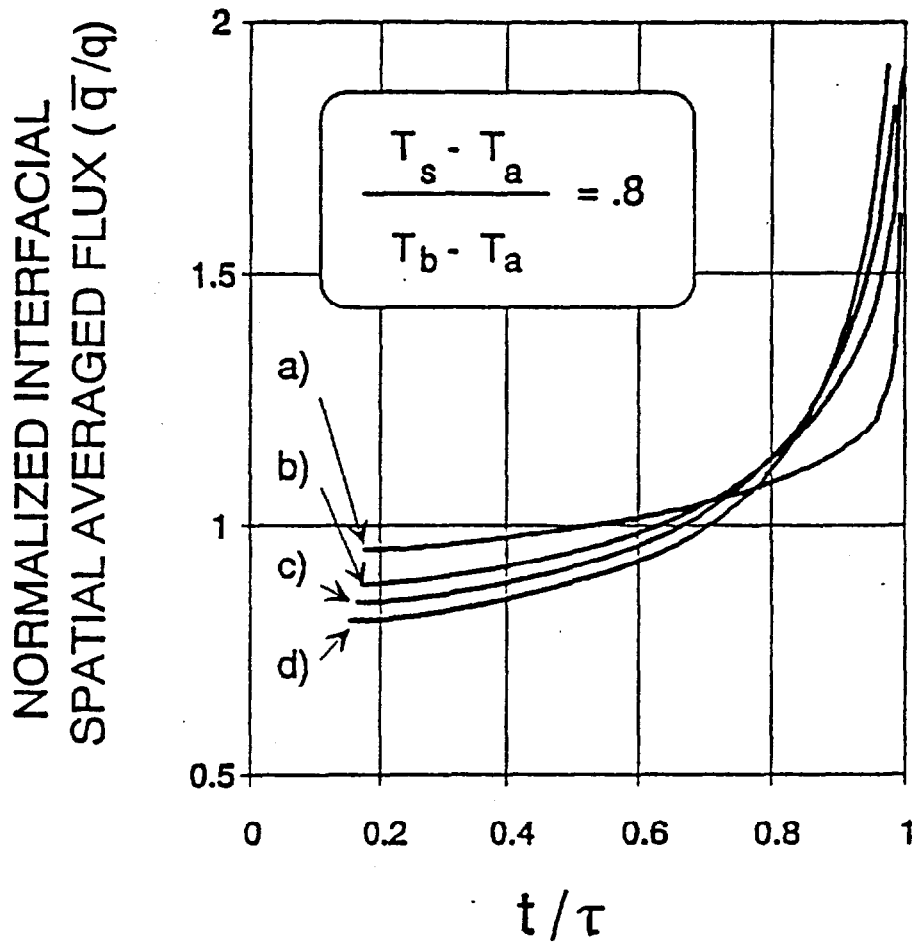

Fig. A7 Normalized spatial averaged liquid-solid interfacial flux for a water droplet with V = 30 μl on a) bakelite with T_s = 230 °C; b) aluminum with T_s = 88 °C; c) marble with T_s = 125 °C; d) steel with T_s = 98 °C; T_b from Eq. (1) and T_a = 20 °C

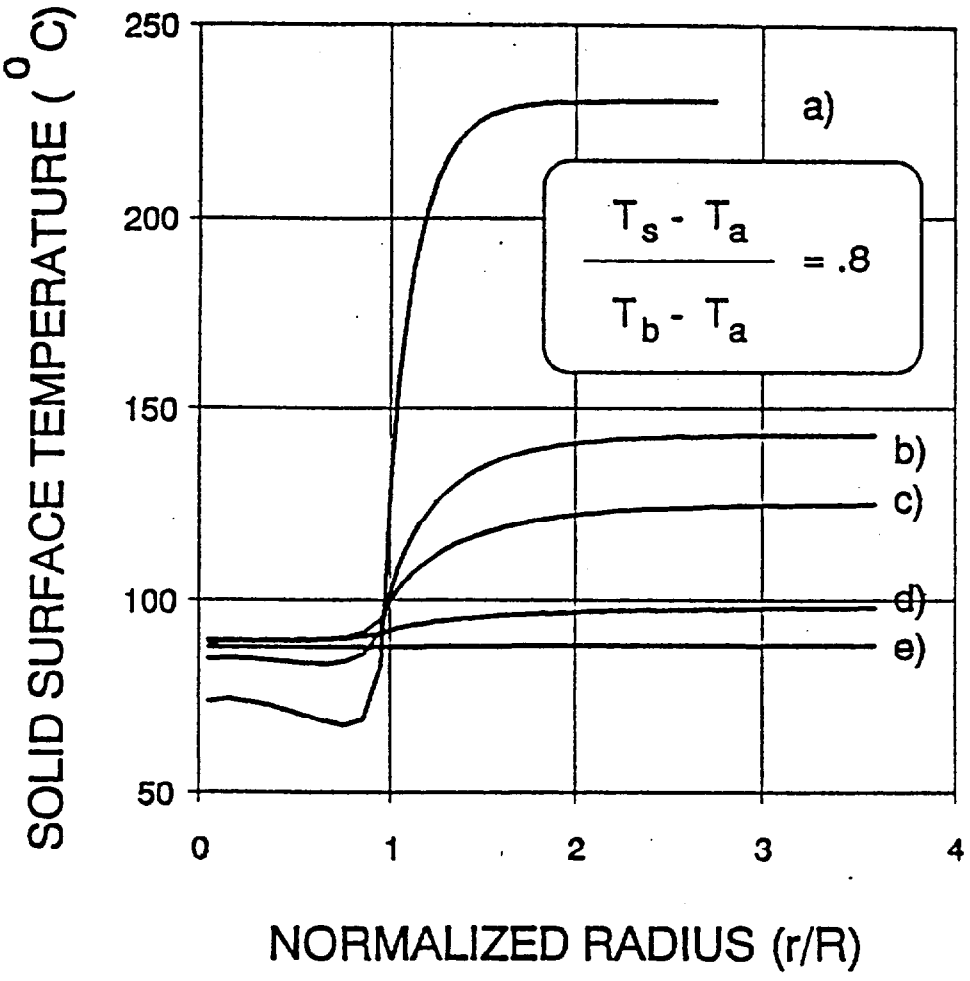

Fig. A8 Typical solid surface temperature profiles for a water droplet with V = 30 μl at t/τ = 0.9 on a) bakelite with T_s = 230 °C; b) macor with T_s = 143 °C; c) marble with T_s = 125 °C; d) steel with T_s = 98 °C; e) aluminum with T_s = 88 °C; T_b from Eq. (1) and T_a = 20 °C

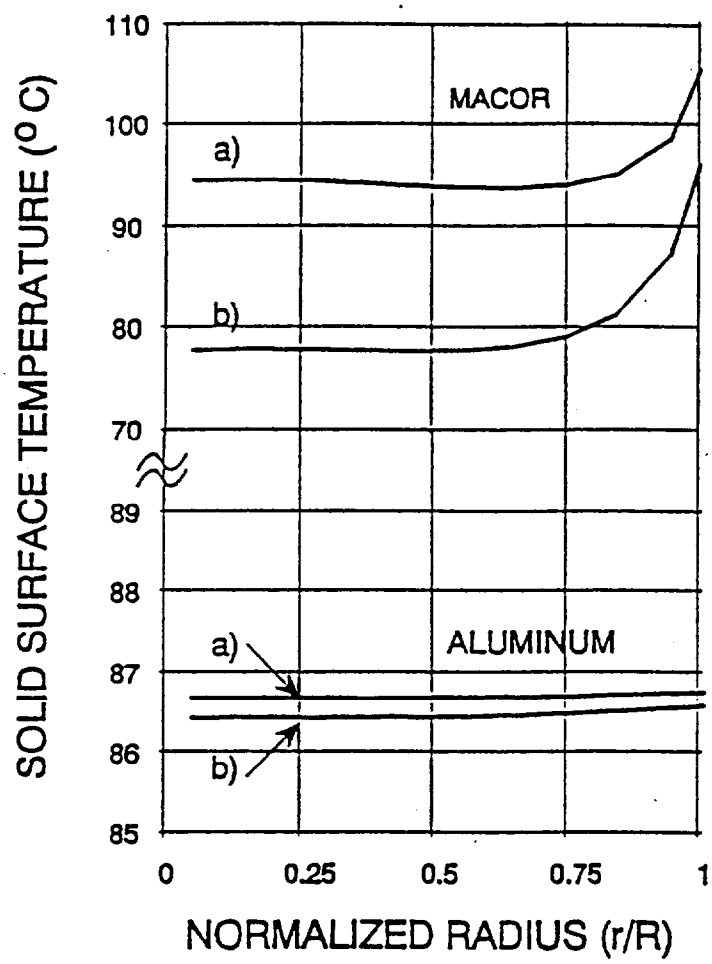

Fig. A9 Typical liquid-solid interfacial temperatures for Macor and aluminum with T_c = 82 °C for water droplets with V = 30 μl at a) t/τ = 0.3 and b) t/τ = 0.9

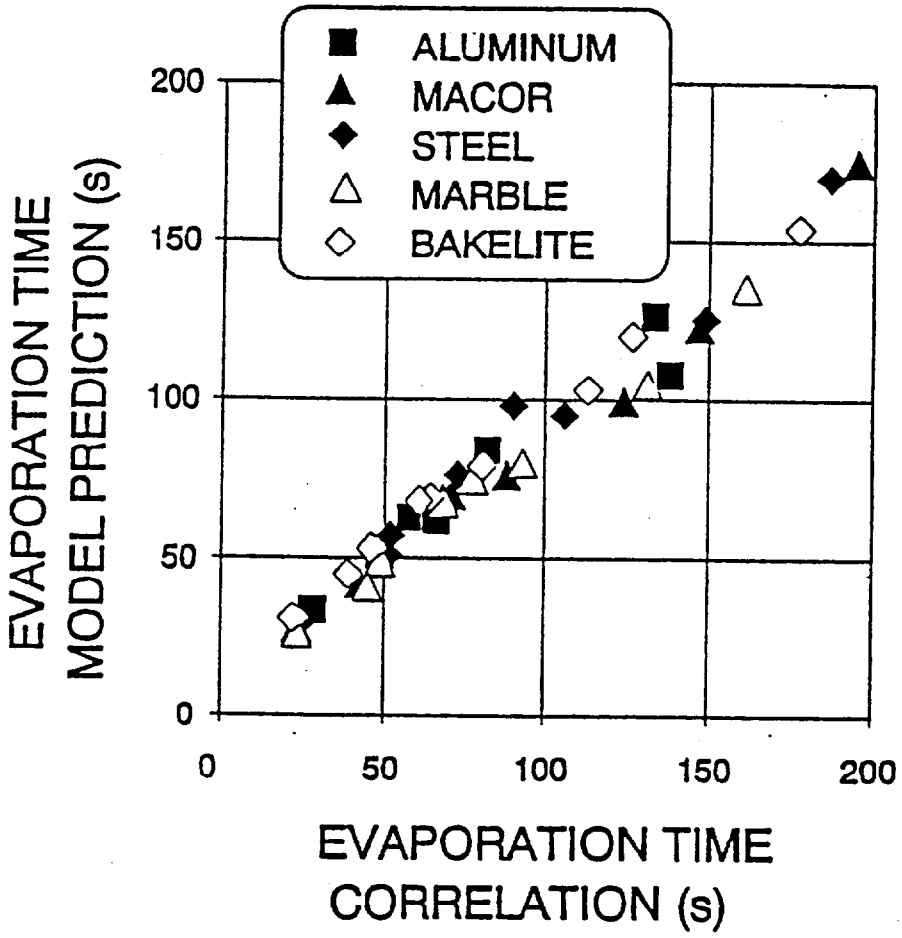

Fig. A10 Evaporation time correlation versus model predictions for water droplets with V = 10, 30, 50 μl on various materials with T_s = 80 ÷ 230 °C

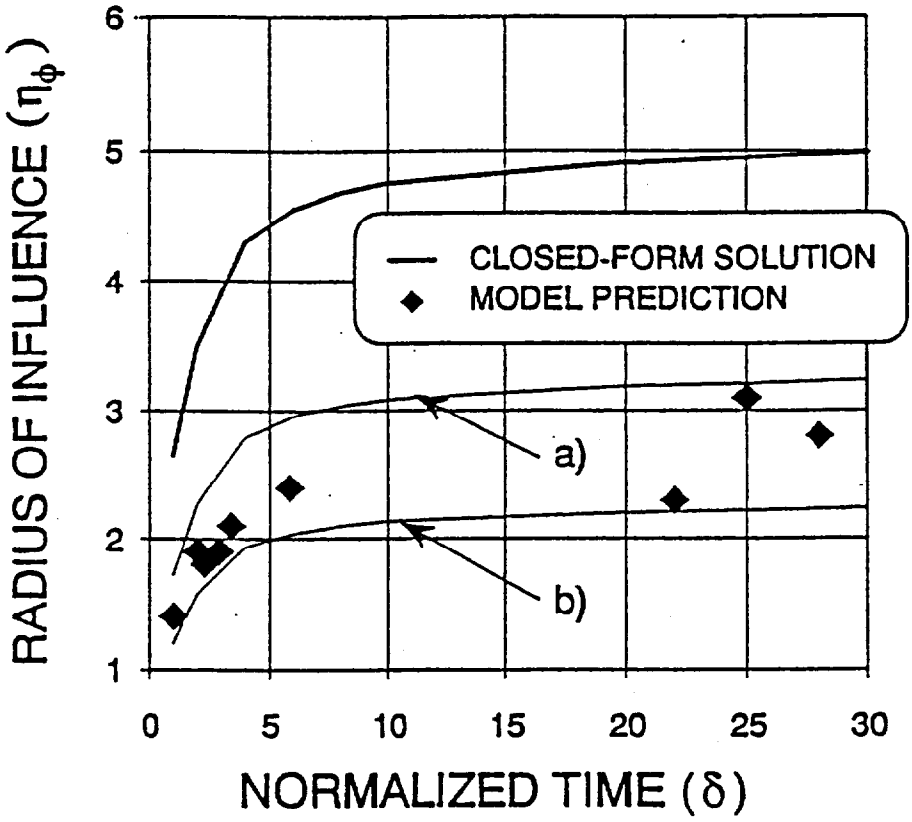

Fig. A11 Radius of influence versus normalized time: closed-form, approximate solution and model predictions where $\phi = \psi = 0.1$; a) $\psi = 0.065$ and b) $\psi = 0.045$

Table 1 - **PROPERTIES OF ALUMINUM AND MACOR**

****

ALUMINUM

Density:	2771	kg/m^3
Thermal Conductivity:	180	$W/(m \cdot K)$
Specific Heat:	962	$J/(kg \cdot K)$

****

MACOR

Density:	2520	kg/m^3
Thermal Conductivity:	1.297	$W/(m \cdot K)$
Specific Heat:	888.9	$J/(kg \cdot K)$

PART B

RADIATION EXPERIMENTS

B1. INTRODUCTION

Quenching of metals, spray cooling and fire suppression with sprinklers are few of the applications that inspired numerous theoretical and experimental investigations. Global approach to spray-surface interactions is addressed in the early investigations by Toda [1] and Bonacina [2]. More detailed numerical and experimental studies followed. In particular, the contributions of Rizza [3], Seki *et al.* [4], Inada *et al.* [5], diMarzo and Evans [6][7] are based on the integration of the transient conduction equation in the solid with a simple boundary condition at the liquid solid interface which prescribes constant and uniform temperature throughout the vaporization process. Grissom and Wierum [8] determined experimentally the lowest surface temperature possible for the existence of spray evaporative cooling and presented a conduction-controlled analytical model of droplet evaporation.

Other experimental works reinforced these modeling assumptions for solids characterized by high thermal conductivity. In particular, Sadhal and Plesset [9] described the droplet shape behavior when the liquid thins and breaks up; Pedersen [10] presented a large number of experimental data, showing that, for impinging droplets, approach velocity is a dominant variable affecting droplet heat transfer; Choi and Yao [11] studied the heat transfer characteristics of impacting sprays, with special attention to the differences between sprays impacting horizontally and vertically. Makino and Michiyosi [12][13][14][15]

investigated the onset of nucleate boiling and the corresponding behavior of the droplets during the different stages of the evaporating process, with particular interest on the influence of the governing parameters such as the droplet size and the initial surface temperature. These investigations span the full range of vaporization phenomena to include evaporation, nucleate boiling and film boiling. Detailed information on the droplet shape [9][13] and on the solid thermal transient [12][14][15] are given.

Recent studies by Abu-Zaid and Atreya [16], diMarzo and Evans [6][7] and Klassen *et al.* [17] concentrated on the evaporative phenomena with temperature ranges below the onset of nucleate boiling. Low thermal conductivity solids are heated from below and the evaporation of a single droplet is investigated [6][7][17]. The behavior of porous and non-porous materials with similar thermal properties are compared [16] and porous materials show higher evaporative cooling rates.

This work is part of a long term research effort aimed at modeling the extinguishment of a solid fuel fire. Water, used as an extinguishing agent, is a primary cause of secondary fire damage. By understanding and predicting fire extinguishment mechanisms, one can optimize the water application (droplet sizes, mass fluxes) and thus minimize the damages associated with the extinguishment process. Previous studies focused on the evaporation of water droplets deposited on surfaces which were heated by conduction from below. Klassen [17] studied droplet evaporation from Macor (a glass-like material) and diMarzo [6][7] reported on the evaporative cooling of aluminum. Most of these data refer to the range where only

evaporation takes place and nucleate boiling is fully suppressed. Some data points are also taken in the nucleate boiling range. In the present study, the heat input is provided by radiant panels located above the Macor to simulate a fire environment. Data are compared with Klassen's previous experiments [17] to determine the differences in the evaporation process due to the heat input characteristics (i.e. radiation from above versus conduction from below). Klassen [17] developed an infrared thermographic technique to obtain transient temperature profiles on the solid surface during the droplet evaporation. This technique is non-intrusive and has no response lag. The primary purposes of this work are: a) to gather data which will be used to validate models of the evaporation phenomena and b) to provide insight into dropwise evaporative cooling.

B2. EXPERIMENTAL APPARATUS

The experimental apparatus (shown schematically in Fig. 1) consists of a Macor tile (of squared shape with 15.2 cm sides and 2.54 thick) mounted onto a steel chilled plate. Contact between the tile and the chilled plate is enhanced by a conductive paste. The Macor is located under two radiant panels facing each other and oriented towards the Macor surface. An infrared camera is mounted above the tile at a 45 degree angle from the vertical axis and looks through a chilled pipe at the Macor surface. A mechanized droplet dispenser rolls in and out of the heated region and is designed to dispense metered water volumes at a precise location and in a repeatable manner (see for details Ref. [6]).

The radiant panels are used to simulate the heat flux output of a fire. These panels are powered by a three-phase 220 volt power supply which is controlled by a 0-10 volts output temperature controller. The panel surface temperatures provide the feedback to the controller.

A chill plate is placed under the Macor tile and is kept at near ambient temperature by controlling the water flowing through it. The heat flux in the vertical direction overwhelms the heat losses through the side of the tile. This set up is designed to obtain (prior to the droplet deposition) a uniform Macor surface temperature by reducing the radial temperature gradients and by providing a linear temperature profile across the tile in the

vertical direction.

The infrared camera (Model 525 Infrared Thermal Imaging System by Inframetrics) is used to observe the temperature distribution on the Macor tile surface. The camera is connected to a VCR which records the transient infrared temperature distribution of the portion of the Macor surface affected by the water droplet. The video image is recorded in real time. A chilled pipe is used to minimize the amount of extraneous infrared radiation that reaches the camera lens. This chilled pipe is constructed with a water cooled copper coil. The interior of the chilled pipe is coated with a high emissivity black paint to minimize the amount of reflection.

A mechanized droplet dispenser is used to place the water droplets onto the Macor surface. The dispenser rolls in and out of the experimental apparatus quickly and easily so that almost no disruption of the radiant heat flux is observed. A microdispenser (Drummond Scientific Corporation 550) is used to measure the droplet volume and to dispense it on the Macor surface. The dispenser is operated by a motor driven cam to obtain a repeatable droplet shape on the surface after deposition.

Macor properties are listed in Table 1. In particular note that it has high emissivity, which minimizes reflection from the surface. Macor can withstand repeated thermal shocks and its surface is smooth and cracks free.

B3. EXPERIMENTAL PROCEDURES

An extensive test matrix is implemented following an identical experimental protocol. These experiments are conducted for droplet sizes of 10, 30 and 50 μl at surface temperatures of 90, 110, 130, 145, 150, 155, and 164 °C. The droplet sizes are a compromise between the sprinkler delivered droplets ($\sim$ 1 μl) and reasonably large volumes to achieve easy repeatable dispensing ($>$ 10 μl). Note that surface tension impairs the delivery of smaller single droplets under the sole gravitational forces. The temperatures are mostly in the evaporative range since onset of nucleate boiling is observed at and above 155 °C.

The experimental protocol consists of 5 steps:

B3.1. Water conditioning

The water used in the experiment is de-ionized and must be completely degassed. De-ionized water is used to maintain a clean, deposit-free Macor surface. Complete degassing must be achieved to avoid degassing during the evaporative process. If gasses come out of solution during the evaporation they may alter the droplet shape and therefore its behavior or they can even shatter the droplet or trigger nucleate boiling.

Degassing is obtained by repeatedly freezing and thawing water kept under vacuum. The water is then removed from the degassing container by bringing it to boil and by extracting

the liquid with a syringe. The syringe is then used to load the mechanized dispenser.

B3.2. Infrared camera, radiant panels, chilled plate and pipe

The radiant panels and the chilled plate are activated and the Macor tile is brought to thermal steady state. The infrared camera sensing enclosure is constantly monitored to insure that adequate cooling by liquid nitrogen is available (a liquid nitrogen charge lasts about 45 minutes). The chilled pipe is also activated and the infrared picture of the Macor surface is obtained. The infrared camera provides a two-dimensional picture where the vertical axis relates to a radiance reading while the horizontal axis is the actual position of the radiance reading on a line which can be arbitrarily set on the Macor surface. This line is carefully positioned through the center of the wetted area (i.e. the liquid-solid interfacial area).

B3.3. Temperature calibration

The radiant panels control set point is adjusted and adequate time is allowed for the system to reach thermal steady state. The infrared picture needs to be calibrated to relate the radiance readings to temperatures. The temperature scale is provided by the infrared camera manufacturer and is also calibrated independently by using a blackbody source. The temperature scale is referenced with one radiance/temperature point. This reference point is obtained by measuring the surface temperature with a hand held probe (OMEGA surface probe series 68000) until a constant reading is observed. By quickly removing the probe while recording the infrared picture of the probe location, one obtains an instantaneous

reading of the same location with the infrared camera and with the temperature probe. Note that the temperature at the probe location changes after the probe removal and that only the picture immediately after the probe removal provides the desired information. Since 30 frames per second are acquired with the VCR, there is no problem in selecting the appropriate frame.

B3.4. Droplet deposition

Prior to the droplet deposition, the surface is cleaned with alcohol and with de-ionized water. When the cleaning water is evaporated the droplet is deposited. The line on which the temperatures are scanned is adjusted to pass exactly through the center of the wetted region. This is a fine tuning adjustment since the mechanized dispenser places the droplet within fractions of a millimeter of the desired location. The evaporative process is then recorded and set aside for post-processing. Each experiment is repeated at least ten times to build sufficient confidence in its repeatability.

B3.5. Test record

A regular black and white camera is used to record (on the same VCR tape) the experimental conditions. In particular, droplet size, Macor surface temperature, chilled plate temperature and radiant panels temperatures are recorded. In addition, an infrared picture of a small coin placed on the Macor surface is also recorded to determine the length scale of the infrared image. All this information is recorded at the beginning and at the end

of a ten tests sequence (which relate to the same droplet size and initial temperature conditions).

B4. DATA PROCESSING

After a sequence of ten tests is completed, data processing is performed. The evaporation time τ for each experiment is measured from the VCR record. The size of the wetted region is identified and the droplet shape is inferred. Extensive visual observations and photographic records show that the droplet shape can be approximated by a segment of a sphere [6][9]. By inspecting the droplet shape and evaporation time information, one representative test is selected out of the ten tests sequence. The rationale for this selection is based on the following concepts:

a) The droplet evaporation time increases as solid-liquid interfacial area decreases. Since the droplet geometry is reasonably approximated by a segment of a sphere, a shape parameter, β [2][6][9], is defined as the radius of the wetted area over the radius of an equal volume droplet of spherical shape. An averaged and most repeatable shape parameter identifies the representative droplet.

b) In spite of the dispenser accuracy, some of the water will cling to the inside of the droplet dispenser. The longer a droplet takes to evaporate, the greater the likelihood that less water is left in the dispenser.

c) The droplet does not always fall in the same location. Sometimes the temperature

scanned line is not positioned exactly through the droplet center. Further, the wetted region shrinks during the evaporation and the center of the wetted region may drift from its initial position. If this occurs, the image may show complete evaporation when water is still present.

These three concepts are the guidelines for the selection of the most representative droplet. Usually there are four or five identical tests. In a few cases, a decision must be made based on item a) with some bias towards higher evaporation times to account for items b) and c).

Images from the record for the selected droplet are obtained at 10, 30, 50 and 100 per cent of the evaporation time and a few images are also analyzed to describe the surface temperature recovery after the evaporation. These images are digitized by a PC-based 641H x 201V frame grabber (by Computer Eyes which also provides the required software). The spatial resolution in the horizontal axis may vary depending on the camera field of view. Usually a pixel corresponds to 0.05 millimeters. The temperature scale is of about 100 °C and the typical thermographic trace is two pixels thick. Therefore, a resolution of 1-2 °C is achieved in the vertical axis (i.e. the temperature scale).

The digitized image is processed with a thresholding and subsequent erosion techniques which are described at length by Klassen [17]. In summary, the intensity of the thermographic traces is differentiated from unwanted noise by thresholding. This technique identifies as noise the pixels with intensities above a set value and retains the pixels with

intensity below this set threshold. In addition, thresholding binarizes the resulting image by assigning the maximum and minimum intensity value respectively to data pixels or "blank" pixels. Further elimination of noise is achieved by erosion which consists in a pixel-by-pixel inspection of the neighboring information to differentiate between isolated information (which is most likely noise) and clustered information (which is most likely useful data). These techniques are applied by trial and error and visual inspection of the images confirms their effectiveness.

The data points isolated by the image processing techniques are then compacted by folding the right side of the image (about the droplet center) onto the left side of the image. Since the temperature profile is symmetric about the droplet center, superimposing one half of the profile on the other half produces twice as many data points to be analyzed and allows a more accurate determination of the symmetry axis through the center of the wetted region. Figure 2 shows the typical transient data after processing. Note that in the figures prior to the complete evaporation ($t < \tau$), the temperature profiles are plotted for $r \geq R$. The radiance signal in the solid surface region covered by the droplet cannot be translated into a significant temperature reading since water is a radiation participating medium. The temperature distributions in the range $0.3\ \tau \leq t \leq 0.9\ \tau$ do not change appreciably and the surface temperature recovers its initial value for $t \geq 1.5\ \tau$.

B5. RESULTS AND DISCUSSION

B5.1. Phenomenology

To set the results and their discussion in the appropriate context it is necessary to briefly review the major differences in the thermal behavior between the case of radiant heat input (from above the surface) and the case of conductive heat input (from below the surface). It is important to note that, for the droplet sizes under investigation, the heat transfer mechanisms in the liquid are conduction and radiation. Convection does not play a significant role since Rayleigh-Benard instabilities require times longer than the evaporative time to develop and Marangoni surface tension driven flows generate very slow motion in these experimental conditions (Ostrach and Pradhan [18]).

In the case of radiant heat input, the initial vertical temperature gradient in the solid shows a higher temperature at the surface and a lower temperature at the chilled plate. The droplet tends to reduce the heat transfer in the vertical direction since it decreases the vertical temperature gradient. In the case of conductive heat input, the initial vertical temperature gradient is opposite since the temperature increases with depth. Droplet cooling increases the heat transfer in the vertical direction since it increases the vertical temperature gradient. This means that the portion of the solid under the droplet contributes greatly to the evaporation of a droplet in the conduction case while it has a lesser role in the radiation case. Note that for both cases the amount of heat required to

evaporate a given size droplet is the same.

The conductively heated surface is certainly supplying more energy to the droplet through conduction than the radiatively heated surface, yet Fig. 3 shows that the radiatively heated surface evaporation times are shorter. This is due to the heat directly supplied by radiation to the water. The radiant panels behave like blackbodies. Their typical surface temperature is in the 600-750 °C range. At these temperatures the maximum emission of the blackbody spectrum occurs in the 3-3.5 micron range (Siegel and Howell [19]). Water has its maximum absorption coefficient of 11,400 cm^{-1} at a wavelength of 3 microns and maintains an elevated value at all wavelengths in the near infrared above 2.6 microns (Siegel and Howell [19]). The absorption coefficient determines the exponential attenuation of the light intensity. By multiplying the absorption coefficient by the thickness of the water layer, one obtains a non-dimensional exponent which determines how much radiant energy is transmitted through the water. Figure 4 shows the percentage of incident radiation which is absorbed by water (10, 30 and 50 μl droplets) at various initial solid surface temperatures, corresponding to various radiant panels temperatures. The line in the figure is the linear regression of the data. The temperature distribution at the exposed solid surface is shown in Fig. 5 for both the radiation and the conduction case. The curves a) and b) represent respectively a radiation and a conduction case with the same initial surface temperature, while curve c) shows the temperature distribution for a radiation case in which the evaporation time is the same of the conduction case b). All curves are obtained for a 30 μl droplet. These three curves are for $t = 0.3\ \tau$ since thereafter the droplet shrinks in the radiation case and a graphical

representation of the temperature profiles would be quite intricate due to the time dependence of the normalizing parameter R.

A direct comparison of the radial heat flux is not possible due to the uncertainty associated with the data at the droplet edge (r = R). However it is apparent that the cooling effect is less pronounced for the radiation case since radiation contributes directly to the vaporization process thus reducing the conduction component.

B5.2. Shape parameter

Figure 6 shows the shape parameter, β, for various droplet sizes and initial solid surface temperatures. The shape parameter is defined as $\beta = R/R_s$; where R is the radius of the wetted region under the deposited droplet and R_s is the radius of a spherical droplet of the same volume. Note that an experimental measurement of β is possible only at the beginning of the evaporative transient, because it is not possible to obtain information about the droplet volume during the evaporation, thus R_s cannot be determined after the initial time t=0.

The droplet size is not significantly affecting β. This holds true for the conduction case. The scatter is overwhelming for temperatures above 155 °C. This temperature corresponds to the onset of nucleate boiling. For the conduction case, nucleate boiling is observed at 164 °C and above. Klassen [17] measured β values that ranged from 1.2 to 1.5. These

values are significantly lower than the values measured for the radiation case. Klassen also showed constant radii of the wetted region. Similar results were obtained by diMarzo [6] for a quartz surface. Both these results were obtained for the conduction case. It appears that, for the conduction case, increasing the solid surface temperature does not affect the water-vapor interfacial temperature. This is reasonable since the heat can only be conducted from the solid surface through the liquid layer.

For the radiation case, β average values range from 1.4 at an initial solid surface temperature of 90 °C to 2.5 at an initial solid surface temperature of 155 °C. This may be due to the direct radiation from above the droplet. The absorption coefficients are high for water in the spectra produced by the radiant panels. This results in substantial amounts of energy absorbed by the surface of the water, causing the droplet surface to heat up and therefore reducing its surface tension. This in turns may cause the droplet to spread out. The higher is the temperature of the heaters, the greater is the amount of heat absorbed by the droplets, which lowers the surface tension and contributes to a wider spreading of the droplet.

Figure 7 shows how the radius of the wetted region changes during the evaporation process for various initial solid surface temperatures. Note that the radius of the wetted region R is normalized with its value at deposition R_o. At higher initial surface temperatures (i.e. at the onset of boiling), a marked decrease in the radius of the wetted region is observed as the evaporation progresses. This shrinking of the wetted region occurs when the solid-liquid

contact angle has reached its receding value (Simon and Hsu [20]). This phenomenon is observed by Klassen [17] at the very end of the evaporative transient.

Although there are many differences between the solid thermal response for the conduction and radiation cases, there are also some similarities. Both cases show an onset of nucleate boiling when the initial surface temperature is in the 155-164 °C range. Both cases show that nucleate boiling drastically disrupts the droplet geometry with large variations of β.

B6. CONCLUSIONS

The experiments describe some aspects of the behavior of a low thermal conductivity material heated by radiation from above when a water droplet is placed on its surface. The results are different from analogous results obtained with the same material heated by conduction from below.

Water absorbs near infrared radiation. More than 95 per cent of the radiant heat supplied from the radiant panels is in the near infrared spectrum. It is estimated that 20 to 30 per cent of the heat of vaporization is supplied to the water droplet from direct absorption of the incident radiation. The remainder is from conduction across the liquid-solid interface.

The shape parameter increases as the surface temperature increases. A contributing factor is the effect of surface tension at different temperatures. For the conduction case, the constant value of β is an indicator that the temperature at the exposed water droplet surface is not affected by the initial solid surface temperature.

The evaporation times for the radiation case are shorter than for the conduction case. The water droplets on the radiatively heated surface are heated from both below and above. Further, the radiatively heated droplets spread across the surface more than in the conduction case thus providing a larger surface area to absorb heat from above and a thinner layer to transfer heat from below by conduction.

B7. NOMENCLATURE

r	radial coordinate on the solid surface
R	radius of the wetted region [f(t) in the radiation case]
R_0	radius of the wetted region at deposition
R_s	radius of a sphere with equal volume of the droplet at deposition
t	time
T_0	initial solid surface temperature
V	volume of the droplet at deposition
β	shape parameter: = R/R_s
τ	total evaporation time

B8. REFERENCES

1. S. Toda, A Study of Mist Cooling. 1st Report: Investigation of Mist Cooling, *Heat Transfer Japanese Research*, vol. 1, pp. 39-50, 1972.
2. C. Bonacina, S. Del Giudice and G. Comini, Dropwise Evaporation, *ASME Journal of Heat Transfer*, vol. 101, pp. 441-446, 1979.
3. J.J. Rizza, A Numerical Solution to Dropwise Evaporation, *Journal of Heat Transfer*, vol. 103, pp. 501-507, 1981.
4. M. Seki, H. Kawamura and K. Sanokawa, K., Transient Temperature Profile of a Hot Wall due to an Impinging Liquid Droplet, *Journal of Heat Transfer*, vol. 100, pp. 167-169, 1978.
5. S. Inada, Y. Miyasaka and K. Nishida, Transient Heat Transfer for a Water Drop Impinging on a Heated Surface, *Bulletin of JSME*, vol. 28, no. 245, pp. 2675-2681, 1985.
6. M. diMarzo and D.D. Evans, Dropwise Evaporative Cooling of High Thermal Conductivity Materials, *Heat and Technology*, vol. 5, no. 1-2, pp. 126-136, 1987.
7. M. diMarzo and D.D. Evans, Evaporation of a Water Droplet Deposited on a Hot High Thermal Conductivity Solid Surface, *ASME Journal of Heat Transfer*, vol.111, pp. 210-213, 1989.
8. W.M. Grissom and F.A. Wierum, Liquid Spray Cooling of a Heated Surface, *Int. J. Heat Mass Transfer*, vol. 24, pp. 261-271, 1981.

9. S.S. Sadhal and M.S. Plesset, Effect of Solid Properties and Contact Angle in Dropwise Condensation and Evaporation, *ASME Journal of Heat Transfer*, vol. 101, pp. 48-54, 1979.

10. C.O. Pedersen, An Experimental Study of the Behavior and Heat transfer Characteristics of Water Droplets Impinging upon a Heated Surface, *Int. J. Heat Mass transfer*, vol. 13, pp. 369-381, 1970.

11. K.J. Choi and S.C. Yao, Mechanism of Film Boiling Heat Transfer of Normally Impacting Spray, *Int. J. Heat Mass Transfer*, vol. 30, no. 2, pp. 311-318, 1987.

12. K. Makino and I. Michiyosi, Heat Transfer Characteristics of Evaporation of a Liquid Droplet on Heated Surfaces, *Int. J. Heat Mass Transfer*, vol. 21, pp. 605-613, 1978.

13. K. Makino and I. Michiyosi, Effects of Initial Size of Water Droplet on its' Evaporation on Heated Surfaces, *Int. J. Heat Mass Transfer*, vol. 22, pp. 979-981, 1979.

14. K. Makino and I. Michiyosi, The Behavior of a Water Droplet on Heated Surfaces, *Int. J. Heat Mass Transfer*, vol. 27, no. 5, pp. 781-791, 1984.

15. K. Makino and I. Michiyosi, Discussion of Transient Heat Transfer to a Water Droplet on Heated Surfaces Under Atmospheric Pressure, *Int. J. Heat Mass Transfer*, vol. 30, no. 9, pp. 1895-1905, 1987.

16. M. Abu-Zaid and A. Atreya, Effect of Water on Piloted Ignition of Cellulosic Materials, *National Institute of Standards and Technology Interagency Report*, NIST-GCR-89-561, 1989.

17. M. Klassen, M. diMarzo and J. Sirkis, Infrared Thermography of Dropwise

Evaporative Cooling, *ASME HTD*, vol. 141, pp. 117-121, 1990.

18. S. Ostrach and A. Pradhan, Surface-Tension Induced Convection at Reduced Gravity, *AIAA Journal*, vol. 16, no. 5, pp. 419-424, 1978.

19. Siegel, R., Howell, J.R., *Thermal Radiation Heat Transfer*, 2nd ed., Hemisphere Publishing Corporation, New York, 1981.

20. F.F. Simon and Y.Y. Hsu, Y.Y., Wetting Dynamics of Evaporating Drops on Various Surfaces, *NASA Technical Memorandum*, NASA TM X-67913, 1971

B9. FIGURES AND TABLE

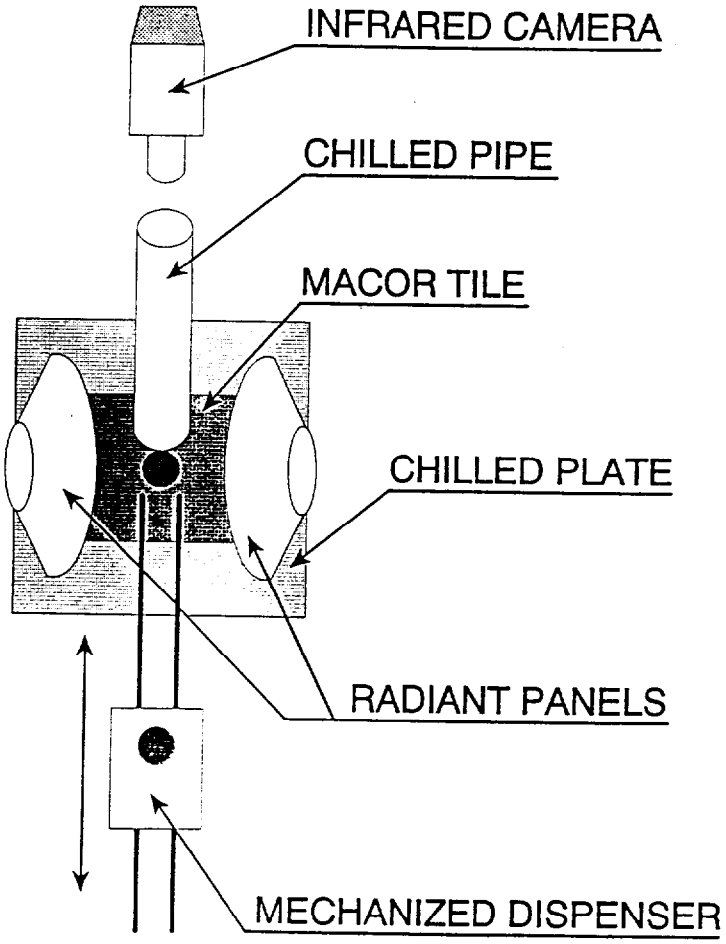

FIGURE 1 - Experimental apparatus (top view)

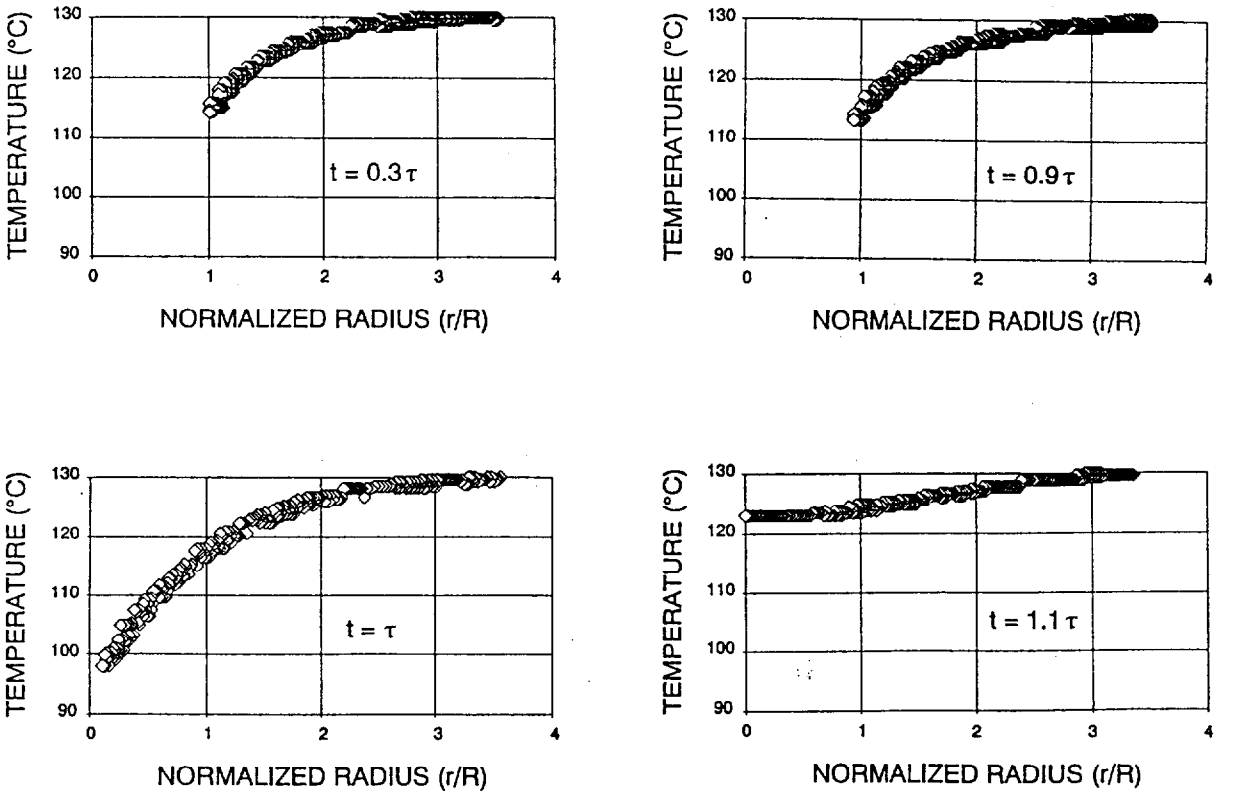

FIGURE 2 - Transient temperature distribution (T_0 = 130 °C; V = 30 μl; τ = 60 s)

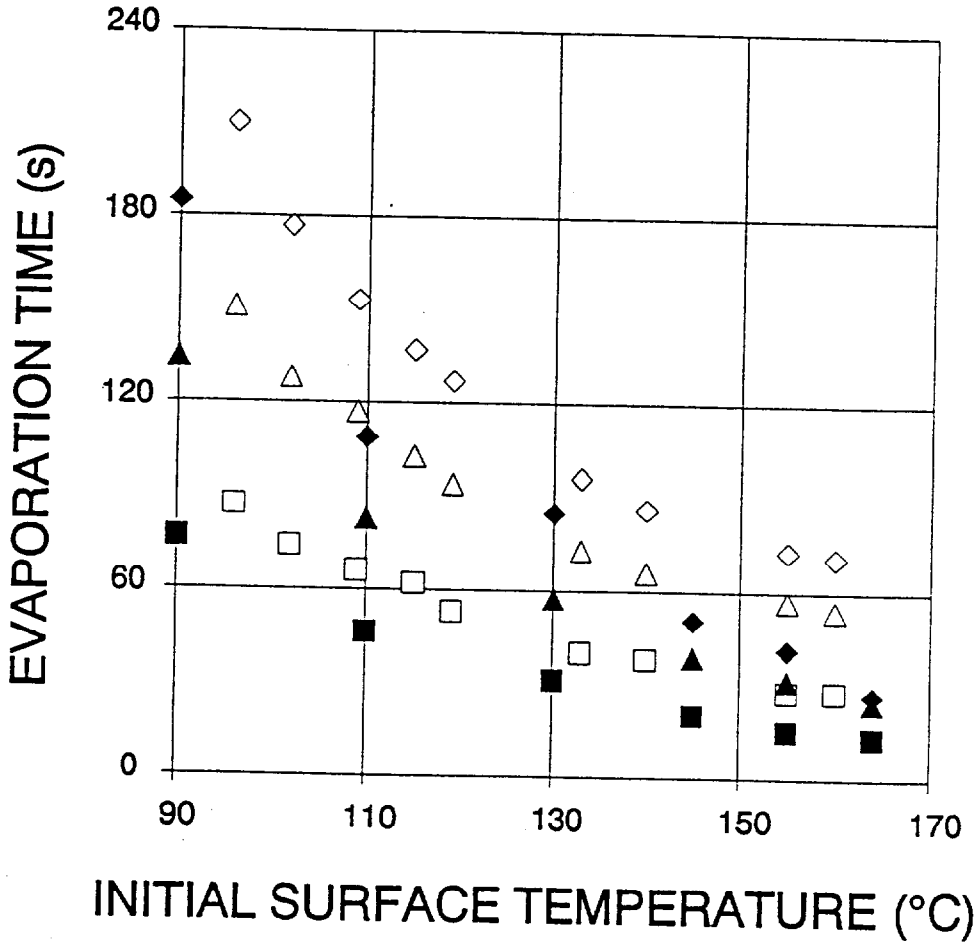

FIGURE 3 - Evaporation time (solid symbols for radiation case; open symbols for conduction case; ◇: V = 50 μl; △: V = 30 μl; □: V = 10 μl)

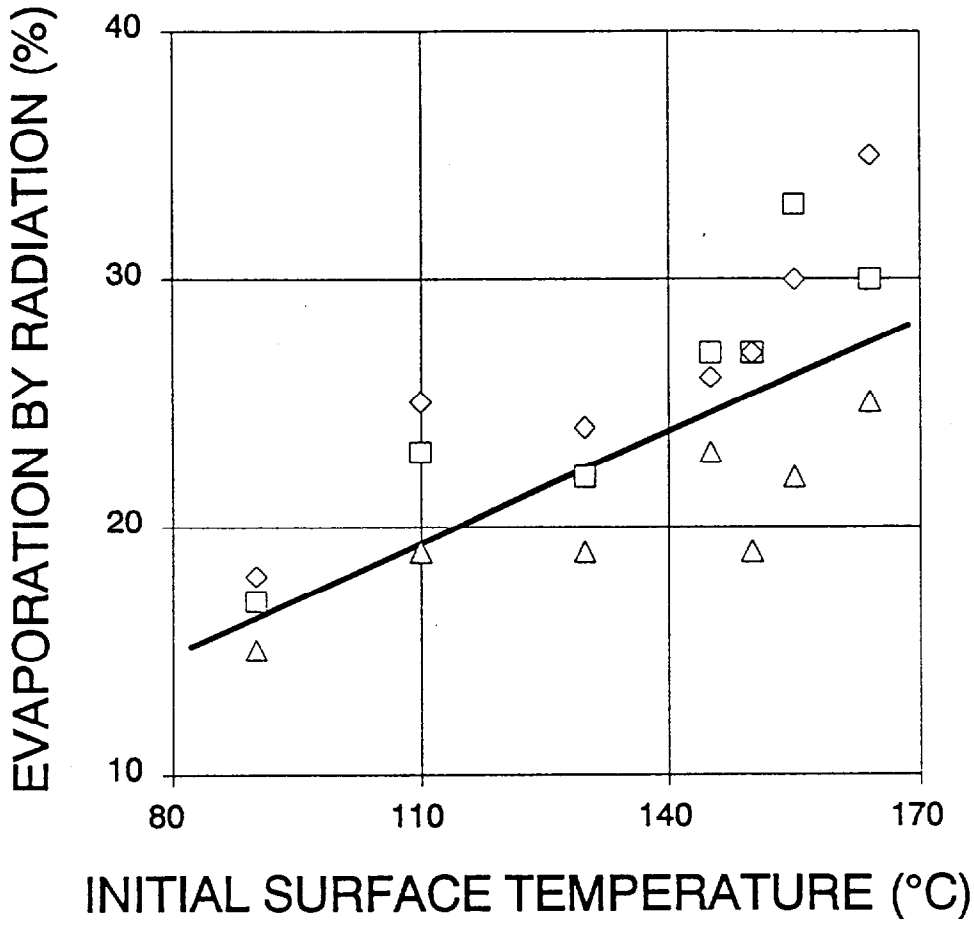

FIGURE 4 - Percentage of vaporization heat by direct radiation (▵: V = 50 μl; ◇: V = 30 μl; □: V = 10 μl)

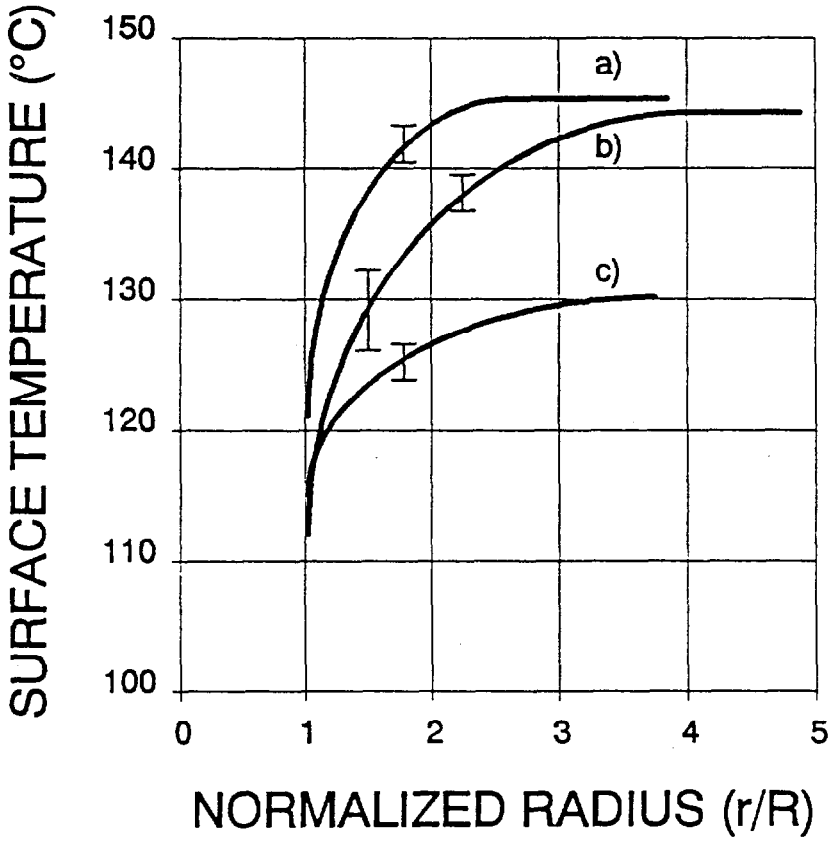

FIGURE 5 - Cooling effect: comparison between radiation and conduction (V= 30 μl; a: radiation T_0 = 145 °C; τ = 40 s ; b: conduction T_0 = 145 °C; τ = 60 s; c: radiation T_0 = 130 °C; τ = 60 s)

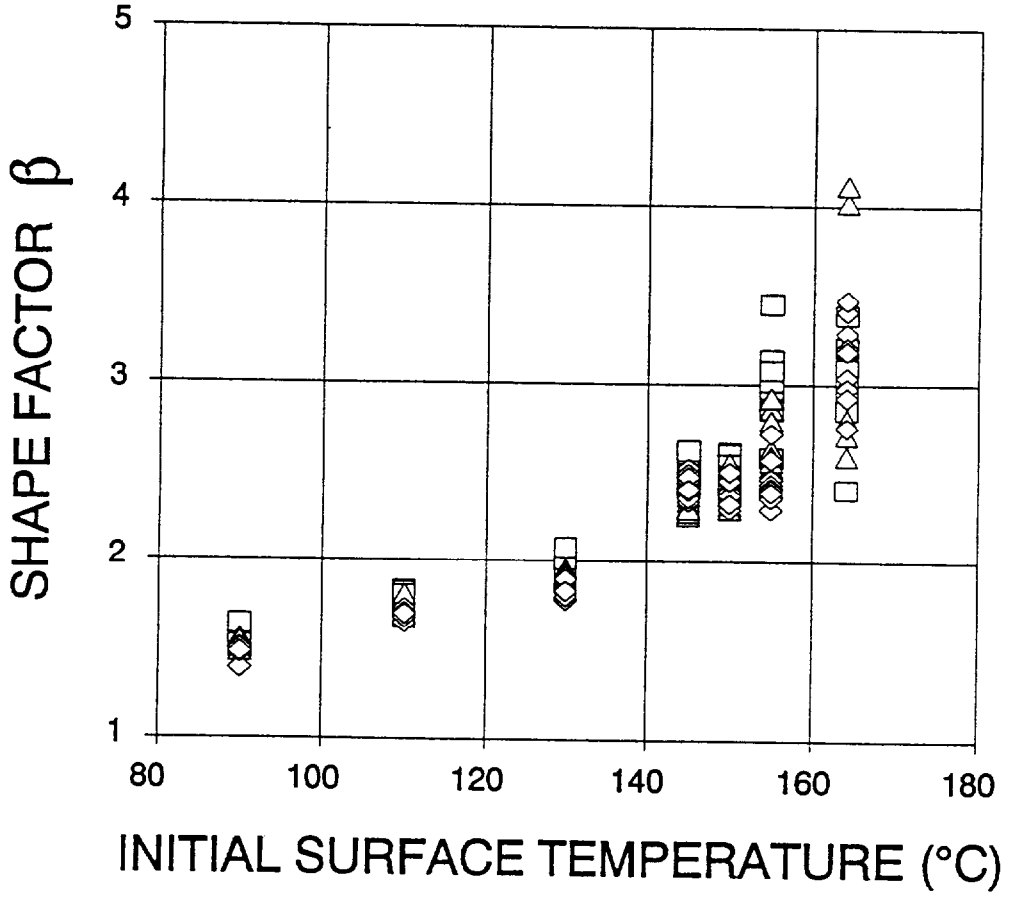

FIGURE 6 - Shape factor (◇: V = 50 μl; △: V = 30 μl; □: V = 10 μl)

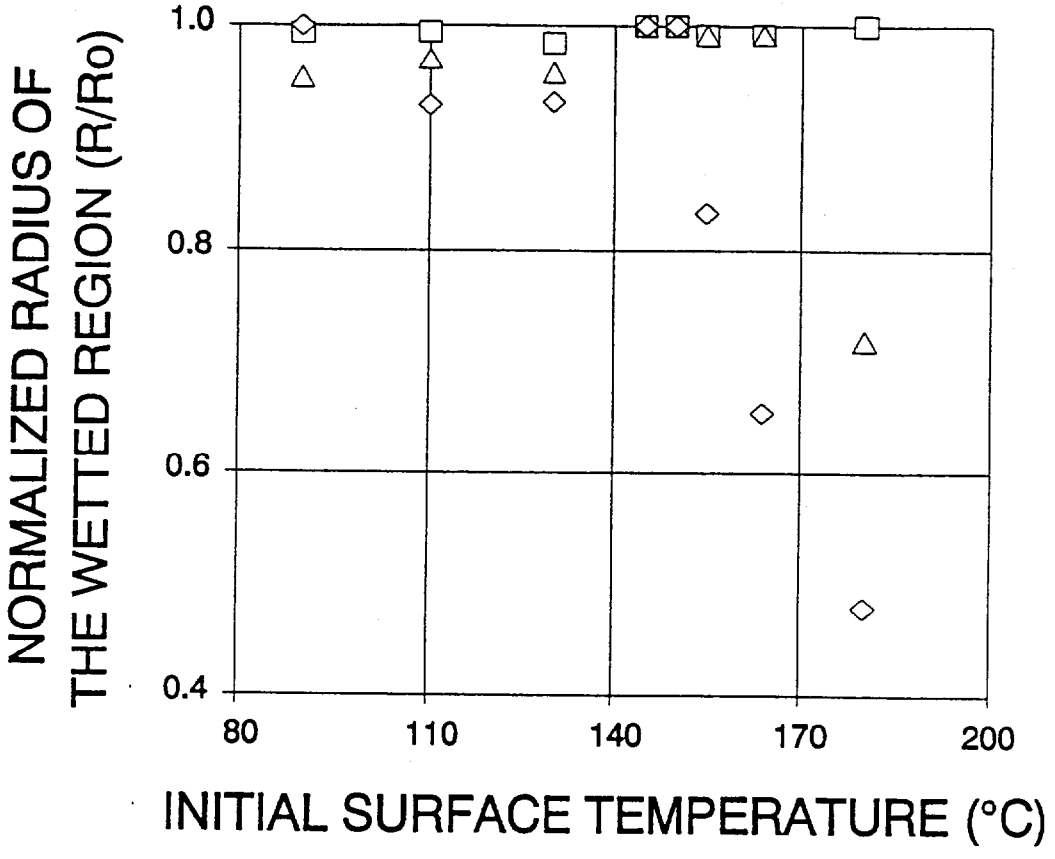

FIGURE 7 - Normalized radius of the wetted region (□: t = 0.3 τ; △: t = 0.6 τ; ◇: t = 0.9 τ)

TABLE 1 - MACOR PROPERTIES

Density:	2520	kg/m^3
Thermal Conductivity:	1.297	$W/(m \cdot K)$
Specific Heat:	888.9	$J/(kg \cdot K)$
Emissivity:	0.94	

B10. APPENDIX - DATA BASE

In the following pages, experimental data from all the tests conducted are presented.

INITIAL VOL. (µl)	*INIT. TEMP. MACOR (°C)*	*CHILL PLATE TEMP. (°C)*	*EVAPORATION TIME (s)*	*BETA (adim.)*
10	180	59	8.41	3.39
10	180	59	7.25	3.81
10	180	59	7.71	3.47
10	180	59	6.46	3.96
10	180	59	6.98	3.88
10	180	59	7.36	3.12
10	180	59	5.81	3.24
10	180	59	7.03	3.64
10	180	59	6.59	3.58
10	180	59	6.59	3.29
30	180	59	10.91	3.86
30	180	59	11.16	3.34
30	180	59	9.65	3.34
30	180	59	9.53	3.36
30	180	59	10.46	3.11
30	180	59	8.64	3.27
30	180	59	8.16	3.29
30	180	59	10.47	3.32
30	180	59	9.34	3.84
30	180	59	9.15	3.92
30	180	59	12.42	3.15
50	180	59	12.42	3.34
50	180	59	14.30	3.26
50	180	59	8.05	3.57
50	180	59	11.81	3.84
50	180	59	13.29	3.06
50	180	59	10.97	3.19
50	180	59	14.36	3.18
50	180	59	5.56	2.32
50	180	59	12.62	3.15

INITIAL VOL. (µl)	*INIT. TEMP. MACOR (°C)*	*CHILL PLATE TEMP. (°C)*	*EVAPORATION TIME (s)*	*BETA (adim.)*
10	164	37	11.90	3.06
10	164	37	13.59	2.98
10	164	37	15.30	2.94
10	164	37	11.84	3.21
10	164	37	12.86	3.39
10	164	37	15.53	2.88
10	164	37	5.79	2.41
10	164	37	13.00	2.86
10	164	37	13.90	3.04
10	164	37	13.09	3.09
30	164	37	24.72	2.60
30	164	37	17.84	4.02
30	164	37	15.22	4.12
30	164	37	23.79	3.03
30	164	37	23.98	3.03
30	164	37	30.99	2.72
30	164	37	16.59	3.23
30	164	37	27.03	2.81
30	164	37	29.55	2.72
50	164	37	22.15	2.98
50	164	37	29.84	3.04
50	164	37	32.00	3.29
50	164	37	29.98	3.41
50	164	37	20.28	2.98
50	164	37	33.09	2.76
50	164	37	28.73	3.21
50	164	37	22.34	3.47
50	164	37	20.36	3.19
50	164	37	25.47	2.93

INITIAL VOL. (µl)	*INIT. TEMP. MACOR (°C)*	*CHILL PLATE TEMP. (°C)*	*EVAPORATION TIME (s)*	*BETA (adim.)*
10	155	36	14.87	2.88
10	155	36	16.03	2.59
10	155	36	16.86	3.02
10	155	36	14.15	3.45
10	155	36	16.96	2.98
10	155	36	16.53	3.08
10	155	36	14.75	3.02
10	155	36	12.59	3.14
10	155	36	16.53	3.08
10	155	36	16.59	2.86
30	155	36	28.44	2.87
30	155	36	33.65	2.60
30	155	36	33.59	2.80
30	155	36	31.21	2.64
30	155	36	27.96	2.93
30	155	36	32.21	2.54
30	155	36	31.30	2.57
30	155	36	32.37	2.60
30	155	36	32.85	2.52
30	155	36	32.80	2.57
50	155	36	39.90	2.47
50	155	36	43.00	2.38
50	155	36	40.90	2.44
50	155	36	38.03	2.42
50	155	36	41.03	2.73
50	155	36	38.55	2.58
50	155	36	37.22	2.30
50	155	36	42.93	2.36
50	155	36	45.97	2.41
50	155	36	45.28	2.39

INITIAL VOL. (µl)	*INIT. TEMP. MACOR (°C)*	*CHILL PLATE TEMP. (°C)*	*EVAPORATION TIME (s)*	*BETA (adim.)*
10	150	35	16.46	2.55
10	150	35	20.15	2.60
10	150	35	14.97	2.43
10	150	35	14.70	2.46
10	150	35	19.58	2.55
10	150	35	17.42	2.62
10	150	35	14.05	2.61
10	150	35	17.89	2.55
10	150	35	18.25	2.44
10	150	35	16.28	2.49
30	150	35	32.90	2.45
30	150	35	32.44	2.32
30	150	35	29.85	2.54
30	150	35	28.46	2.56
30	150	35	33.46	2.40
30	150	35	35.42	2.38
30	150	35	28.47	2.50
30	150	35	34.53	2.30
30	150	35	31.40	2.41
30	150	35	32.24	2.42
50	150	35	38.74	2.47
50	150	35	39.36	2.40
50	150	35	42.53	2.34
50	150	35	38.36	2.51
50	150	35	37.30	2.32
50	150	35	39.22	2.38
50	150	35	33.85	2.46
50	150	35	38.66	2.51
50	150	35	39.09	2.30
50	150	35	36.41	2.33

INITIAL VOL. (µl)	*INIT. TEMP. MACOR (°C)*	*CHILL PLATE TEMP. (°C)*	*EVAPORATION TIME (s)*	*BETA (adim.)*
10	145	35	21.78	2.48
10	145	35	19.59	2.43
10	145	35	22.86	2.57
10	145	35	17.34	2.52
10	145	35	20.87	2.61
10	145	35	21.47	2.52
10	145	35	19.34	2.63
10	145	35	20.03	2.50
10	145	35	19.42	2.49
10	145	35	21.54	2.50
30	145	35	38.36	2.34
30	145	35	40.91	2.31
30	145	35	40.40	2.31
30	145	35	36.91	2.37
30	145	35	37.06	2.42
30	145	35	40.65	2.26
30	145	35	35.96	2.28
30	145	35	39.06	2.31
30	145	35	38.37	2.30
30	145	35	41.35	2.30
50	145	35	48.10	2.34
50	145	35	49.09	2.36
50	145	35	55.35	2.40
50	145	35	46.00	2.44
50	145	35	52.80	2.46
50	145	35	51.03	2.51
50	145	35	47.06	2.53
50	145	35	50.28	2.50
50	145	35	51.92	2.48
50	145	35	52.97	2.41

INITIAL VOL. (µl)	*INIT. TEMP. MACOR (°C)*	*CHILL PLATE TEMP. (°C)*	*EVAPORATION TIME (s)*	*BETA (adim.)*
10	130	34	30.40	1.96
10	130	34	31.81	1.93
10	130	34	32.00	2.01
10	130	34	32.15	2.05
10	130	34	30.59	1.93
10	130	34	33.15	1.91
10	130	34	29.71	1.89
10	130	34	29.30	1.93
10	130	34	31.12	2.01
10	130	34	31.90	2.08
30	130	34	55.46	1.96
30	130	34	59.71	1.94
30	130	34	59.96	1.93
30	130	34	54.40	1.88
30	130	34	55.87	1.84
30	130	34	57.21	1.90
30	130	34	54.03	1.94
30	130	34	58.90	1.93
30	130	34	58.96	1.90
30	130	34	59.15	1.93
50	130	34	87.00	1.79
50	130	34	83.71	1.78
50	130	34	86.21	1.82
50	130	34	84.04	1.84
50	130	34	81.53	1.91
50	130	34	84.43	1.83
50	130	34	84.53	1.84
50	130	34	85.97	1.90
50	130	34	84.31	1.80
50	130	34	85.35	1.83

INITIAL VOL. (µl)	*INIT. TEMP. MACOR (°C)*	*CHILL PLATE TEMP. (°C)*	*EVAPORATION TIME (s)*	*BETA (adim.)*
10	110	33	45.21	1.81
10	110	33	45.90	1.83
10	110	33	46.28	1.75
10	110	33	46.59	1.73
10	110	33	47.42	1.80
10	110	33	46.71	1.79
10	110	33	45.53	1.75
10	110	33	44.84	1.82
10	110	33	46.34	1.73
10	110	33	46.71	1.80
30	110	33	83.60	1.69
30	110	33	85.00	1.73
30	110	33	84.23	1.76
30	110	33	81.23	1.81
30	110	33	82.16	1.70
30	110	33	85.67	1.71
30	110	33	72.53	1.68
30	110	33	84.00	1.70
30	110	33	84.24	1.71
30	110	33	83.40	1.70
50	110	33	110.21	1.73
50	110	33	110.84	1.71
50	110	33	110.92	1.69
50	110	33	112.60	1.71
50	110	33	110.21	1.65
50	110	33	110.97	1.69
50	110	33	107.84	1.70
50	110	33	101.96	1.71
50	110	33	102.59	1.68
50	110	33	109.53	1.70

INITIAL VOL. (µl)	*INIT. TEMP. MACOR (°C)*	*CHILL PLATE TEMP. (°C)*	*EVAPORATION TIME (s)*	*BETA (adim.)*
10	90	30	75.66	1.63
10	90	30	75.40	1.62
10	90	30	76.30	1.62
10	90	30	76.30	1.58
10	90	30	77.23	1.60
10	90	30	79.21	1.61
10	90	30	78.46	1.58
10	90	30	76.68	1.55
10	90	30	74.75	1.63
10	90	30	74.71	1.64
30	90	30	134.15	1.52
30	90	30	136.34	1.51
30	90	30	135.84	1.50
30	90	30	137.40	1.53
30	90	30	137.34	1.50
30	90	30	135.24	1.48
30	90	30	133.03	1.56
30	90	30	133.62	1.52
30	90	30	130.54	1.54
30	90	30	132.37	1.51
50	90	30	193.03	1.39
50	90	30	194.05	1.48
50	90	30	187.17	1.50
50	90	30	174.42	1.49
50	90	30	187.96	1.39
50	90	30	188.53	1.48
50	90	30	180.46	1.51
50	90	30	184.40	1.50
50	90	30	182.35	1.47
50	90	30	179.00	1.48

EVAPORATION TIME AND SHAPE FACTOR OF THE DROPLETS WHICH HAVE BEEN SELECTED AS REPRESENTATIVE CASES

	Initial Temperature of the solid surface (°C)	*Evaporation Time (s)*	*Shape Factor β (adim.)*
50 microliters			
	180	14.4	3.18
	164	33.1	2.76
	155	45.3	2.39
	150	42.5	2.34
	145	52.8	2.46
	130	86.2	1.82
	110	110.8	1.71
	90	194.1	1.48
30 microliters			
	180	11.2	3.34
	164	31.0	2.72
	155	32.9	2.52
	150	35.4	2.38
	145	41.4	2.30
	130	58.9	1.93
	110	85.7	1.71
	90	137.4	1.53
10 microliters			
	180	8.4	3.39
	164	15.3	2.94
	155	16.5	3.08
	150	20.2	2.60
	145	22.9	2.57
	130	32.2	2.05
	110	47.4	1.80
	90	79.2	1.61

INITIAL TEMPERATURE OF THE SOLID SURFACE, OF THE CHILL PLATE AND OF THE HEATERS FOR EACH TEST SERIES

Initial Temperature of the solid surface (°C)	Chill Plate Temperature (°C)	Temperature of the Heaters (°C)
90	30	525
110	33	635
130	34	655
145	35	675
150	35	702
155	36	715
164	37	730
180	59	750

PERCENTAGE OF HEAT FLUX DIRECTLY ABSORBED BY THE DROPLET

10 microliters (vaporization heat = 22 joules)

HEATERS TEMP. (°C)	*SURF. TEMP. (°C)*	*INCIDENT FLUX (KW/M^2)*	*EVAP. TIME (s)*	*BETA*	*ABSORBED HEAT (J)*	*% OF H E A T ABS.*
750	180	11.1	8.4	3.39	5.1	23
730	164	10.2	15.3	2.94	6.5	30
715	155	9.6	16.5	3.08	7.2	33
702	150	9.1	20.2	2.60	6.0	27
675	145	8.2	22.9	2.57	5.9	27
655	130	7.5	32.2	2.05	4.8	22
635	110	6.9	47.4	1.80	5.0	23
525	90	4.1	79.2	1.61	3.8	17

30 microliters (vaporization heat = 67 joules)

HEATERS TEMP. (°C)	*SURF. TEMP. (°C)*	*INCIDENT FLUX (KW/M^2)*	*EVAP. TIME (s)*	*BETA*	*ABSORBED HEAT (J)*	*% OF H E A T ABS.*
750	180	11.1	11.2	3.34	13.8	21
730	164	10.2	31.0	2.72	23.4	35
715	155	9.6	32.9	2.52	20.0	30
702	150	9.1	35.4	2.38	18.2	27
675	145	8.2	41.4	2.30	17.6	26
655	130	7.5	58.9	1.93	16.1	24
635	110	6.9	85.7	1.71	16.8	25
525	90	4.1	137.4	1.53	12.3	18

50 microliters (vaporization heat = 112 joules)

HEATERS TEMP. (°C)	*SURF. TEMP. (°C)*	*INCIDENT FLUX (KW/M^2)*	*EVAP. TIME (s)*	*BETA*	*ABSORBED HEAT (J)*	*% OF HEAT ABS.*
750	180	11.1	14.4	3.18	16.1	14
730	164	10.2	33.1	2.76	28.0	25
715	155	9.6	45.3	2.39	24.8	22
702	150	9.1	42.5	2.34	21.1	19
675	145	8.2	52.8	2.46	25.7	23
655	130	7.5	86.2	1.82	21.0	19
635	110	6.9	110.8	1.71	21.7	19
525	90	4.1	194.1	1.48	16.3	15

ABSORPTION COEFFICIENT VALUES FOR WATER IN THE RANGE 1-10 MICRON
(Siegel et al. 1981)

Wavelength (micron)	Absorption Coefficient (cm^{-1})
1.0	3.63×10^{-1}
1.2	1.04
1.4	1.24×10^{1}
1.6	6.72
1.8	8.03
2.0	6.91×10^{1}
2.2	1.65×10^{1}
2.4	5.01×10^{1}
2.6	1.53×10^{2}
2.8	5.16×10^{3}
3.0	1.14×10^{4}
3.2	3.63×10^{3}
3.4	7.21×10^{2}
3.6	1.80×10^{2}
3.8	1.12×10^{2}
4.0	1.45×10^{2}
4.2	2.06×10^{2}
4.4	2.94×10^{2}
4.6	4.02×10^{2}
4.8	3.93×10^{2}
5.0	3.12×10^{2}
5.5	2.65×10^{2}
6.0	2.24×10^{3}
6.5	7.58×10^{2}
7.0	5.74×10^{2}
7.5	5.46×10^{2}
8.0	5.39×10^{2}
8.5	5.43×10^{2}
9.0	5.57×10^{2}
9.5	5.87×10^{2}
10.0	6.38×10^{2}

RADIATION ABSORPTION IN WATER

The water droplets absorb most of the radiation present on the surface of the water droplets. The following is a chart showing the percentage of radiation which is absorbed by water for various thicknesses and various spectrums produced by the heaters at different temperatures. These numbers were calculated by a simple computer program.

THICKNESS (mm)	*HEATERS TEMP. (°C)*	*RADIATION ABSORBED (%)*
1.0	750	97.4
1.0	725	97.7
1.0	700	98.0
1.0	675	98.2
1.0	650	98.4
1.0	625	98.7
1.0	600	98.8
0.5	750	94.8
0.5	725	95.3
0.5	700	95.8
0.5	675	96.3
0.5	650	96.7
0.5	625	97.1
0.5	600	97.4
0.1	750	82.0
0.1	725	83.0
0.1	700	84.0
0.1	675	85.0
0.1	650	86.0
0.1	625	86.9
0.1	600	87.8
0.01	750	41.3
0.01	725	41.7
0.01	700	42.1
0.01	675	42.5
0.01	650	42.9
0.01	625	43.2
0.01	600	43.5

PART C

MULTI-DROPLET MODEL

C1. INTRODUCTION

The spray cooling associated with the solid fuel fire extinguishment process is numerically simulated in this portion of the report. On the basis of the results provided by the single-droplet code, a data base is built to extend the analysis to a multi-droplet scenario. A closed form solution is developed to approximate the surface temperature at times and locations remote with respect to the point considered.

The surface temperature calculation in the multi-droplet model is performed by superimposing the appropriate elements selected from the data base. A detailed temperature distribution on the solid surface under the spray cooling is obtained.

A spatial average temperature of the solid surface is calculated and its significance is discussed in relation with the influence of dominating parameters such as droplets mass flow rate, impingement area and initial solid surface temperature.

C2. MULTI-DROPLET MODELING

In the study of spray cooling, a major objective is the determination of the average temperature of the solid surface as a function of time. Eventually, one would also need to know when a steady state temperature is reached for a given spray mass flow rate. Other information of interest concern the solid surface temperature distribution, the initial cooling effect of the impinging spray, etc.

In order to model a multi-droplet evaporative cooling transient, two basic steps have to be completed: the droplet distribution simulation and the temperature distribution calculation.

C2.1. Droplet distribution simulation

As well as for single droplet cooling, also for multi-droplet situations the solid surface starts from an initial condition of uniform temperature. During the cooling process, the droplets are randomly deposited (in terms of landing time and position) on the surface. In order to obtain a suitable droplet distribution pattern for later use in multi-droplet temperature calculations, a numerical model is created which simulates a random droplet distributer. The program is able to provide the information such as the deposition time and the location on the surface for all droplets.

The distributer moves with initial constant speed within the boundaries of a circle of fixed radius, hits the walls and bounces back on a new trajectory like in a "Pin-ball" game (see

Fig. C1). During this movement, it releases the droplets with constant frequency. The numerical simulation of this behavior can be described as follows. The droplet dispenser is represented by a moving point, whose initial position and initial velocity are assigned. It starts to move freely inside the circle and delivers a droplet at each given time interval. This behavior is simulated by recording the point location at the moment corresponding to the fall of each droplet. During each time period, the trace of the point is followed by tracking the position and velocity of the point in small time intervals. Periodically the point approaches the boundary. Assuming that all contacts are elastic, the rebounding angle and velocity can be computed by applying the principle that the impact angle is equal to the rebounding angle and that the velocity remains unchanged. It has to be pointed out that when the point passes through the center of the circle or very close to that region, it will keep rebounding within that area, since the impact and rebounding angles become very small. In order to avoid such repeating moves, one can force the point velocity vector to change its direction when it happens to pass through the center point of the circle or the nearby region. Further improvement can be obtained by assuming that the circle boundary wall rotates against its center point with a time dependent frequency, for example a sinusoidal function, so that the rebounding angle can be different from the impact angle. An additional feature is included in the model in order to avoid overlapping among the droplets which have been deposited on the same or very nearby location. This is due to the purpose of applying the results obtained from the single droplet model, as it will be discussed later. The program simply forces the distance between those droplets which are deposited within a given period to be no less than a twice the size of a single droplet

diameter.

A typical plot showing the random distribution of droplets on the surface which is obtained with this numerical simulation is displayed in Fig. C2.

C2.2. Temperature distribution calculation

The solid surface which is interested by the cooling effect of the spray evaporation is the same that is described for the single droplet cases, i.e., its initial temperature is constant and uniform, and its depth and width are big enough to be considered as infinite. The other major assumptions used in both single- and multi-droplet modeling are:

1) The wetted area between each liquid droplet and the solid surface is a circle and remains constant during the evaporation process.
2) At any moment, each droplet has a spherical segment shape.
3) Nucleate boiling is suppressed in the liquid-solid interface.
4) Conduction is the only effective heat transfer mode considered inside the liquid droplets.

Since the conduction is the dominant heat transfer mode, the governing equation for this multi-droplet cooling can be written, for both the droplets and the solid, as:

$$\frac{\partial T}{\partial t} = \alpha \nabla^2 T \qquad \text{(C1)}$$

Similarly to the single droplet model, the initial conditions can be expressed as:

$$T = T_0 \qquad at \quad t = 0 \qquad \text{(C2)}$$

For each droplet, the corresponding initial surface temperature is different because of the

different time and location of impingement. This condition can be written as:

$$T = T_{i_{s0}} \qquad at\ location\ i\ ; \quad t = t_i\ ; \quad i = 1, ND \qquad (C3)$$

This condition is used during the entire multi-droplet evaporation modeling, as discussed in detail in later sections. The assumption that the surface temperature T_{is0} in each droplet region at the initial moment is uniform and equal to the temperature at the center point of the wetted area is implicitly used. This assumption is reasonable if the wetted area under each droplet is small, as well as the temperature gradient in this region. From the surface temperature profiles in the single droplet model, it can be seen that the large temperature gradients on the solid surface occur near the droplet edge.

In analogy with the single droplet case, the boundary conditions are assigned as:

$$\frac{\partial T}{\partial r} = 0 \qquad when \quad r \to \infty \qquad (C4)$$

$$\frac{\partial T}{\partial z} = 0 \qquad when \quad z \to -\infty \qquad (C5)$$

$$k_s\left(\frac{\partial T}{\partial z}\right)_s = k_l\left(\frac{\partial T}{\partial z}\right)_l \qquad at \quad z = 0 \quad droplets\ locations \qquad (C6)$$

$$-k_s\frac{\partial T}{\partial z} = h(T - T_a) \qquad at \quad z = 0 \quad elsewhere \qquad (C7)$$

In general, the temperature difference used here is defined as:

where T_{s0} is the initial solid surface temperature. By using Eq. (C8), the governing equation

$$U = T - T_{s0} \tag{C8}$$

and the initial and boundary conditions become:

$$\frac{\partial U}{\partial t} = \alpha \nabla^2 U \tag{C9}$$

$$U = 0 \qquad at \quad t = 0 \tag{C10}$$

$$\frac{\partial U}{\partial r} = 0 \qquad when \quad r \to \infty \tag{C11}$$

$$\frac{\partial U}{\partial z} = 0 \qquad when \quad z \to -\infty \tag{C12}$$

$$k_s \left(\frac{\partial U}{\partial z}\right)_s = k_l \left(\frac{\partial U}{\partial z}\right)_l \quad at \quad z = 0, \quad droplets\ locations \tag{C13}$$

$$-k_s \frac{\partial U}{\partial z} = hU \quad at\ z=0 \quad elsewhere \tag{C14}$$

The governing equation and the associated conditions can be solved for the droplets and the solid surface temperature by using the Boundary Element Method (BEM) and the Control Volume Method (CVM) as discussed in the single droplet modeling presented in Part A and more extensively in a previous report (Tartarini et al., 1990). Unlike the single droplet calculation, this three dimensional conduction problem can not be reduced to a two dimensional case by applying the symmetry for both the droplet and the solid surface. For thousands droplets on the relatively large solid surface, the calculation procedure would be

huge in terms of computer memory and CPU.

The governing conduction equation (C1) applied to a multi-droplet scenario constitutes a linear system; therefore, superposition can be used for this multi-droplet modeling.

Assume U_i is the temperature difference for a single droplet $_i$ deposited on a solid surface at uniform initial surface temperature T_{is0} at the time t_i:

$$U_i = T_i - T_{i_{s0}} \tag{C15}$$

The governing equation for the solid in single droplet model is written as:

$$\frac{\partial U_i}{\partial t} = \alpha \nabla^2 U_i \tag{C16}$$

and the associated boundary conditions are:

$$\frac{\partial U_i}{\partial r} = 0 \qquad when \quad r \to \infty \tag{C17}$$

$$\frac{\partial U_i}{\partial z} = 0 \qquad when \quad z \to \infty \tag{C18}$$

$$k_s \frac{\partial U_i}{\partial z} = k_l \frac{\partial U_i}{\partial z} \qquad at \quad z = 0 \tag{C19}$$

$$\frac{\partial U_i}{\partial z} = h U_i \qquad elsewhere \tag{C20}$$

The initial condition is:

$$U_i = 0 \qquad at \quad t = t_i, \quad i = 1, ND \tag{C21}$$

Now one can assume:

$$U = \sum_{i=1}^{ND} U_i \tag{C22}$$

Thus, the governing equation becomes:

$$\frac{\partial U}{\partial t} = \alpha \nabla^2 U \tag{C23}$$

and the boundary conditions are:

$$\frac{\partial U}{\partial r} = 0 \qquad when \quad r \to \infty \tag{C24}$$

$$\frac{\partial U}{\partial z} = 0 \qquad when \quad z \to -\infty \tag{C25}$$

$$k_s \left(\frac{\partial U}{\partial z}\right)_s = k_l \left(\frac{\partial U}{\partial z}\right)_l \qquad at \quad droplets \quad locations \tag{C26}$$

$$\frac{\partial U}{\partial z} = hU \qquad elsewhere \tag{C27}$$

The initial condition is:

$$U = 0 \qquad at \quad t = 0 \tag{C28}$$

These equations coincide with those which have been written for the multi-droplet model.

Therefore U, as it is defined in Eq. (C29), is indeed the solution for the multi-droplet cooling on the solid surface:

$$U = T - T_{s0} = \sum U_i = \sum (T_i - T_{i_{s0}}) \qquad (C29)$$

or, in more general form:

$$T = T_{s0} + \sum_{i=1}^{ND} (T_i - T_{i_{s0}}) \qquad (C30)$$

It can also be shown that the heat flux for the multi-droplet model can be calculated by superposition due to the linear relation between the temperature and the heat flux.

There are different approaches for solving the multi-droplet problem by applying the superposition technique. However, since the studies presented in this section of this report are still in progress, only a summary of the procedures utilized until now is contained here.

The single-droplet code has been used to calculate transient temperatures and heat fluxes. A data base has been built with the results from the single-droplet code. Then, in order to avoid the huge computational expenses connected with the run of the single-droplet code for thousands of droplets, proper values for the temperatures at various time step and location have been selected from the data base.

In order to complete the data base, one has to calculate the temperature difference T-T_{s0} for those locations and times which are not contained in the part of the data base originated

by the single-droplet code. This is obtained by means of closed form solutions which had to be created for this specific purpose. For the present purposes, it is only necessary to have the final expressions of those solutions, which are based on the following expression for the temperature difference for a semi-infinite solid surface:

$$T - T_{s0} = \Delta T = -\frac{V_d \frac{\rho_l}{\rho_s} \frac{\Lambda}{C_{ps}}}{4\,(\pi \alpha_s t)^{3/2}} \exp\left(-\frac{r^2}{4\alpha_s t}\right) \qquad \text{(C31)}$$

The first solution is the recovery function, which yields the temperature difference T-T_{s0} for the far-field region after the complete evaporation of the first droplets. This function is obtained by substituting a modified time t-τ into Eq. (C31). The resulting expression is:

$$T - T_{s0} = -\frac{V_d \frac{\rho_l}{\rho_s} \frac{\Lambda}{C_{ps}}}{4\,(\pi \alpha_s (t-\tau))^{3/2}} \exp\left(-\frac{r^2}{4\alpha_s (t-\tau)}\right) \qquad \text{(C32)}$$

The second solution is the evaporation function, which yields the temperature difference in the far-field during the evaporation process. It is obtained as a modification of the recovery solution. By using a small value of time δt, Eq. (C31) can be written as follows:

$$T - T_{s0} = -\frac{V_d \frac{\rho_l}{\rho_s} \frac{\Lambda}{C_{ps}}}{4\,(\pi \alpha_s \delta t)^{3/2}} \exp\left(-\frac{r^2}{4\alpha_s \delta t}\right) \cos\left(\frac{\pi}{2}\left(1 - \frac{t}{\tau}\right)\right) \qquad \text{(C33)}$$

where the factor

$$\cos\left(\frac{\pi}{2}\left(1 - \frac{t}{\tau}\right)\right)$$

is 0 at $t=0$ and 1 at $t=\tau$.

Figure C3 shows a comparison between the calculated temperature and the closed form solutions.

The full data base consists of results from the single-droplet model and calculations performed with the closed form solutions mentioned above. At this point, the data base can provide all the required information for applying the superposition criterion to the multi-droplet modeling. The major advantage related to the use of this data base is the saving of computational time. Since all the single-droplet calculations are performed at a preliminary stage, the execution of the multi-droplet program is very rapid. On the other hand, this results in the need of a very large computer storage where the data base has to be contained.

The multi-droplet program, which has been created on the basis of the concepts above summarized, is listed in the section C6. The latest version of the single-droplet code is also included.

C3. RESULTS

The main objective of the multi-droplet model is to calculate the temperature distribution of the solid surface as a function of time during a spray evaporative cooling. As described in the previous section, the temperature at any point of the solid surface can be obtained by superimposing the results from many runs of the single-droplet code.

Given an initial solid surface temperature and a pre-determined droplet distribution pattern, the detailed temperature distribution at any selected time can be obtained. Figures C4, C5 and C6 show some typical three dimensional temperature plots for a portion of the solid surface at different times.

During the first seconds of the transient, the region influenced by the cooling effect of a single droplet is easily individuated and, at a sufficient distance from the droplet, the solid temperature remains constant and uniform. Consequently, the temperature drop is very sharp in the areas where a droplet is evaporating. After few seconds, more droplets are deposited on the solid surface, and the temperature at any point becomes a combination of the cooling effect generated by all the droplets together. At this point, the single droplets influence cannot be individuated as easily as before. After a longer time, the plot shows an overall temperature drop and the solid surface temperature is everywhere below its initial value.

Obviously, the lowest solid temperature at any time is always higher than the initial temperature of the liquid droplets (20°C).

The most useful parameter to describe the temperature distribution for multi-droplet cooling is the spatial average temperature of the considered portion of the solid surface. It is defined as follows:

$$T_{avg} = \frac{\int\int T\,dx\,dy}{\int\int dx\,dy} = \frac{\sum_{i=1}^{N_{pi}} \sum_{j=1}^{N_{pj}} T_{ij}\,\Delta x_i \Delta y_j}{\sum_{i=1}^{N_{pi}} \sum_{j=1}^{N_{pj}} \Delta x_i \Delta y_j} \qquad (C34)$$

Further simplification can be obtained if the same distance is imposed between the grid points in both directions of the mesh. Then the spatial average temperature is interpreted as the temperature summation for all the considered points on the surface divided by the total number of grid points:

$$T_{avg} = \frac{\sum_{k=1}^{N_p} T_k}{N_p} \qquad (C35)$$

Figure C7 shows an average temperature curve versus time. In this plot, the average temperature is calculated at every second. Fluctuations of the average temperature are observed.

Since the droplets distribution is irregular in time and space, the cooling effect around a single point cannot be monotonic. This explains the oscillatory behavior of the average temperature curve, that could be smooth only if the droplets distribution were uniform both

in time and in space.

The governing parameters for the multi-droplet cooling include the initial solid surface temperature, the physical properties of the solid surface and the mass flow rate of the droplets. In this study, only Macor is considered, but other materials characteristics are already implemented in the code for future tests. The initial solid surface temperature is always less than 160°C to prevent boiling, as described in the previous sections, i.e. Part A and B. The mass flow rate is added to the cooling parameters which refer to the properties of the solid. Without losing generality, one can assume that all the droplets have the same initial volume V_0. Under this assumption, the definition of the mass flow rate can be written as:

$$\dot{m} = \frac{\rho f V_0}{A} \qquad (C36)$$

where f is the droplets depositing frequency, and A is the area over which the averaging process is performed. In this definition, the liquid density and the droplet initial volume are assumed to be constant values, so that the effective variables for the mass flow rate are the frequency and the area.

Figures C8 to C10 show some different average temperature curves for a common initial solid temperature of 160°C, a constant total area, A1 = 0.0314 m^2, and different frequencies of 1, 2, and 5 droplets per second respectively. Figures C11 to C13 show other average temperature curves for A2 = 2 A1, and a frequency of 2, 4, and 10 droplets per second

respectively. Figures C14 to C16 display the curves for A3 = 4 A1 and frequencies of 4, 8 and 20 droplets/s. The higher is the frequency, the lower is the average temperature. If one defines the droplet distribution density is:

$$d = \frac{f}{A} \tag{C37}$$

then the mass flow rate can be expressed as:

$$\dot{m} = \rho V_0 d \tag{C38}$$

Figure C17 illustrates some different average temperature curves versus the number of droplets. For this plot, the droplet distribution density, as well as the mass flow rate, is constant. The mass flow rate appears to be a dominant factor, since all the average temperature plots show the same trend for the same value of the mass flow rate.

All the average temperature plots indicate that the average temperature tends to reach constant values, i.e. a steady state average temperature. The existence of the steady state average temperature can be demonstrated by applying an energy balance to a control volume of the solid surface of concern. From the first law of thermodynamics, the energy balance is expressed as:

$$\frac{\partial Q}{\partial t} = \dot{Q}_{in} - \dot{Q}_{out} \tag{C39}$$

where Q is the total heat stored in the control volume, which can be written as:

$$Q = \int_{V_c} \rho c_p T \, dV \tag{C40}$$

By selecting very small and constant thickness dz for the control volume, being $dV = dz\,dA$, the expression for the total heat becomes:

$$Q = \rho c_p dz \int_{A_c} T\,dA \qquad \text{(C41)}$$

Recalling the definition of the average temperature, the total heat Q can be further expressed as:

$$Q = (\rho c_p dz A_c)\ T_{avg} \qquad \text{(C42)}$$

so that the energy balance equation (C46) becomes:

$$(\rho c_p dz A)\ \frac{\partial T_{avg}}{\partial t} = \dot{Q}_{in} - \dot{Q}_{out} \qquad \text{(C43)}$$

When the outgoing heat flux due to the evaporation is equal to the incoming heat flux supplied from the rest of the semi-infinite solid, the right hand side of the above equation becomes zero, and one has:

$$\frac{\partial T_{avg}}{\partial t} = 0 \qquad \text{(C44)}$$

Then a steady state average temperature is reached.

Figures C18 to C20 show some average temperature curves for the same mass flow rate at different initial solid temperatures. They all show a quick temperature decrease in initial portion of the transient. This can be explained if one remembers that the evaporation time for Macor under these initial conditions is in the range between 25 and 100 seconds; therefore, during this initial period the solid surface is consistently cooled by the evaporating

droplets, and the average temperature continuously decreases. After this, some of the droplets are completely evaporated and the recovery process starts in those area previously covered by the water, thus the temperature increases again locally. Since there are always some evaporating droplets and recovery areas in the same region, the combined process results in a relatively smooth and slow variation in the average temperature. The steady state average temperature is approached as time tends to infinity.

C4. CONCLUSIONS

A multi-droplet model has been developed to obtain the transient temperature distribution on a hot solid surface subjected to evaporative cooling. The numerical simulation can be applied to a broad range of solid materials, from low thermal conductivity materials like Macor to high thermal conductivity materials like aluminum.

The single-droplet model, which has been previously validated, provides numerical predictions of the evaporation time. It also provides temperature distribution, as well as heat flux, inside the droplets and along the solid surface. These results are used to generate the data based used by the multi-droplet program.

By applying the characteristic of linearity of the conduction equation and assuming homogeneous boundary conditions along the exposed solid surface, the superposition technique is used for the multi-droplet simulation. Given a pre-determined droplet distribution pattern on the solid surface, the temperature distribution is obtained by superposition of results from the single-droplet model with different initial and boundary conditions. The summation of these contributions provides the detailed temperature distributions as a function of time during the multi-droplet evaporative cooling.

A spatial average temperature is used to summarize the cooling effect for the solid surface. The influence of the spray mass flow rate and the initial solid temperature is studied and

it is observed that the mass flow rate is a dominating factor in the multi-droplet evaporation process. A steady state value of the spatial average temperature is also calculated.

C5. FIGURES

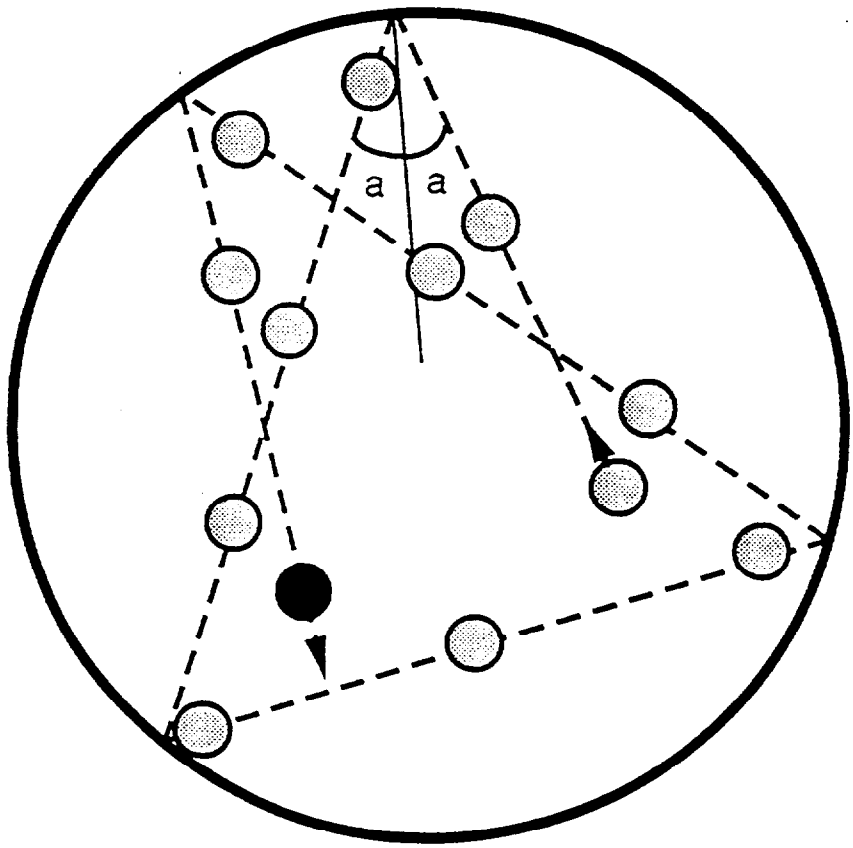

Fig. C1 Droplet distribution simulation; a = angle of impact = angle of reflection

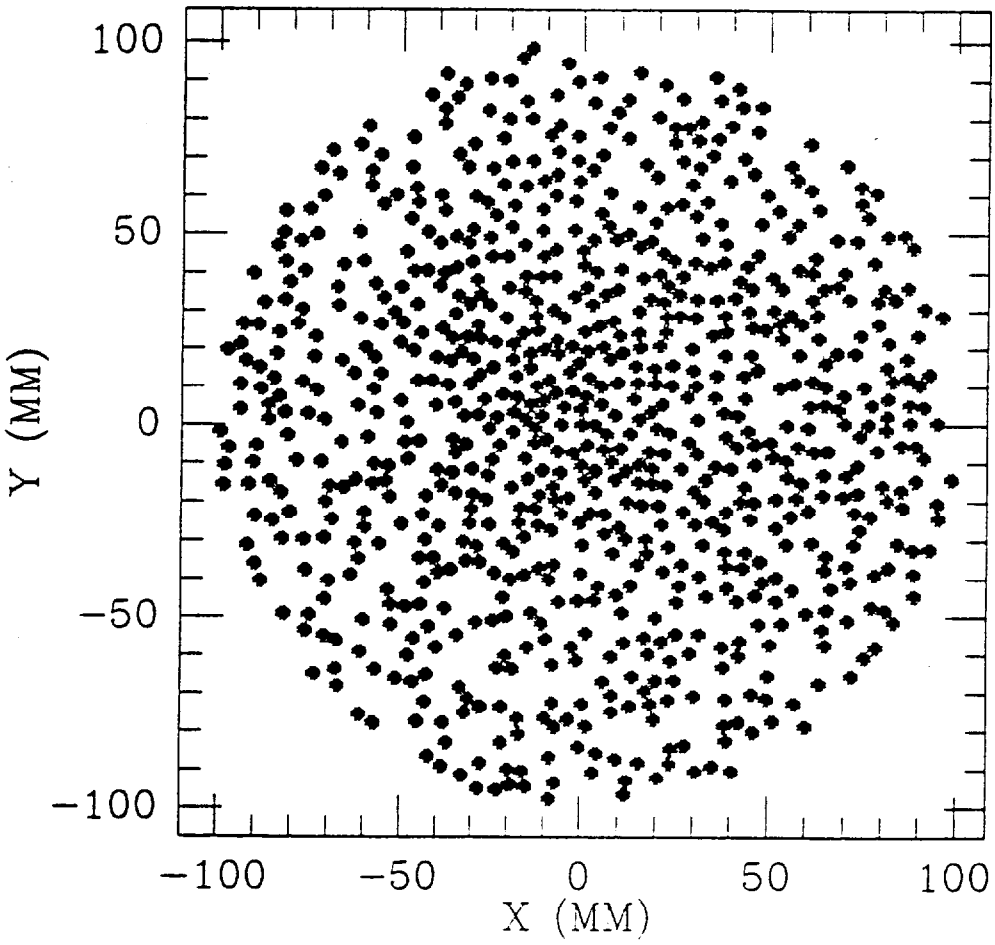

Fig. C2 Typical distribution of droplets on the surface

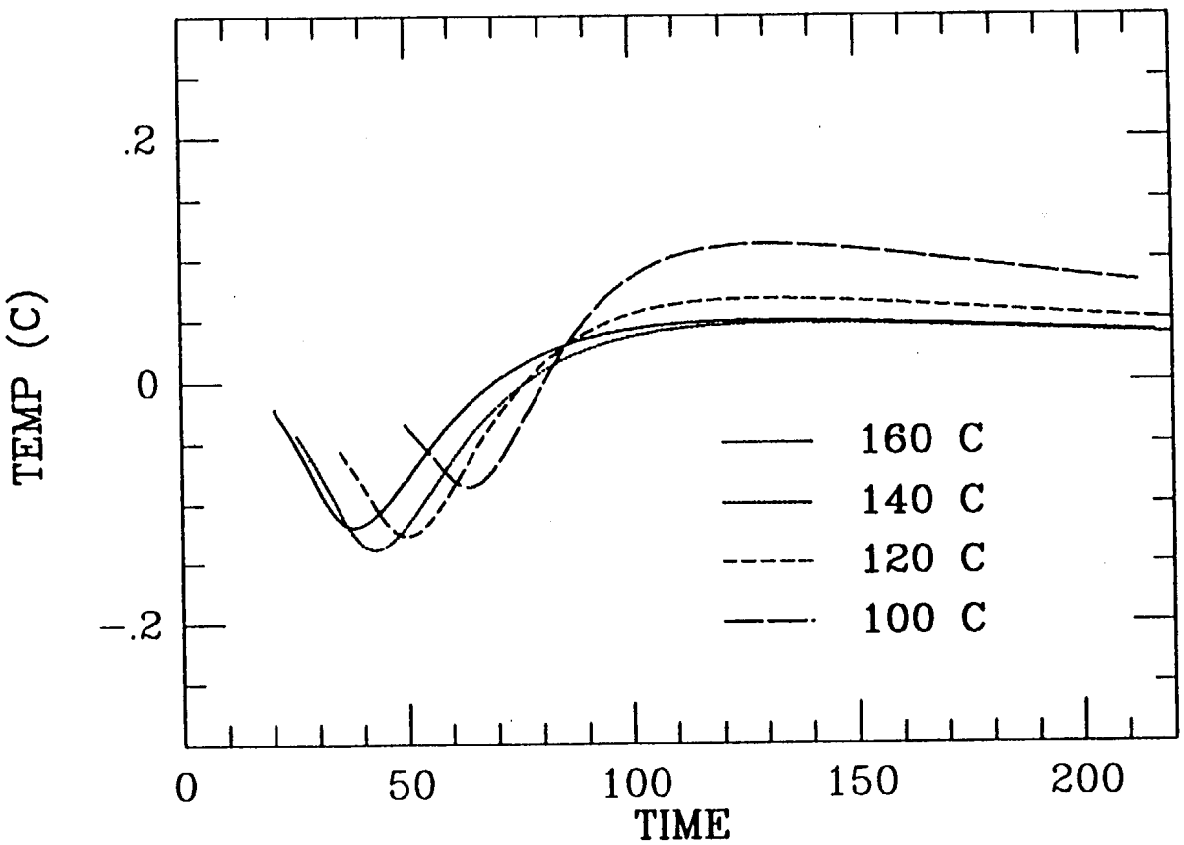

Fig. C3

TEMP DIFFERENCE (CODE – FUNCTIONS)
FOR FAR FIELD POINT (MACOR: V0=5, BETA=1.4)

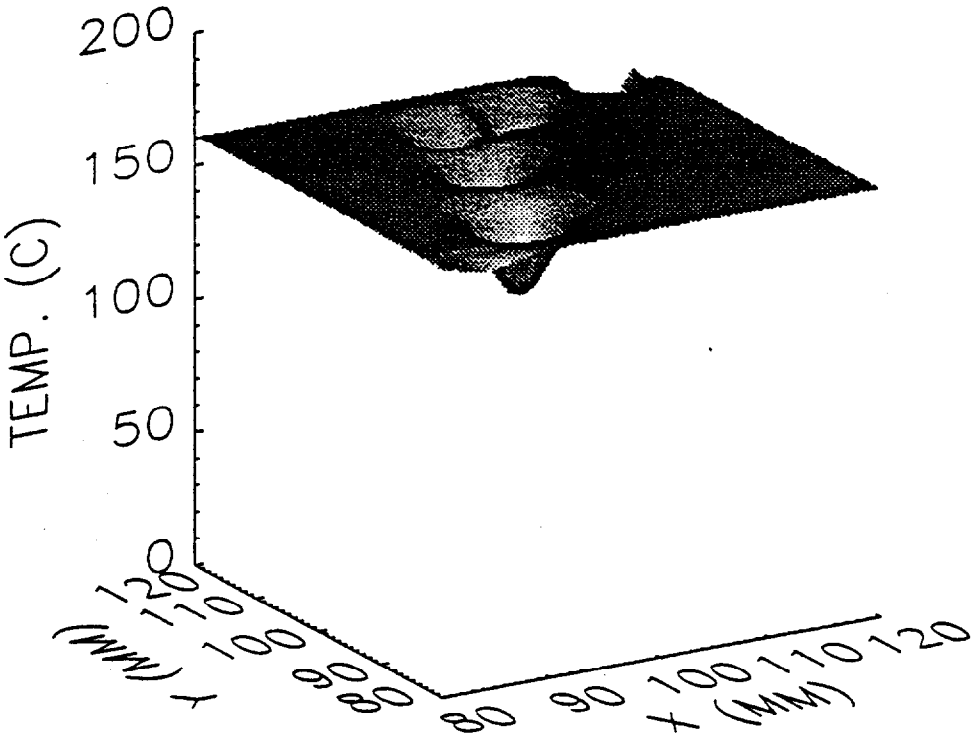

Fig. C4 Temperature distribution on the solid surface; t = 10 s, f = 2 droplets/s, V_0 = 5 μl

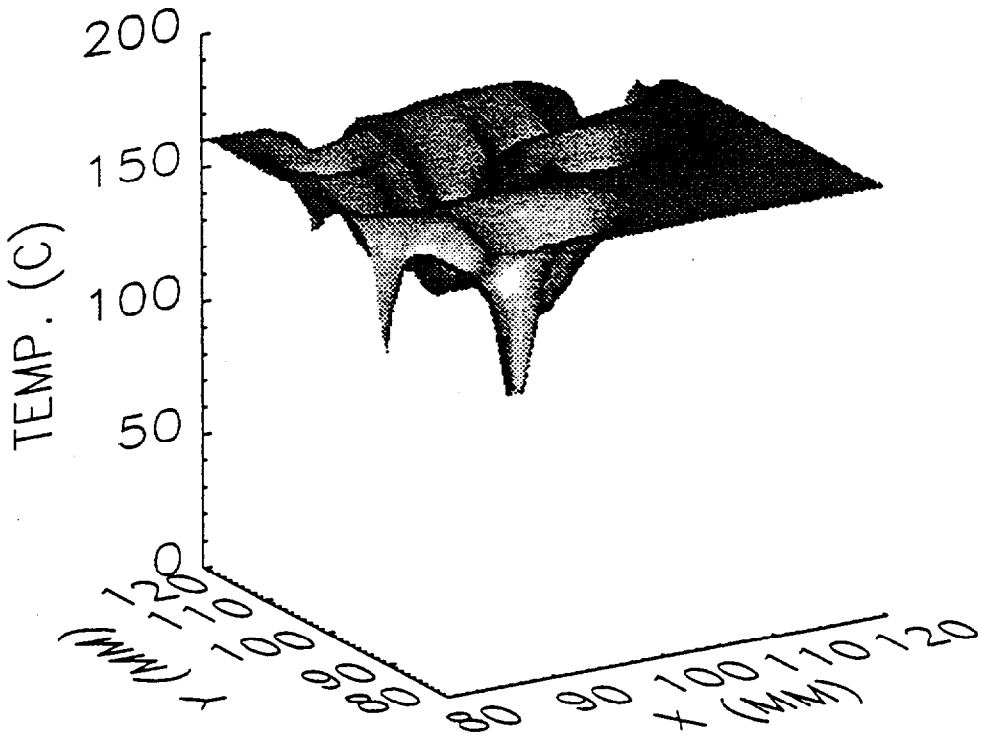

Fig. C5 Temperature distribution on the solid surface; t = 10 s, f = 10 droplets/s, V_0 = 5 μl

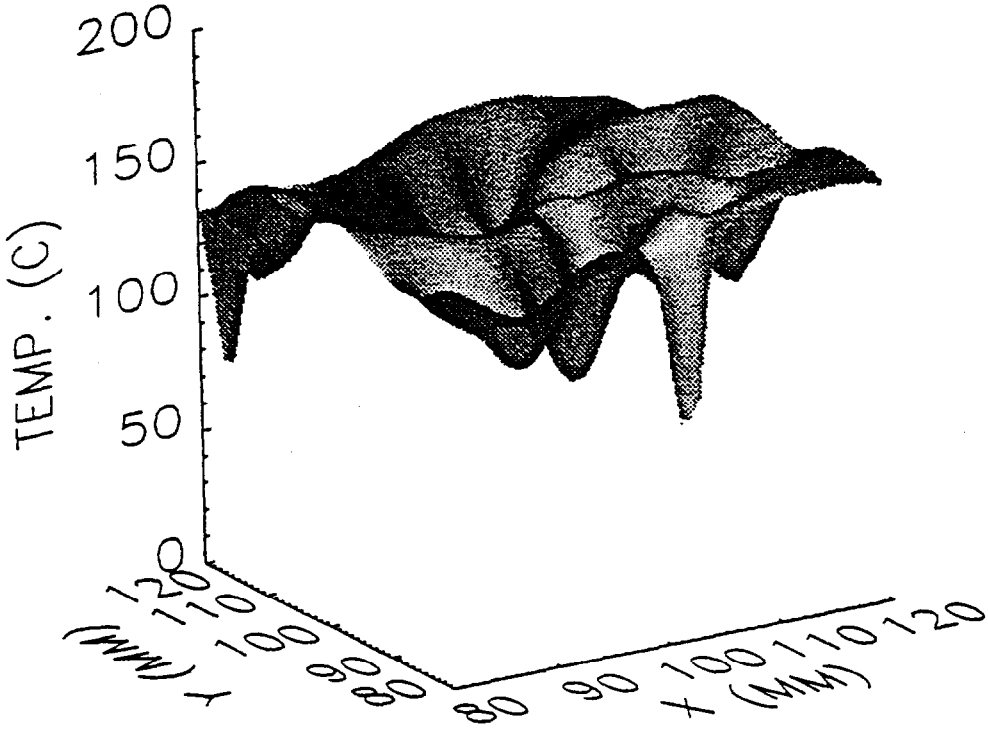

Fig. C6 Temperature distribution on the solid surface; t = 30 s, f = 10 droplets/s, V_0 = 5 μl

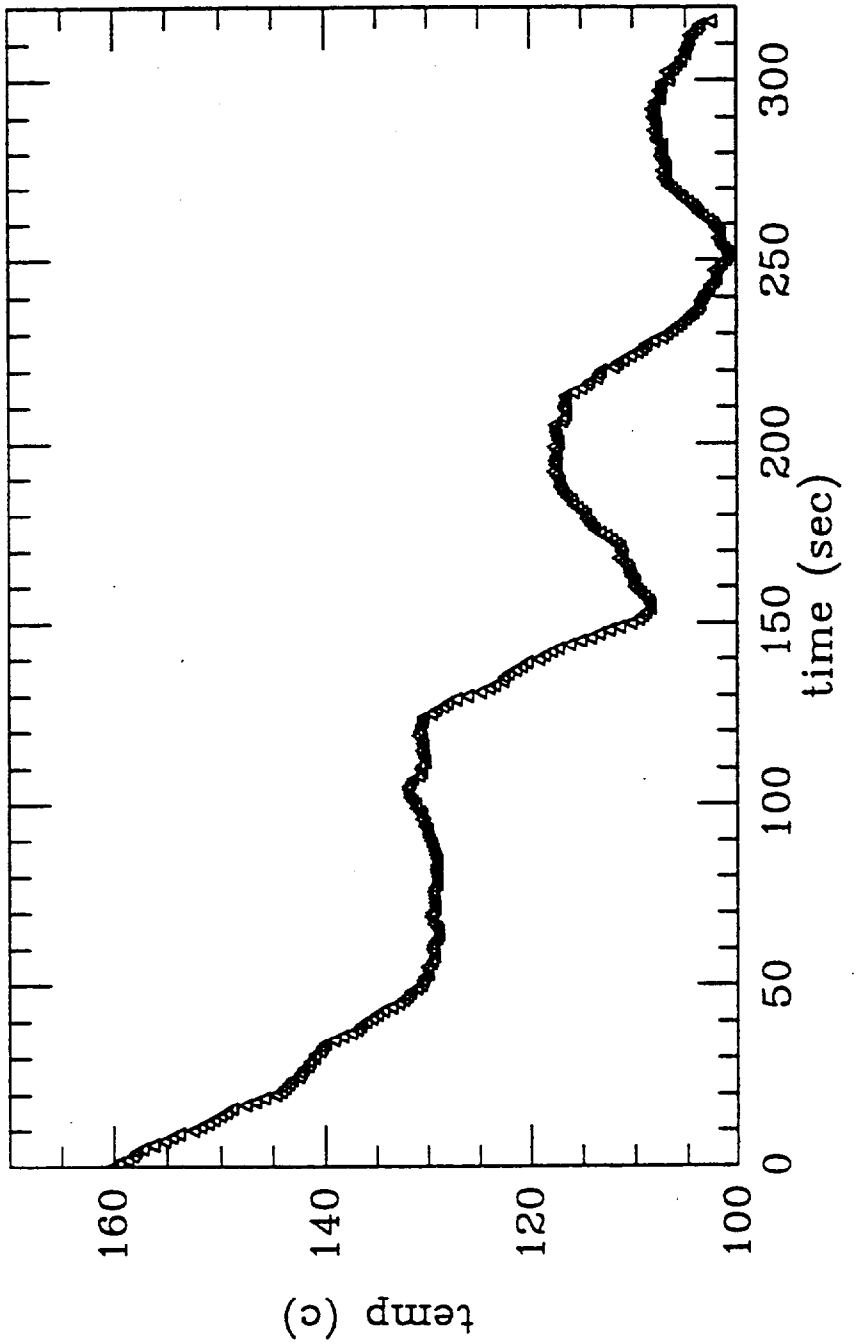

Fig. C7 Average temperature distribution vs. time; R = 100 mm, f = 10 droplets/s, V_0 = 5 μl, T_0 = 160 °C

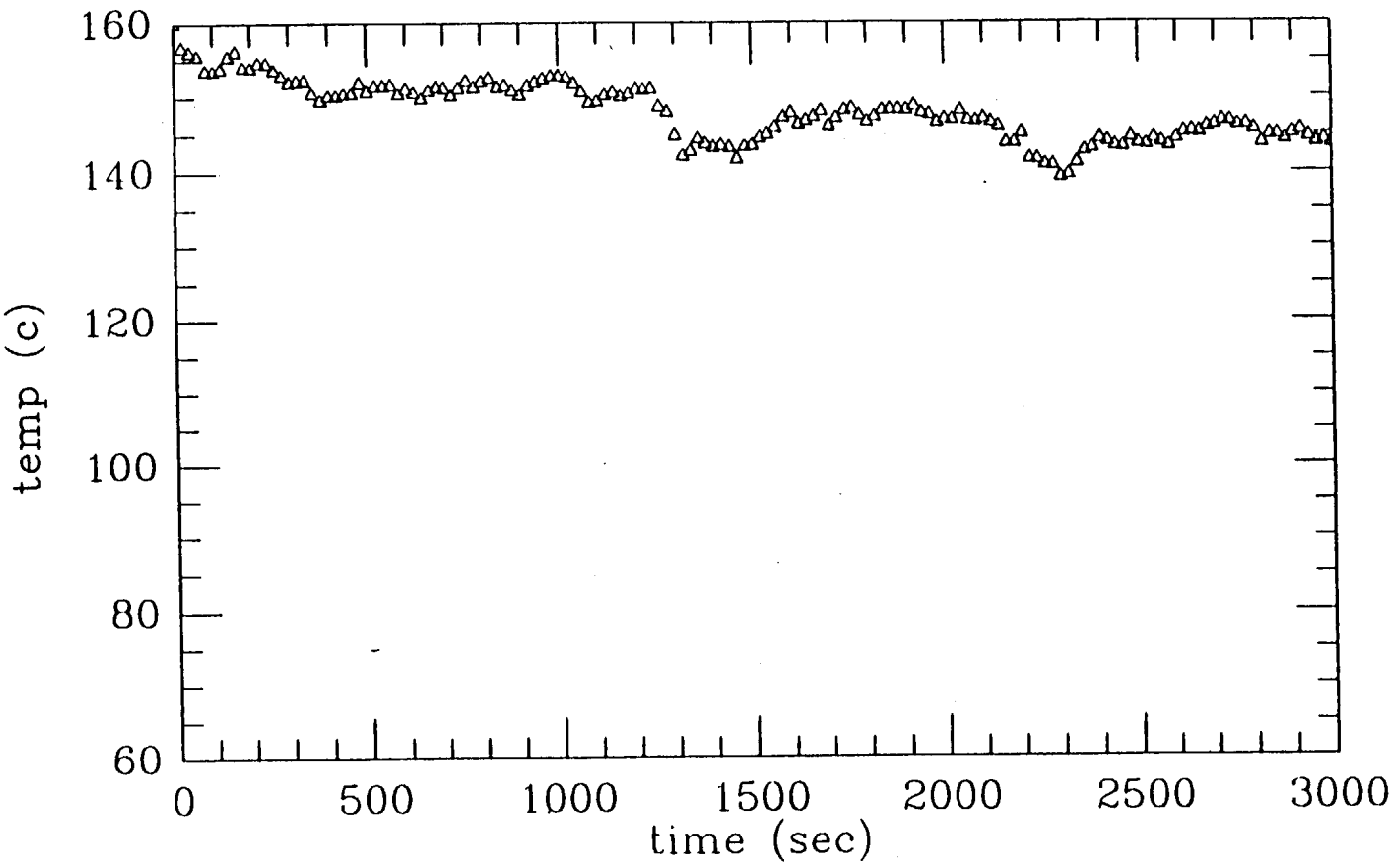

Fig. C8 Average temperature distribution vs. time; A = 0.0314 m^2, f = 1 droplet/s

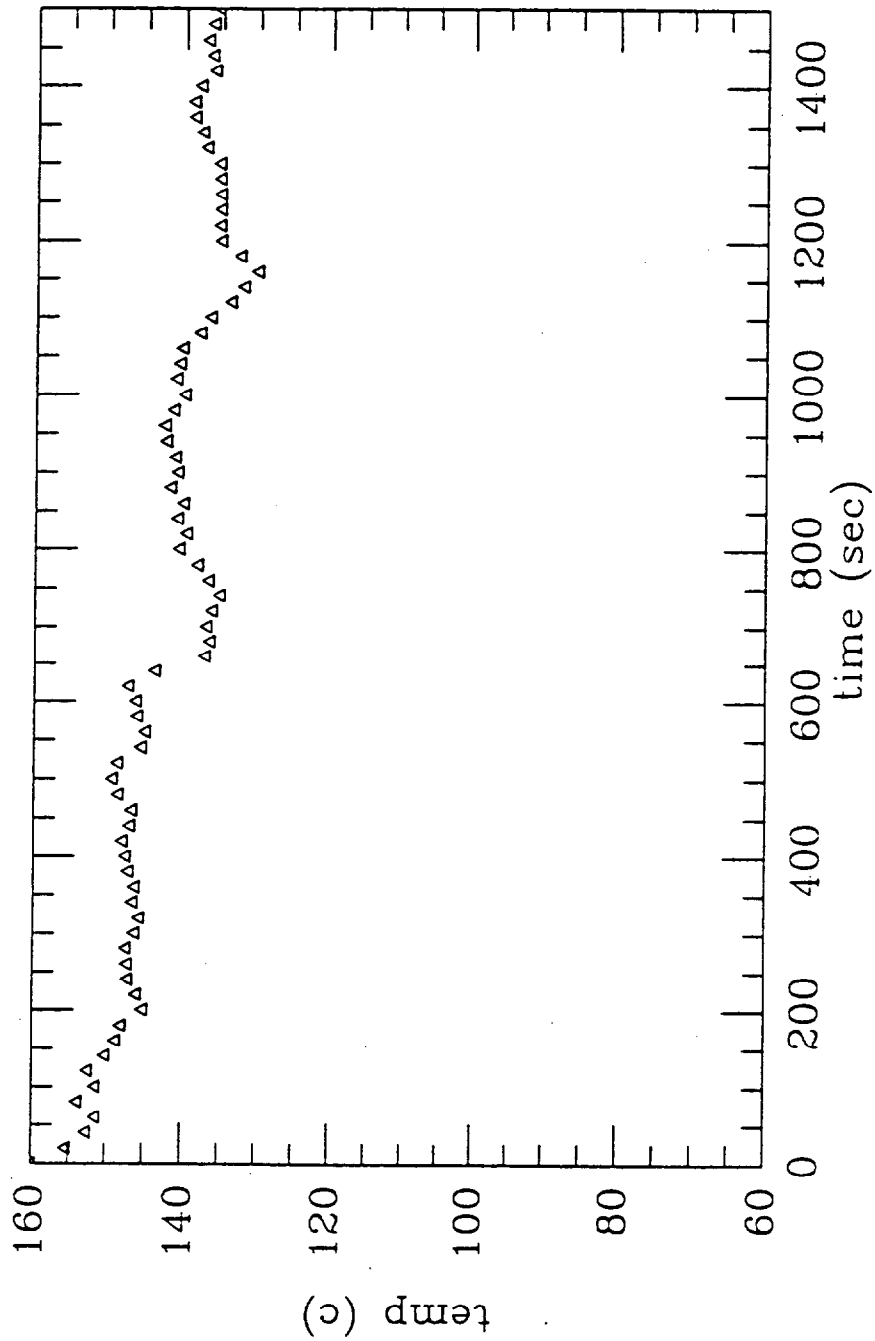

Fig. C9 Average temperature distribution vs. time; $A = 0.0314\ m^2$, $f = 2$ droplets/s

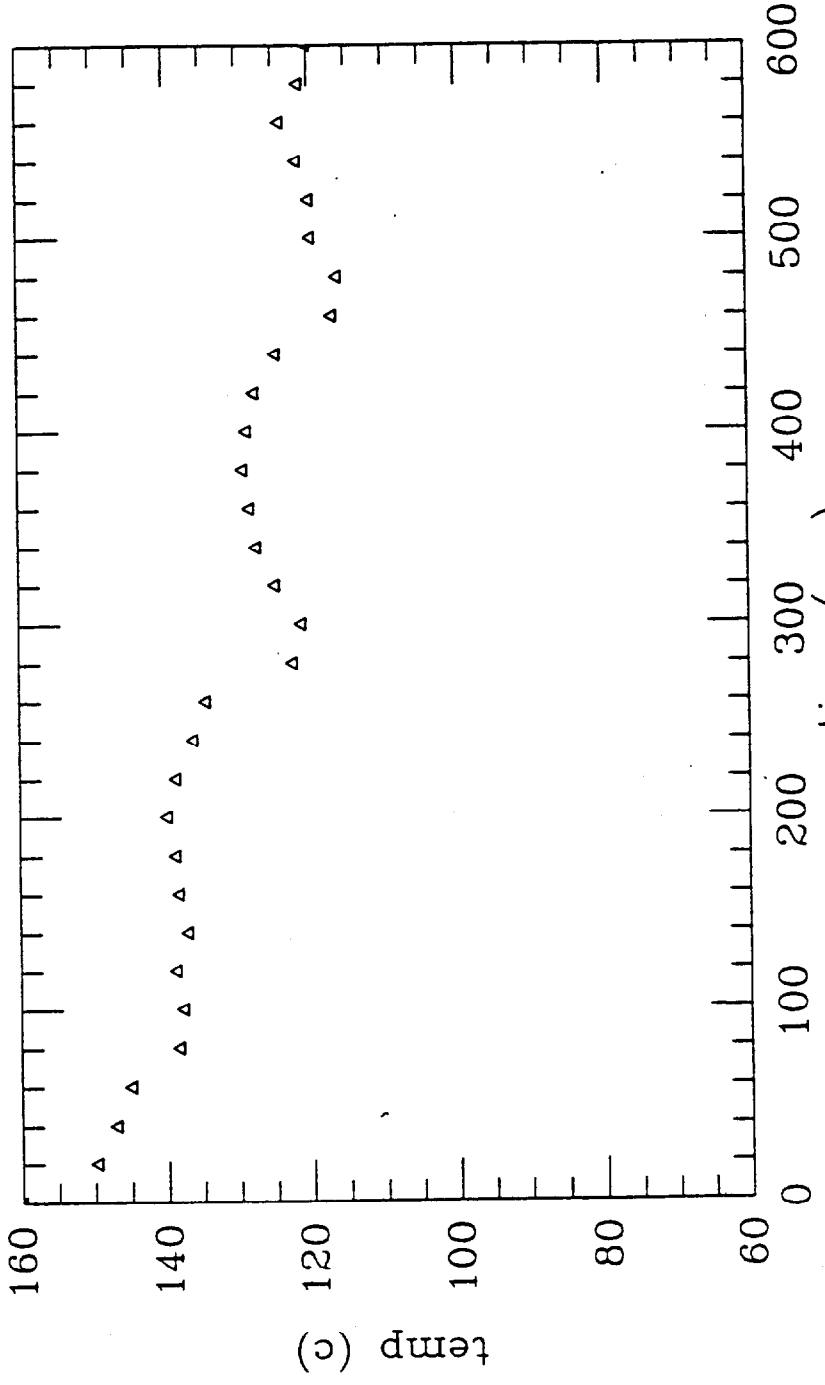

Fig. C10 Average temperature distribution vs. time; A = 0.0314 m^2, f = 5 droplets/s

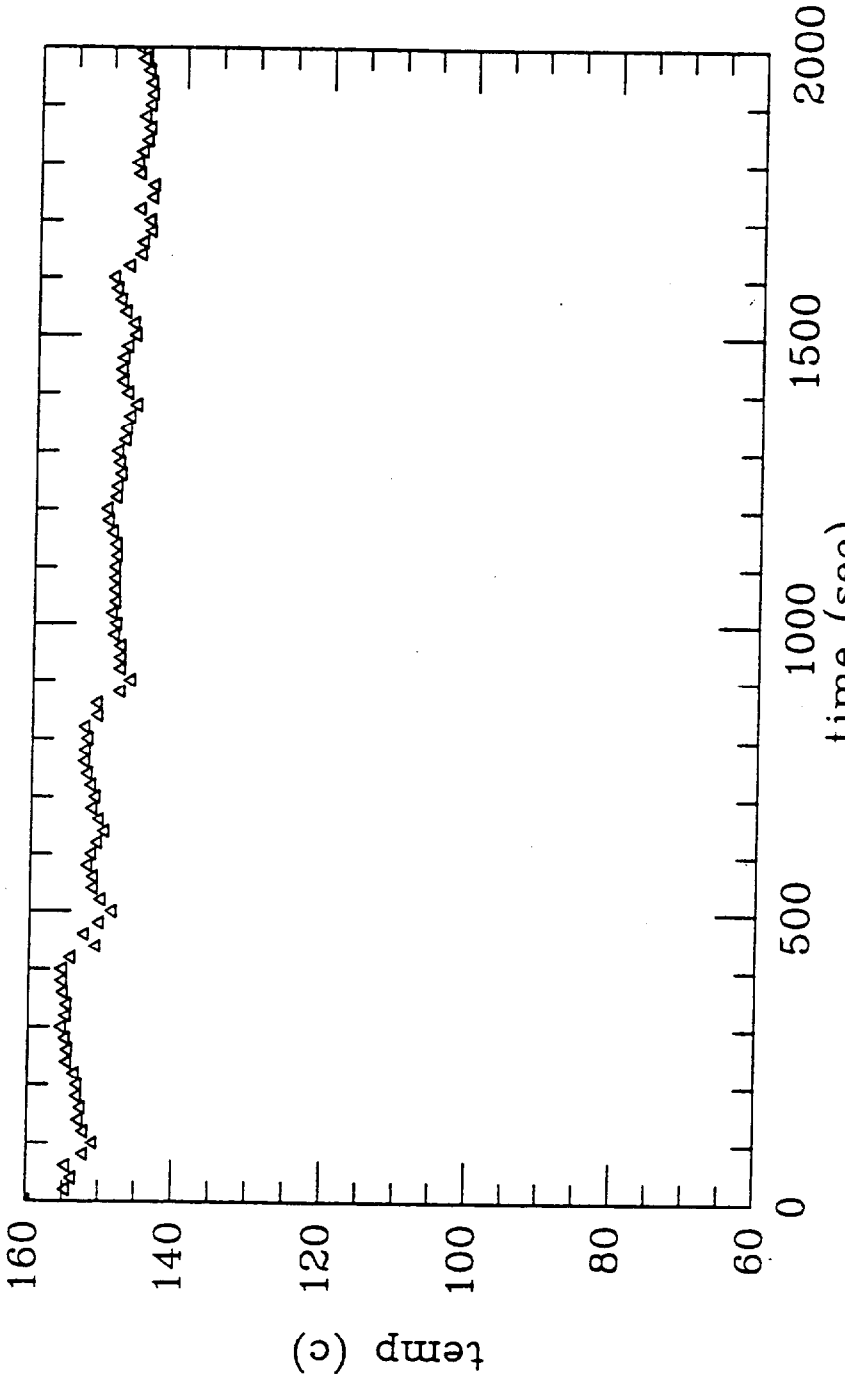

Fig. C11 Average temperature distribution vs. time; A = 0.0628 m^2, f = 2 droplets/s

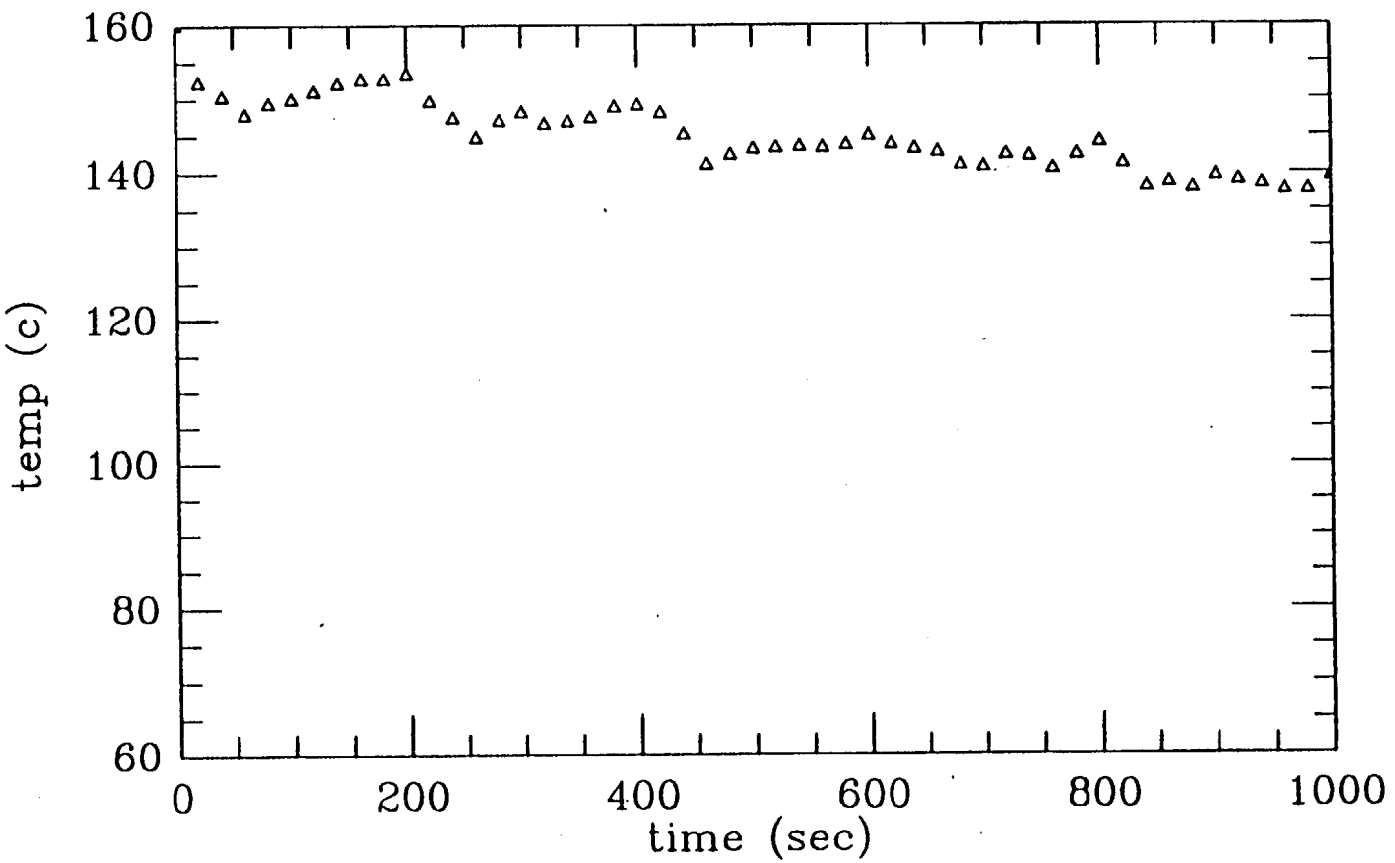

Fig. C12 Average temperature distribution vs. time; A = 0.0628 m^2, f = 4 droplets/s

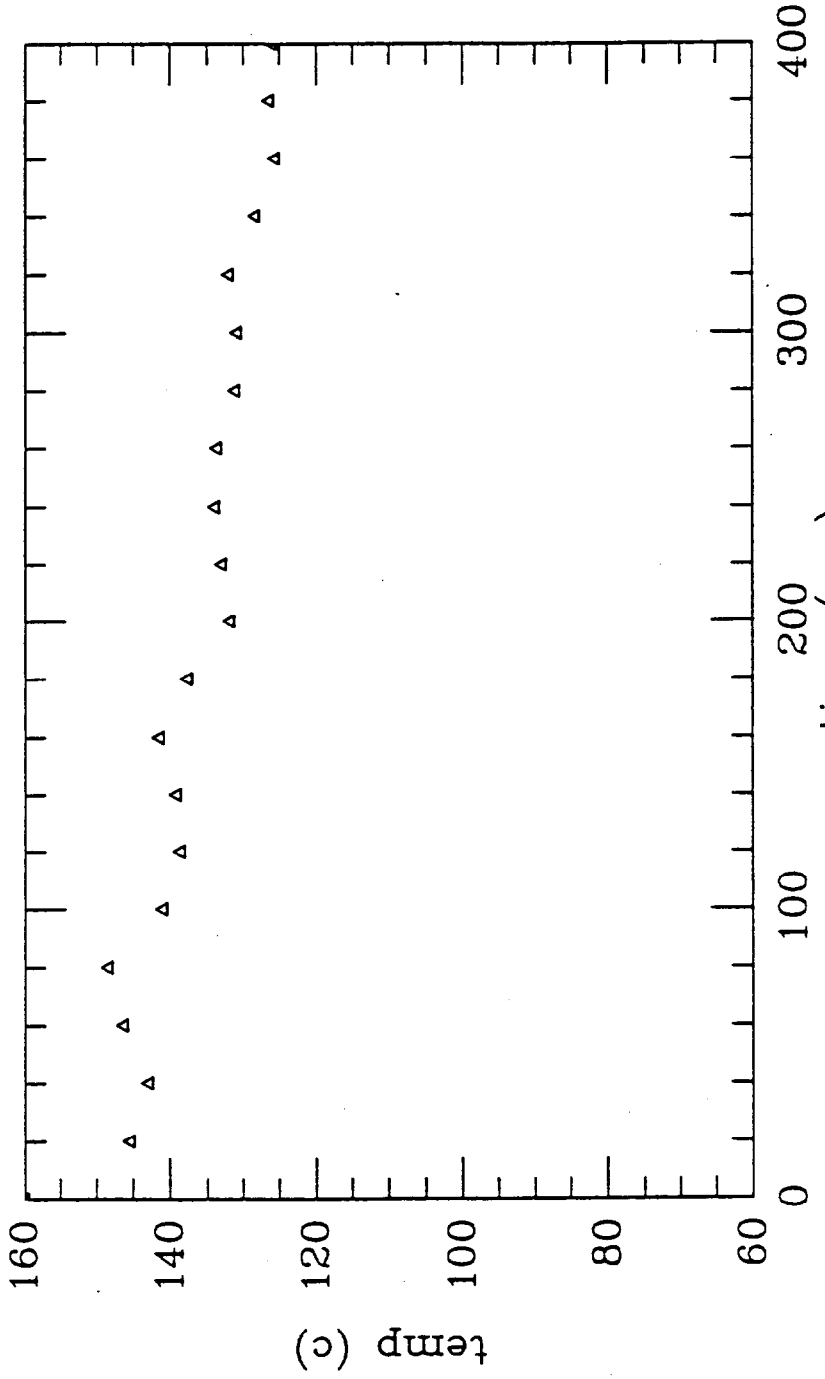

Fig. C13 Average temperature distribution vs. time; A = 0.0628 m^2, f = 10 droplets/s

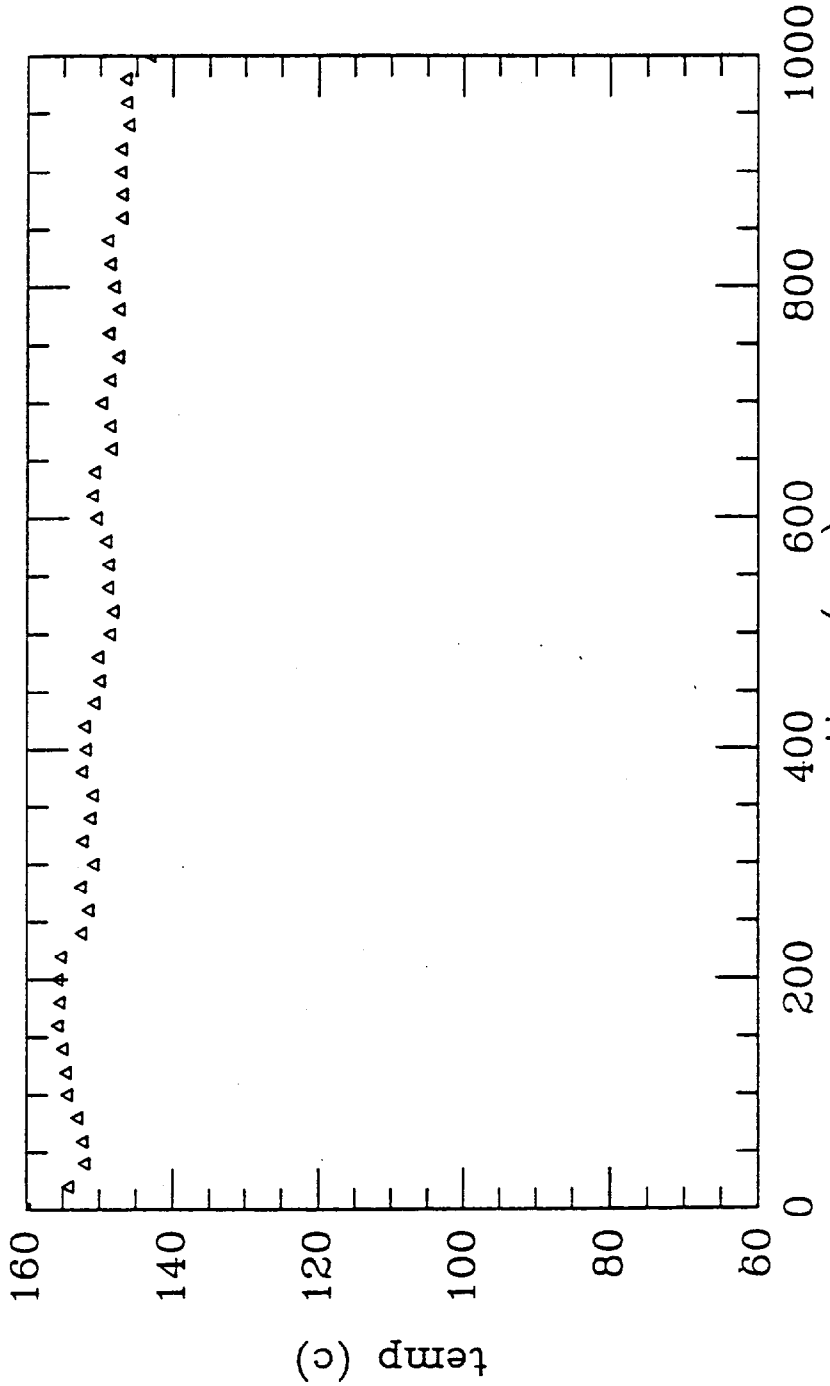

Fig. C14 Average temperature distribution vs. time; A = 0.1256 m^2, f = 4 droplets/s

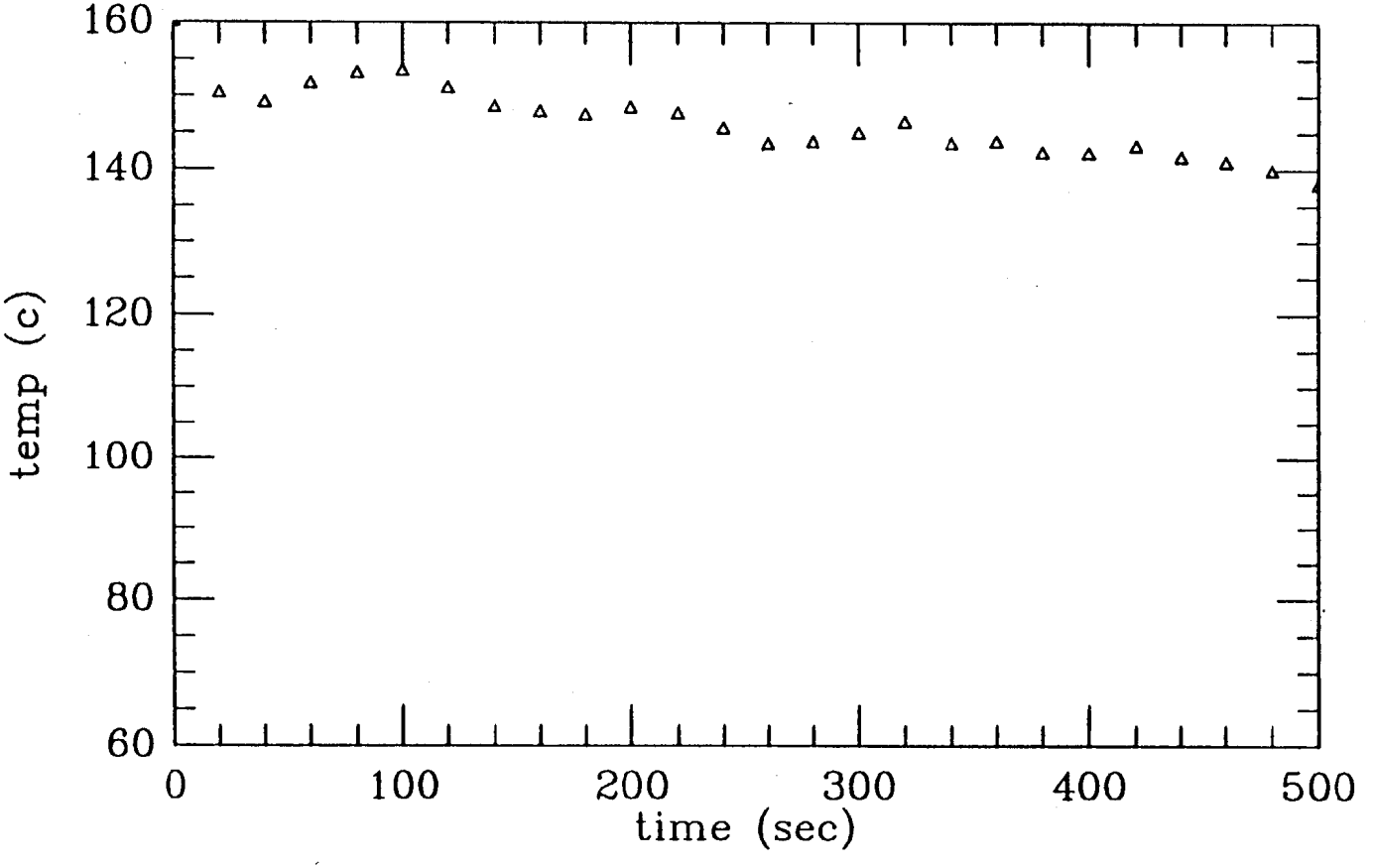

Fig. C15 Average temperature distribution vs. time; A = 0.1256 m^2, f = 8 droplets/s

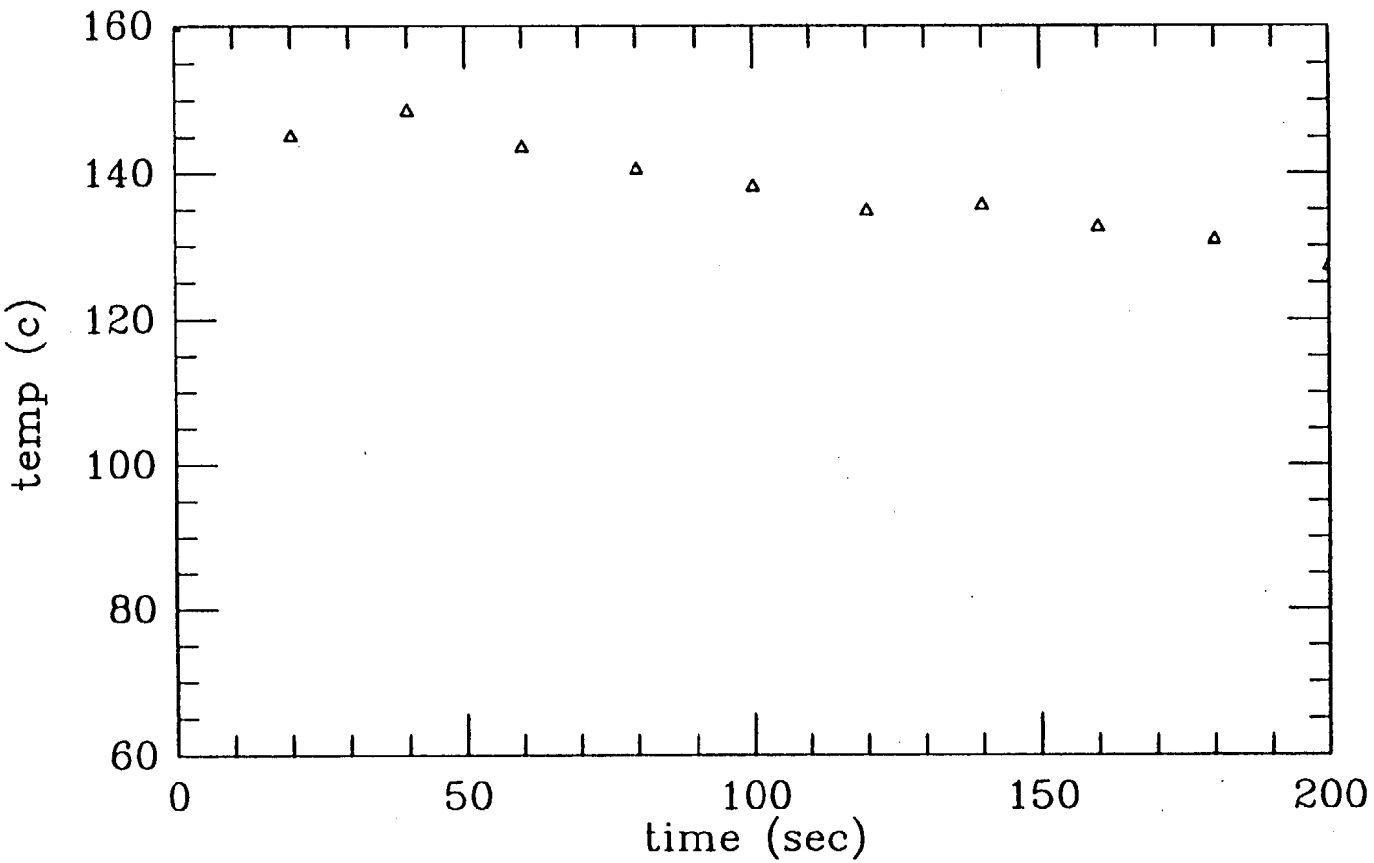

Fig. C16 Average temperature distribution vs. time; A = 0.1256 m^2, f = 20 droplets/s

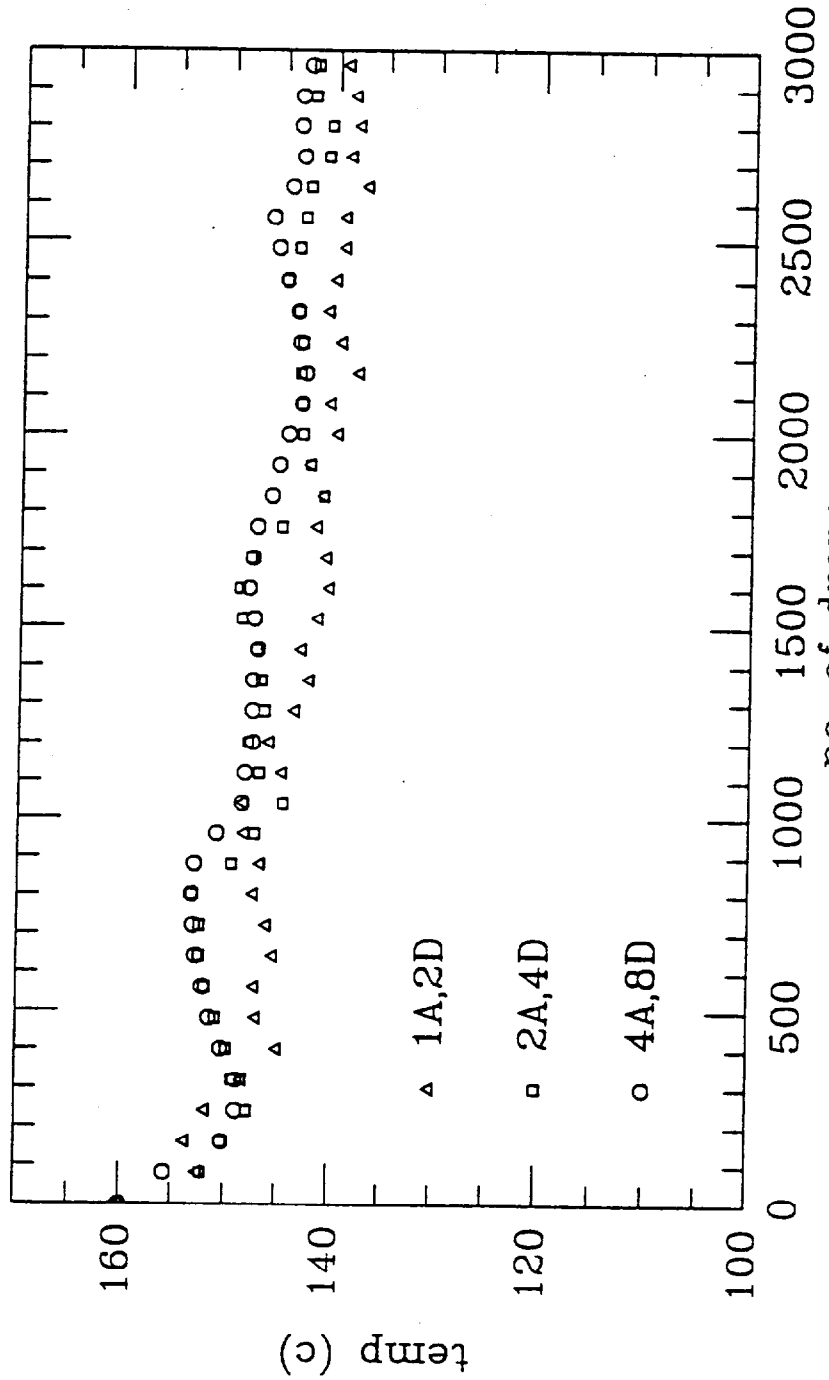

Fig. C17 Average temperature vs. number of droplets; V_0 = 5 μl, T_0 = 160 °C

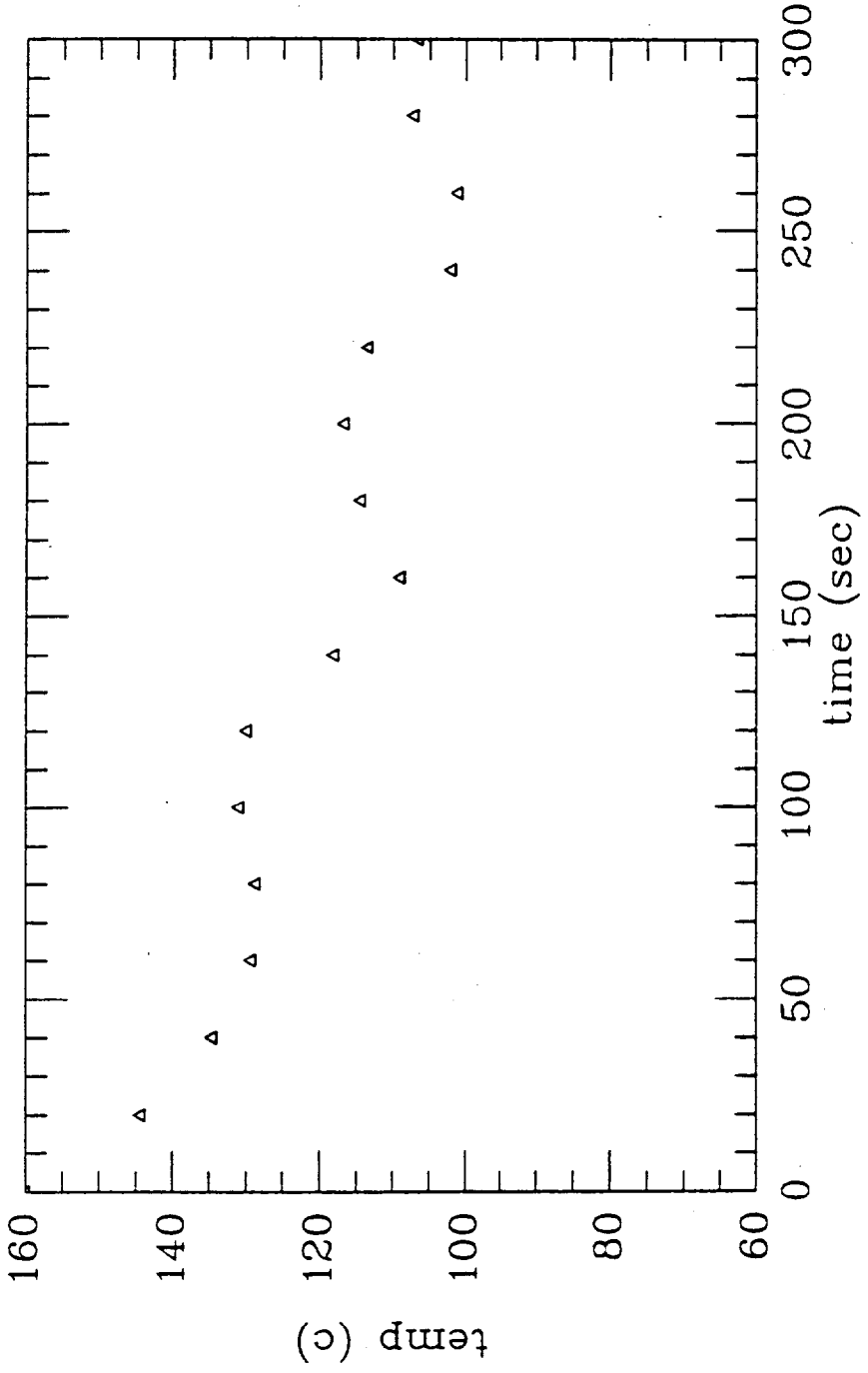

Fig. C18 Average temperature vs. time; f = 10 droplets/s, T_0 = 160 °C

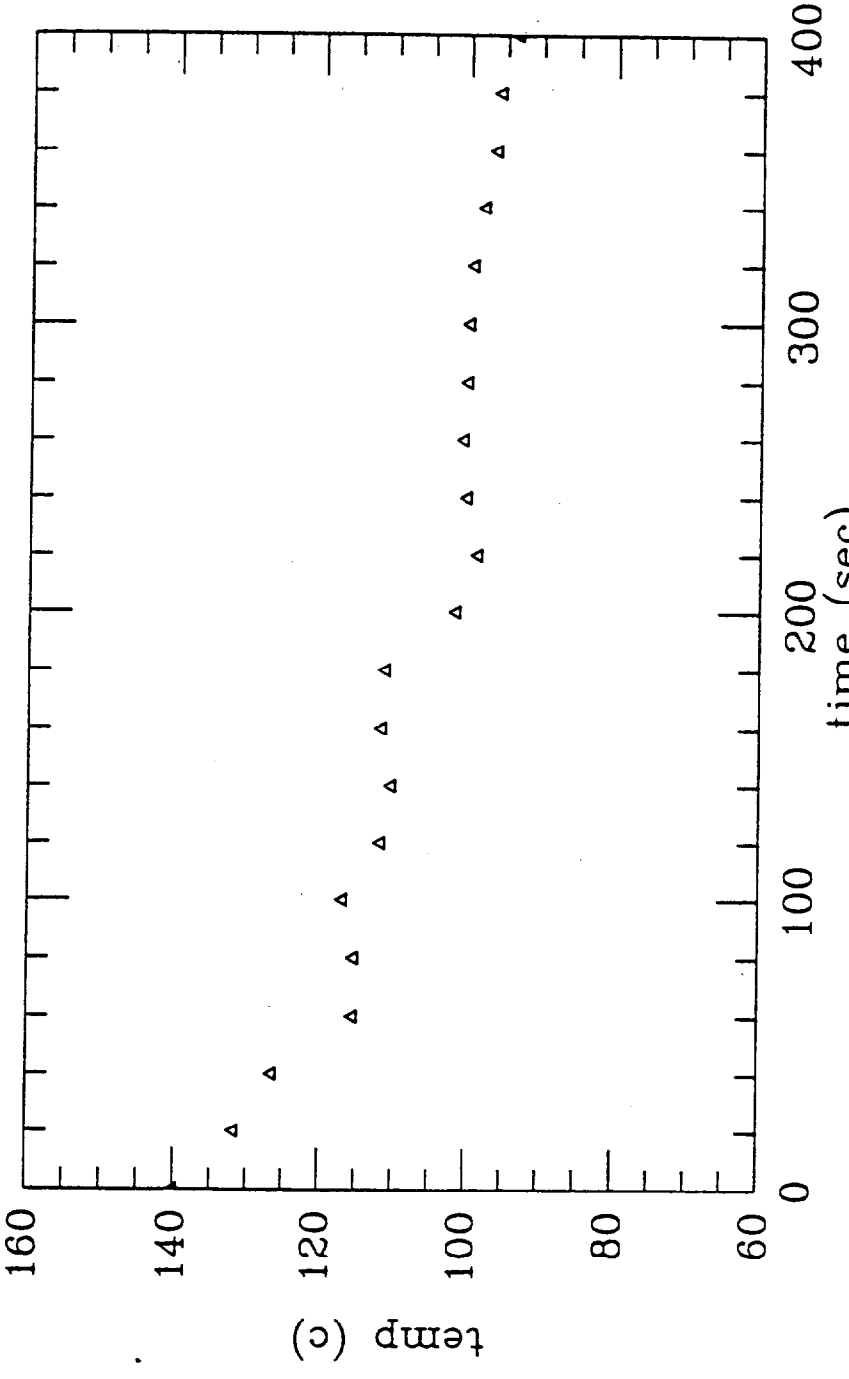

Fig. C19 Average temperature vs. time; f = 10 droplets/s, T_0 = 140 °C

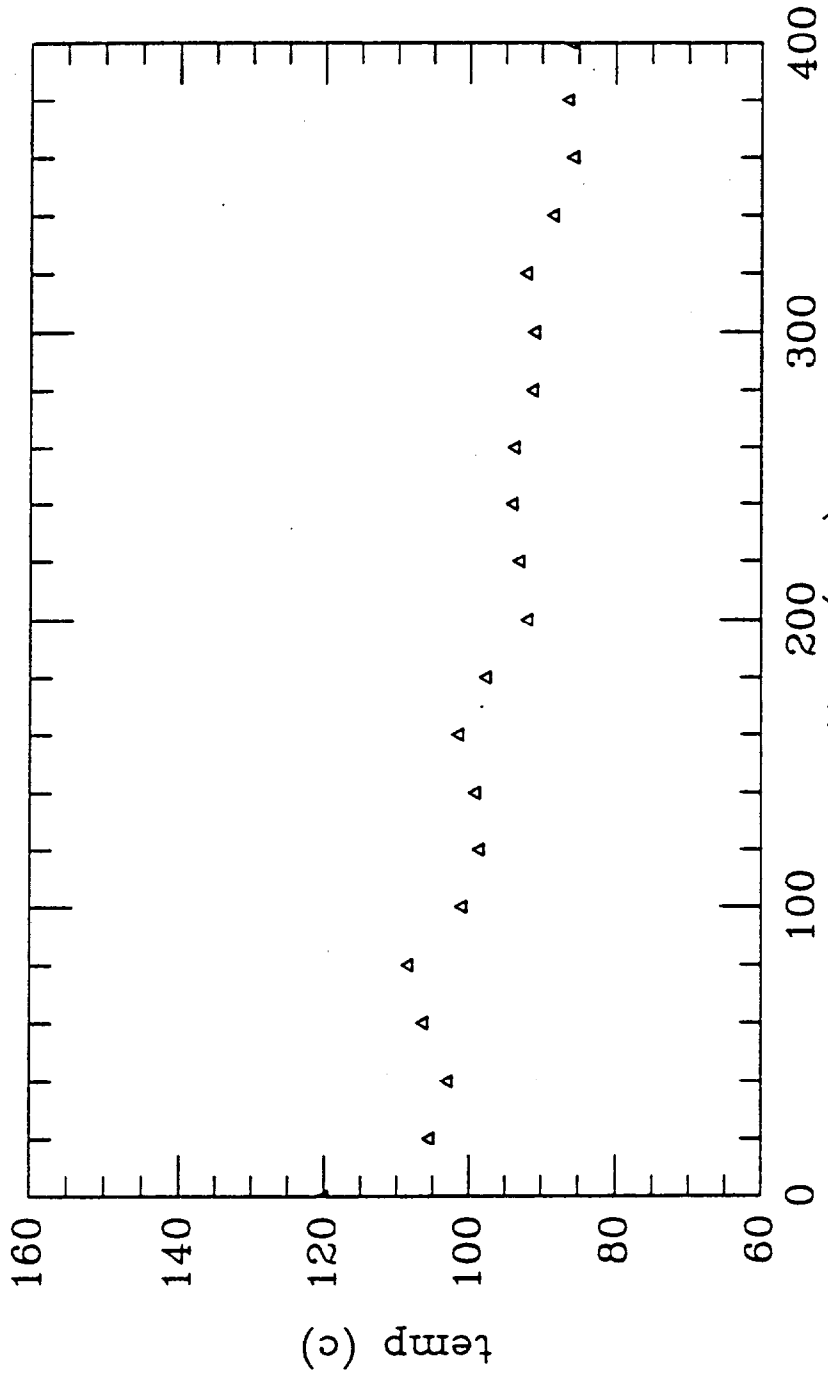

Fig. C20 Average temperature vs. time; f = 10 droplets/s, T_0 = 120 °C

C6. APPENDIX - MULTI-DROPLET CODE

In the following pages, the current version of the multi-droplet code is presented. It includes: a) the main program for multi-droplet calculations; b) the program calculating the recovery process which follows the evaporation of a droplet and c) the single-droplet program which is used to build the multi-droplet data base.

```
C...MULTI-DROPLET MODEL (MACOR)
      DIMENSION U(41,41),TR(3000,5)
      DIMENSION UDATA(27,1,1,15,973),TEND(27),TEVAP(27)
      DIMENSION PT(50)
C...NIX=41,NIY=41,NDROP=30,MNTS0=20,MNV0=1,MNBETA=1,MNRL=30,MNTL=60
C....DIMENSION U(NIX,NIY),TR(NDROP,5),TEND(MNTS0),TEVAP(MNTS0)
C....DIMENSION UDATA(MNTS0,MNV0,MNBETA,MNRL,MNTL)
      COMMON /DDATA/DTS0,DTL,DRL,T0,DTIME
      COMMON /DROP/TS0,V0,BETA,TL
      COMMON /NDATA/MNTS0,MNV0,MNBETA,MNRL,MNTL
      COMMON /NUMR/NRL,NOD,NDROP
      COMMON /GEOM/BLX,BLY,OBX,OBY,DBLX,DBLY
      COMMON /XY/NIX,NIY,NOX,NOY
      COMMON /FR/XM0,YM0,TDROP,FLOWR
      OPEN(UNIT=66,FILE='MD1.DAT',STATUS='NEW')
C..GIVE INITIAL SOLID SURFACE TEMP. T0
      PRINT *,'INITIAL SOLID TEMP (< 160 C) T0=?'
      READ(5,*)T0
C..PLOT INFORMATION
      PRINT *,'HOW MANY PLOTS?'
      READ(5,*)NNPT
      PRINT *,'PLOT AT (SECOND)?'
      READ(5,*)(PT(I),I=1,NNPT)
C..NUMBER OF DROPS PER SECOND (STANDARD 10 D/SEC)
C       NDS=10
      PRINT *,'NUMBER OF DROPS PER SECOND NDS='
      READ(5,*)NDS
      FNDS=10./(1.*NDS)
C..GEOMETRY
C...LOWER LEFT POINT OF THE BLOCK
      OBX=121.4214
      OBY=121.4214
C       OBX=80.
C       OBY=80.
C...SIZE OF THE BLOCK
      BLX=40.
      BLY=40.
C...SIZE OF THE CELL
      DBLX=1.
      DBLY=1.
C..
      NDROP=3000
      NOD=0
C..V0=5
      MNTS0=27
      MNV0=1
      MNBETA=1
C..V0=5
      MNRL=15
C..V0=5
      MNTL=973
```

```
C..
      KPT=1
C..
      CALL MDXY
C...
      CALL MDTR(TR,FNDS)
C...
      CALL MDDATA(UDATA,TEND,TEVAP)
C...
      DO 15 ID=1,NDROP
      TR(ID,2)=T0
  15  CONTINUE
C...
      TIME=0.
      DTIME=20.
      TSTOP=(1.*NDROP)/(1.*NDS)
C...
C...MASS FLOW RATE CALCULATION (KG/M^2 S)
      PI=4.*ATAN(1.)
      RHOW=996.
      AREA=PI*(XM0*1.E-3)**2
      VOLUME=NDROP*V0*1.E-9
      TMASS=VOLUME*RHOW
      FLOWR=TMASS/TDROP/AREA
      PRINT *,'NUMBER OF DROPLETS=',NDROP,'   V0=',V0,'(MM^3)',
     $ '  TOTAL TIME=',TDROP,'(SECOND)'
      PRINT *,'THE MASS FLOW RATE IS',FLOWR,'(KG/M^2 S)'
C...
  1   CONTINUE
C...
      CALL MDIN(TIME,TR,U,UDATA,UMD,TEND,TEVAP)
C...SPACIAL AVERAGED TEMP. IN BLOCK
      TAVE=0.
      DO 50 J=1,NIY-1
      DO 50 I=1,NIX-1
      TAVE=TAVE+.25*(U(I,J)+U(I+1,J)+U(I,J+1)+U(I+1,J+1))+T0
  50  CONTINUE
      TAVE=TAVE/((NIX-1)*(NIY-1))
      PRINT *,'TAVE=',TAVE
      WRITE(66,*)TIME,TAVE
C...PLOT
      NPT=0
      DO 70 IPT=1,NNPT
      IF(PT(IPT).EQ.TIME)NPT=1
  70  CONTINUE
      IF(NPT.EQ.1)THEN
      PRINT *,'A PLOT AT TIME=',TIME
      CALL MDPLOT(KPT,TIME,TAVE,U)
      ENDIF
C..
      IF(TIME.EQ.TSTOP)GO TO 2
```

```
        TIME=TIME+DTIME
        GO TO 1
  2     STOP
        END
C....SUB. FOR DEFINING THE GRID POINTS IN THE TEMP. CALCULATING
BLOCK FOR
C....PROGRAM MD.FOR
        SUBROUTINE MDXY
        COMMON /DDATA/DTS0,DTL,DRL,T0,DTIME
        COMMON /DROP/TS0,V0,BETA,TL
        COMMON /NDATA/MNTS0,MNV0,MNBETA,MNRL,MNTL
        COMMON /NUMR/NRL,NOD,NDROP
        COMMON /GEOM/BLX,BLY,OBX,OBY,DBLX,DBLY
        COMMON /XY/NIX,NIY,NOX,NOY
C...INDEX NUMBERS FOR CORRESPONDING X AND Y DIRECTION
        NIX=INT(BLX/DBLX+1+.000001)
        NIY=INT(BLY/DBLY+1+.000001)
        NOX=INT(OBX/DBLX+1+.000001)
        NOY=INT(OBY/DBLY+1+.000001)
        RETURN
        END
C....SUB. FOR ASSIGNING THE DROPLETS DISTRIBUTION IN TERMS OF THE
TIME THEY
C....ARE DEPOSITED ON THE SOLID AND THE LOCATION
C..TR(ID,1):TIME TO START
C..TR(ID,2):INITIAL SURFACE TEMP
C..TR(ID,3):X
C..TR(ID,4):Y
C..TR(ID,5):INDICATOR OF INSIDE OR OUTSIDE THE CALCULATION BLOCK
        SUBROUTINE MDTR(TR,FNDS)
        DIMENSION TR(NDROP,5)
        COMMON /DDATA/DTS0,DTL,DRL,T0,DTIME
        COMMON /DROP/TS0,V0,BETA,TL
        COMMON /NDATA/MNTS0,MNV0,MNBETA,MNRL,MNTL
        COMMON /NUMR/NRL,NOD,NDROP
        COMMON /GEOM/BLX,BLY,OBX,OBY,DBLX,DBLY
        COMMON /XY/NIX,NIY,NOX,NOY
        COMMON /FR/XM0,YM0,TDROP,FLOWR
C...MDTR10.DAT: R=100 MM
C...MDTR2A.DAT: R=141.4124 MM
C...MDTR200.DAT: R=200 MM
        OPEN(UNIT=15,FILE='MDTR2A.DAT',STATUS='OLD')
C...DISTANCE FROM CENTER OF THE PLATE TO THE EDGES IN X AND Y DIR.
        READ(15,*)XM0,YM0
C...XM0,YM0 (MM)
        READ(15,*)NNDROP
        DO 10 I=1,NDROP
        READ(15,*)ID
C....ID=I
        READ(15,*)TID
        READ(15,*)XI,YI
```

```
        TR(I,1)=TID*FNDS
C...TR(I,2):TEMPID0 IS NEEDED TO BE DETERMINED.
C....MM
        TR(I,3)=XI+XM0
        TR(I,4)=YI+YM0
        TR(I,5)=0.
C...IO=1:INSIDE; IO=0:OUTSIDE
        IF((TR(I,3).GE.OBX.AND.TR(I,3).LE.(OBX+BLX)).AND.
     $     (TR(I,4).GE.OBY.AND.TR(I,4).LE.(OBY+BLY)))TR(I,5)=1.
  10    CONTINUE
        TDROP=TR(NDROP,1)-TR(1,1)
        CLOSE(15)
        RETURN
        END
C...SUB. FOR CREATING A DATABASE FOR TEMP. DISTRIBUTION
C...AT DIFFERENT INITIAL SOLID SURFACE TEMP. (TS0),
C...             INITIAL DROPLET VOLUME (V0)
C...             BETA (BETA)
C...             LOCAL TIME (TL)
C...             LOCAL RADIUS (RL)
        SUBROUTINE MDDATA(UDATA,TEND,TEVAP)
C        PARAMETER (MNTS0=6,MNV0=1,MNBETA=1,MNRL=4,MNTL=4)
        DIMENSION UDATA(MNTS0,MNV0,MNBETA,MNRL,MNTL)
        DIMENSION TEND(MNTS0),TEVAP(MNTS0)
        COMMON /DDATA/DTS0,DTL,DRL,T0,DTIME
        COMMON /DROP/TS0,V0,BETA,TL
        COMMON /NDATA/MNTS0,MNV0,MNBETA,MNRL,MNTL
        COMMON /NUMR/NRL,NOD,NDROP
        COMMON /GEOM/BLX,BLY,OBX,OBY,DBLX,DBLY
        COMMON /XY/NIX,NIY,NOX,NOY
C...MDDATA2.DAT: V0=5, BETA=1.4,TS0=160 - 30
        OPEN(UNIT=25,FILE='MDDATA2.DAT',STATUS='OLD')
C......UDATA: TEMP. (C)
C......ITS0=1: TS0=160 (C)
C......      2: TS0=155
C......      3: TS0=150
C......NV0=1: V0=10 (MM^3)
C......NBETA=1: BETA=1.4
C......RL=NRL*DRL (MM)
C......TL=NTL*DTL (SECOND)
C..........'M': MAXIMUM
C..
C...FOR IV0=1
        READ(25,*)V0
        READ(25,*)TT0
        READ(25,*)DTS0
        READ(25,*)DTL
        READ(25,*)DRL
C.
        READ(25,*)NTS0
        IV0=1
```

```
C.
      IBETA=1
C...FOR IBETA=1
      BETA=1.4
C.
      READ(25,*)NRL
      DO 10 ITS0=1,NTS0
      READ(25,*)IITS0
      READ(25,*)TS0I
      READ(25,*)NTEVAP,NTEND
      TEVAP(ITS0)=NTEVAP
      TEND(ITS0)=NTEND
C....
      DO 20 ITL=1,NTEND
      READ(25,*)(UDATA(ITS0,IV0,IBETA,IRL,ITL),IRL=1,NRL)
      DO 21 IIRL=1,NRL
      IF(UDATA(ITS0,IV0,IBETA,IIRL,ITL).GT.0.)THEN
      UDATA(ITS0,IV0,IBETA,IIRL,ITL)=0.
      ENDIF
 21   CONTINUE
 20   CONTINUE
C....
 10   CONTINUE
      CLOSE(25)
      RETURN
      END
C...SUB. FOR CALCULATING THE TEMP. ON ALL GRID POINTS IN THE
CALCULATION
C...BLOCK.
      SUBROUTINE MDIN(TIME,TR,U,UDATA,UMD,TEND,TEVAP)
      DIMENSION U(NIX,NIY),TR(NDROP,5)
      DIMENSION UDATA(MNTS0,MNV0,MNBETA,MNRL,MNTL)
      DIMENSION TEND(MNTS0),TEVAP(MNTS0)
      COMMON /DDATA/DTS0,DTL,DRL,T0,DTIME
      COMMON /DROP/TS0,V0,BETA,TL
      COMMON /NDATA/MNTS0,MNV0,MNBETA,MNRL,MNTL
      COMMON /NUMR/NRL,NOD,NDROP
      COMMON /GEOM/BLX,BLY,OBX,OBY,DBLX,DBLY
      COMMON /XY/NIX,NIY,NOX,NOY
      EXTERNAL UFEV
      EXTERNAL UFRE
      DO 11 I=1,NIX
      DO 11 J=1,NIY
      U(I,J)=0.
 11   CONTINUE
      TS0=T0
C      PRINT *,'   NOD=',NOD,'    TR(ID,2):'
C      PRINT *,(TR(ID,2),ID=1,NOD)
      DO 10 ID=1,NOD
C...DETERMINE TS0,V0,BETA,TL
      TS0=TR(ID,2)
```

```
        IF(TS0.LT.30.)PRINT *,'TS0=',TS0,
     $ 'MORE DATA NEEDED FOR TS0 BELOW 30 C'
        KTS0=0
        DO 12 K=1,MNTS0+1
        IF(TS0.LE.T0-(K-1)*DTS0.AND.TS0.GT.T0-K*DTS0)KTS0=K
  12    CONTINUE
C...TL=(ITL-1)*DTL
        TL=TIME-TR(ID,1)
C..FOR EVERY POINT IN THE BLOCK, DETERMINE RL
        DO 20 I=1,NIX
        DO 20 J=1,NIY
        RL=SQRT((TR(ID,3)-(NOX+I-1)*DBLX)**2
     $         +(TR(ID,4)-(NOY+J-1)*DBLY)**2)
C...RL=(IRL-1)*DRL
C        IF(RL.LE.(MNRL-1)*DRL.AND.TL.LE.MNTL*DTL)THEN
        IF(RL.LE.(MNRL-1)*DRL.AND.
     $    TL.LE.TEND(KTS0).AND.TL.LE.TEND(KTS0+1))THEN
        CALL MDU(UDATA,TS0,TL,RL,UMD)
        UIJ=UMD
        ELSE
C..CALL FUNCTION
        IF(TL.LT.TEVAP(KTS0))THEN
        UIJ=UFEV(TS0,V0,BETA,TL,RL,KTS0,TEVAP,TEND)
        ELSE
        UIJ=UFRE(TS0,V0,BETA,TL,RL,KTS0,TEVAP,TEND)
        ENDIF
        ENDIF
C..SUMMATION
        U(I,J)=U(I,J)+UIJ
  20    CONTINUE
  10    CONTINUE
C..DETERMINE TR(ID,2) AND NEW NOD (NUMBER OF ON-RUN DROPLETS)
        NOD1=NOD
        TS0=T0
        DO 100 ID=NOD1,NDROP
        UOUT=0.
C..WHEN THE DROPLET IS DEPOSITED
        IF(TR(ID,1).GE.TIME.AND.TR(ID,1).LT.TIME+DTIME)THEN
C..PTS INSIDE OF BLOCK
        IF(TR(ID,5).EQ.1)THEN
        I=INT(TR(ID,3)/DBLX)-NOX+1
        J=INT(TR(ID,4)/DBLY)-NOY+1
C..INTERPOLATION TO GET TR(ID,2)
C....FROM U(I,J),U(I,J+1),U(I+1,J+1) AND U(I+1,J)
        UX1=(U(I+1,J)-U(I,J))*(TR(ID,3)-(NOX+I-1)*DBLX)/DBLX
     $    +U(I,J)
        UX2=(U(I+1,J+1)-U(I,J+1))*(TR(ID,3)-(NOX+I-1)*DBLX)/DBLX
     $    +U(I,J+1)
        UXY=(UX2-UX1)*(TR(ID,4)-(NOY+J-1)*DBLY)/DBLY+UX1
C..DEFINITION OF U ?
        TR(ID,2)=UXY+T0
```

```
        ELSE
C..PTS OUTSIDE OF BLOCK
        DO 200 ID1=1,NOD1
        IF(ID.NE.ID1)THEN
        TS0=TR(ID1,2)
        KTS0=0
        DO 212 K=1,MNTS0+1
        IF(TS0.LE.T0-(K-1)*DTS0.AND.TS0.GT.T0-K*DTS0)KTS0=K
  212   CONTINUE
C...TL=(ITL-1)*DTL, RL=(IRL-1)*DRL
        TL=TIME-TR(ID1,1)
        RL=SQRT((TR(ID,3)-TR(ID1,3))**2
     $         +(TR(ID,4)-TR(ID1,4))**2)
        IF(RL.LE.(MNRL-1)*DRL.AND.
     $    TL.LE.TEND(KTS0).AND.TL.LE.TEND(KTS0+1))THEN
C..CALL MDU
        CALL MDU(UDATA,TS0,TL,RL,UMD)
        UIJ=UMD
        ELSE
C..CALL FUNCTION
        IF(TL.LT.TEVAP(KTS0))THEN
        UIJ=UFEV(TS0,V0,BETA,TL,RL,KTS0,TEVAP,TEND)
        ELSE
        UIJ=UFRE(TS0,V0,BETA,TL,RL,KTS0,TEVAP,TEND)
        ENDIF
        ENDIF
        UOUT=UIJ+UOUT
        ENDIF
  200   CONTINUE
C..DEFINITION OF U=T-T0
        TR(ID,2)=UOUT+T0
        ENDIF
C..NEW NOD
        NOD=NOD+1
        ELSE
        IF(TR(ID,1).GE.TIME+DTIME)GO TO 300
        ENDIF
  100   CONTINUE
  300   CONTINUE
        RETURN
        END
C.....SUB. FOR FINDING A TEMP. (DIFFERENCE BETWEEN REAL
C.....SOLID SURFACE TEMP. AND INITIAL SOLID SURFACE TEMP.)
C.....FUNCTION VARIABLES ARE:
C.        TS0:  INITIAL SOLID SURFACE TEMP.
C.        V0:   INITIAL DROPLET VOLUME
C.        BETA: RATIO BETWEEN THE RADIUS OF THE WET AREA
C.              AND RADIUS OF THE EQUIVALENT SPHERICAL VOLUME
C.        TL:   LOCAL TIME IN WHICH TL=0 REPRESENTS THE
C.              MOMENT THE DROPLET STARTS TO EVAPORATE
C.        RL:   LOCAL RADIUS WITH ORIGIN DEFINED AT
```

```
C.              THE CENTER OF THE DROPLET
      SUBROUTINE MDU(UDATA,TS0,TL,RL,UMD)
      DIMENSION UDATA(MNTS0,MNV0,MNBETA,MNRL,MNTL)
      COMMON /DDATA/DTS0,DTL,DRL,T0,DTIME
      COMMON /NDATA/MNTS0,MNV0,MNBETA,MNRL,MNTL
      COMMON /NUMR/NRL,NOD,NDROP
      COMMON /GEOM/BLX,BLY,OBX,OBY,DBLX,DBLY
      COMMON /XY/NIX,NIY,NOX,NOY
C      MNTS0=MN1
C      MNV0=MN2
C      MNBETA=MN3
C      MNRL=MN4
C      MNTL=MN5
C...
C.....FIND ITS0 TS0=T0-(ITS0-1)*DTS0
      DO 10 I=1,MNTS0+1
      IF(TS0.LE.T0-(I-1)*DTS0.AND.TS0.GT.T0-I*DTS0)THEN
      ITS0=I
      ENDIF
  10  CONTINUE
C.....FIND IV0
      IV0=1
C.....FIND IBETA
      IBETA=1
C.....FIND ITL TL=(ITL-1)*DTL
      ITL=INT(TL/DTL)+1
C.....FIND IRL RL=(IRL-1)*DRL
      DO 20 I=1,MNRL
      IF(RL.GE.(I-1)*DRL.AND.RL.LT.I*DRL)THEN
      IRL=I
      ENDIF
  20  CONTINUE
C.....INTERPOLATION IN T
      UT1=UDATA(ITS0,1,1,IRL,ITL)
      UT2=UDATA(ITS0,1,1,IRL,ITL+1)
      IF(UT1.GT.0..OR.UT2.GT.0.)PRINT *,ITS0,IRL,ITL
      UR1=(UT2-UT1)*(TL-(ITL-1)*DTL)/DTL+UT1
      UT1=UDATA(ITS0,1,1,IRL+1,ITL)
      UT2=UDATA(ITS0,1,1,IRL+1,ITL+1)
      IF(UT1.GT.0..OR.UT2.GT.0.)PRINT *,ITS0,IRL,ITL
      UR2=(UT2-UT1)*(TL-(ITL-1)*DTL)/DTL+UT1
      UT1=UDATA(ITS0+1,1,1,IRL,ITL)
      UT2=UDATA(ITS0+1,1,1,IRL,ITL+1)
      IF(UT1.GT.0..OR.UT2.GT.0.)PRINT *,ITS0,IRL,ITL
      UR3=(UT2-UT1)*(TL-(ITL-1)*DTL)/DTL+UT1
      UT1=UDATA(ITS0+1,1,1,IRL+1,ITL)
      UT2=UDATA(ITS0+1,1,1,IRL+1,ITL+1)
      IF(UT1.GT.0..OR.UT2.GT.0.)PRINT *,ITS0,IRL,ITL
      UR4=(UT2-UT1)*(TL-(ITL-1)*DTL)/DTL+UT1
C.....INTERPOLATION IN R
      UMD1=(UR2-UR1)*(RL-(IRL-1)*DRL)/DRL+UR1
```

```
        UMD2=(UR4-UR3)*(RL-(IRL-1)*DRL)/DRL+UR3
        IF(UMD1.GT.0..OR.UMD2.GT.0.)PRINT *,'UMD1,UMD2',UMD1,UMD2
C.....INTERPOLATION IN TS0
        UMD=-(UMD2-UMD1)*(TS0-(T0-(ITS0-1)*DTS0))/DTS0+UMD1
        IF(UMD.GT.0.)PRINT *,'UMD: TS0,RL,TL,UMD',TS0,RL,TL,UMD
        RETURN
        END
C......FUNCTION OF U FOR RL BEYOND (MNRL-1)*DRL DURING EVAPORATION
        FUNCTION UFEV(TS0,V0,BETA,TL,RL,KTS0,TEVAP,TEND)
        DIMENSION TEND(MNTS0),TEVAP(MNTS0)
        COMMON /NDATA/MNTS0,MNV0,MNBETA,MNRL,MNTL
        PI=4.*ATAN(1.)
C.......MACOR:
         SK=1.297E-3
         SR=2520.E-9
         SC=888.9
C....DIFFUSIVITY OF MACOR
        ALPHAS=SK/(SR*SC)
C....LATENT HEAT (J/KG K)
        ALAMDA=2500.*1000.
C....WATER DENSITY (KG/MM^3)
        RHOW=997.6E-9
C....LOCAL TIME IN FUNCTION (+1 TO AVOID THE TL0 TO BE 0)
        TL0=TL
C....EVAP. TIME TEVAP1
        TEVAP1=TEVAP(KTS0)
        IF(TL0.LE.0.)THEN
        TL1=1.
        ELSE
        TL1=TL0
        ENDIF
        TSUB=TEVAP1-TL1
        UFEV=-2.*V0*(RHOW/SR)*(ALAMDA/SC)/(8.*(PI*ALPHAS*TSUB)**1.5)
     $ *EXP(-RL**2/(4.*ALPHAS*TSUB))*COS(PI/2.*(1.-TL0/TEVAP1))
        RETURN
        END
C......FUNCTION OF U FOR RL BEYOND (MNRL-1)*DRL DURING THE
C......RECOVERING PROCESS AND FOR TL EXCEEDING MNTL*DTL
        FUNCTION UFRE(TS0,V0,BETA,TL,RL,KTS0,TEVAP,TEND)
        DIMENSION TEND(MNTS0),TEVAP(MNTS0)
        COMMON /NDATA/MNTS0,MNV0,MNBETA,MNRL,MNTL
        PI=4.*ATAN(1.)
C.......MACOR:
         SK=1.297E-3
         SR=2520.E-9
         SC=888.9
C....DIFFUSIVITY OF MACOR
        ALPHAS=SK/(SR*SC)
C....LATENT HEAT (J/KG K)
        ALAMDA=2500.*1000.
C....WATER DENSITY (KG/MM^3)
```

```
        RHOW=997.6E-9
C....LOCAL TIME IN FUNCTION (+1 TO AVOID THE TL0 TO BE 0)
        TL0=TL-TEVAP(KTS0)
C...UFRE=?
        IF(TL0.LE.0.)TL0=.01
        UFRE=-2.*V0*(RHOW/SR)*(ALAMDA/SC)/(8.*(PI*ALPHAS*TL0)**1.5)
     $ *EXP(-RL**2/(4.*ALPHAS*TL0))
        RETURN
        END
```

```
C......PROGRAM FOR SOLVING A CONDUCTION HEAT TRANSFER PROBLEM IN
C......SOLID.
C......RECOVERY PROCESS
C......CONNECTED WITH TEST.FOR
       PARAMETER (JM=11,JE=4*(JM-1),NIMSL=JM+JE,KNT=5000)
       DIMENSION TN1(JM+JE),THALF(JM+JE)
       DIMENSION TX(JM+JE),TR(JM+JE),TB(JM+JE,JM+JE)
       DIMENSION W(JM+JE-1,JM+JE-1),FTIM(JM+JE-1,KNT),F(JM+JE-1)
       DIMENSION W1(JM+JE-1,JM+JE-1,KNT)
       DIMENSION RHS(JM+JE-1),W0(JM+JE-1,JM+JE-1)
       DIMENSION RS0(JM+JE-1),WF(JM+JE-1),TBM(JM+JE)
       DIMENSION PTT(50)
       DIMENSION IWK(NIMSL),WK(NIMSL+NIMSL*(NIMSL-1)/2)
       DIMENSION TMD(300)
         COMMON /WORKSP/RWKSP
         COMMON /CONST/ ALFA,PI,KT,KKNT
         COMMON /GRID/ DR0,DT0,NDP,NP
         COMMON /INTG/ AT0,ERRREL,IRULE
         COMMON /SOLID/ SK,SC,SR
         COMMON /TSTEP/ NT
       CALL IWKIN(NIMSL+NIMSL*(NIMSL-1)/2)
C...GET ALL INFORMATION FROM THE EVAPORATION PROCESS
C...AS THE INITIAL CONDITION OF THE RECOVERY PROCESS
       READ(15,*)ETIME,DTIME,TMPAIR,TSLD0,RR,RHK,KT,MMD
       READ(15,*)VO,BETA,IDMAT,DT0,NDP,NP,AT0,ERRREL,IRULE,ALFA,PI
       DO 10 I=1,JM+JE-1
       READ(15,*)(W0(I,J),J=1,JM+JE-1)
  10   CONTINUE
       READ(15,*)(TN1(I),I=1,JM+JE)
       READ(15,*)(RS0(I),I=1,JM+JE-1)
       READ(15,*)(RHS(I),I=1,JM+JE-1)
       DO 11 K=1,KT
       READ(15,*)(FTIM(I,K),I=1,JM+JE-1)
  11   CONTINUE
       PRINT *,'NUMBER OF PLOTS?'
       READ(5,*)NPT
       PRINT *,'AT WHAT TIME (SECOND)'
       READ(5,*)(PTT(NN),NN=1,NPT)
C...
       TIME=-DTIME
       NT=0
       KKNT=1
       DTEMP=.005
C....SET 0 MATRIX
       DO 90 I=1,JM+JE
       DO 90 J=1,JM+JE
       TB(I,J)=0.
  90   CONTINUE
C....
       DO 150 J=2,JM+JE
       DO 155 JJ=2,JM+JE
```

```
        TB(J,JJ)=RHK*W0(J-1,JJ-1)
  155      CONTINUE
        TB(J,J)=1.+RHK*W0(J-1,J-1)
  150      CONTINUE
C...FOR J=1. B.C. T(I,1)=T(I,2)
        J=1
        TB(J,1)=1.
        TB(J,2)=-1.
        TR(J)=0.
C......NORMALIZING THE MATRIX
        DO 133 I=1,JM+JE
        TBM(I)=TB(I,I)
        DO 133 J=1,JM+JE
        TB(I,J)=TB(I,J)/TBM(I)
  133       CONTINUE
C..
        CALL SOLVE1(JM+JE,TB,TR,TX,IWK,WK)
C.....................
  1     NT=NT+1
C.....................
        TIME=TIME+DTIME
C.............................................................
        TN10=TN1(2)
C....FOR PTS ON SOLID EXPOSED SURFACE
        DO 151 J=2,JM+JE
        SWJ=0.
        DO 157 JJ=2,JM+JE
        SWJ=SWJ+W0(J-1,JJ-1)
  157   CONTINUE
        TR(J)=RHS(J-1)+(TSLD0-TMPAIR)*(1.+RHK*SWJ)
  151      CONTINUE
C......NORMALIZING THE MATRIX
        DO 143 I=1,JM+JE
        TR(I)=TR(I)/TBM(I)
  143       CONTINUE
C.............................................................
        CALL SOLVE2(JM+JE,TB,TR,TX)
C...
        DO 300 J=1,JM+JE
        THALF(J)=.5*(TN1(J)+TX(J))
        TN1(J)=TX(J)
  300       CONTINUE
C..... UPDATE THE FLUX MATRIX
        KKT=KT+NT
        DO 417 KK=KKT,2,-1
        DO 417 II=1,JM+JE-1
        FTIM(II,KK)=FTIM(II,KK-1)
  417   CONTINUE
        DO 418 JJ=2,JM+JE
C...FLUXES
        FTIM(JJ-1,1)=-RHK*(TN1(JJ)+TMPAIR-TSLD0)
```

```
 418    CONTINUE
C.....................................
       CALL NEXTR(NT,KKT,FTIM,RHS,TIME,W,F,WF,RS0,W1)
C...TEST FOR CENTER POINT TEMPERATURE DIFFERENCE
       IF(NT.GT.1.AND.ABS(TN10-TN1(2)).LE.DTEMP)GO TO 3
       GO TO 1
C.....................................................................
  3    PRINT *,'THE SOLID IS RECOVERED AT TIME=',TIME
       STOP
       END
C
         SUBROUTINE NEXTR(NT,KT,FTIM,R,TIME,W,F,WF,RS0,W1)
         DIMENSION W(NP,NP),F(NP),FTIM(NP,KT)
         DIMENSION WF(NP),R(NP),RS0(NP)
         DIMENSION W1(NP,NP,500)
         COMMON /CONST/ ALFA,PI,KNT,KKNT
         COMMON /GRID/ DR0,DT0,NDP,NP
         COMMON /INTG/ AT0,ERRREL,IRULE
         COMMON /MATER/ LMAT
         DO 149 II=1,NP
         R(II)=0.
 149      CONTINUE
         KKT=KT
         DO 150 IT=1,KKT
C   SELECT PROPER WEIGHTS
         T0=IT*DT0
C..
       IF(IT.LE.KKNT)THEN
        DO 151 I=1,NP
        DO 151 J=1,NP
        W(I,J)=W1(I,J,IT)
 151    CONTINUE
       ELSE
C.....
         CALL WEIGHT(T0,W,RS0)
C...
        DO 152 I=1,NP
        DO 152 J=1,NP
        W1(I,J,IT)=W(I,J)
 152    CONTINUE
       ENDIF
C   PICK UP CORRESPONDING FLUX
         DO 100 I=1,NP
         F(I)=FTIM(I,IT)
 100     CONTINUE
C   SUMMATION IN SPACE
         CALL MULT(NP,NP,W,F,WF)
C   SUMMATION IN TIME
         CALL ADD(NP,WF,R)
 150     CONTINUE
       KKNT=KKT
```

```
      RETURN
      END
C
      SUBROUTINE MULT(M,N,W,F,WF)
      REAL W(M,N),F(N),WF(N)
      DO 50 I=1,M
      WF(I)=0.0
      DO 50 K=1,N
      WF(I)=WF(I)+W(I,K)*F(K)
 50   CONTINUE
      RETURN
      END
C
      SUBROUTINE ADD(NP,WF,R)
      REAL WF(NP),R(NP)
      DO 50 I=1,NP
      R(I)=R(I)+WF(I)
 50   CONTINUE
      RETURN
      END
C
      SUBROUTINE WEIGHT(T0,W,RS0)
      REAL W(NP,NP),RS0(NP)
      REAL QDAG,BSI0E,ERF
      EXTERNAL F1
C
      COMMON /CONST/ ALFA,PI,KNT,KKNT
      COMMON /GRID/ DR0,DT0,NDP,NP
      COMMON /INTG/ AT0,ERRREL,IRULE
      COMMON /RR0/ R,R0
      COMMON /MATER/ LMAT
C
      DO 50 I=1,NP
      DO 50 J=1,NP
      IF(J.EQ.1)THEN
      DR0=2.*RS0(J)
      ELSE
      IF(J.EQ.NP)THEN
      DR0=DR0
      ELSE
      DR0=.5*(RS0(J+1)-RS0(J-1))
      ENDIF
      ENDIF
      R=RS0(I)
      R0=RS0(J)
C      PRINT *,DR0,R,R0
C   SET UP (W) FOR T0 < DT0
      ERRABS=0.0
      IF(T0.LT.DT0)THEN
      W(I,J)=QDAG(F1,AT0,.5,ERRABS,ERRREL,IRULE,RESULT,ERREST)
      W(I,J)=RESULT
```

```
          END IF
C    SET UP (W) FOR T0 > DT0
          IF(T0.GE.DT0)THEN
          ARG1=DR0/SQRT(16*ALFA*T0)
          ARG3=(R-R0)**2/(4*ALFA*T0)
          ARG4=0.5*R*R0/(ALFA*T0)
          IF(I.NE.J)THEN
          W(I,J)=(1.0/SQRT(4.0*PI*ALFA))*R0*(T0**(-1.5))*
     &           BSI0E(ARG4)*EXP(-ARG3)*DR0*DT0
          ELSE
          W(I,J)=(R/T0)*BSI0E(ARG4)*ERF(ARG1)*DT0
          END IF
          END IF
C
   50     CONTINUE
          RETURN
          END
C
          FUNCTION F1(T0)
          REAL BSI0E,ERF
          COMMON /CONST/ ALFA,PI,KNT,KKNT
          COMMON /GRID/ DR0,DT0,NP
          COMMON /RR0/ R,R0
C
          ARG1=DR0/SQRT(16*ALFA*T0)
          ARG3=(R-R0)**2/(4*ALFA*T0)
          ARG4=0.5*R*R0/(ALFA*T0)
          E=0.0
          IF(ARG3.LE.100.0)E=EXP(-ARG3)
          IF(R.NE.R0)THEN
          F1=(1.0/SQRT(4.0*PI*ALFA))*R0*(T0**(-1.5))*
     &      BSI0E(ARG4)*E*DR0
          ELSE
          F1=(R/T0)*BSI0E(ARG4)*ERF(ARG1)
          END IF
          RETURN
          END
        SUBROUTINE SOLVE1(N,A,B,X,IWK,WK)
C
C.....SUBROUTINE FOR SOLVING MATRIX
C...'LINK XXX,SOLVE,IMSL/LIB'....
        DIMENSION A(N,N),B(N),X(N)
        DIMENSION IWK(N),WK(N+N*(N-1)/2)
        INTEGER N
        COMMON /WORKSP/RWKSP
        CALL L2NRG(N,A,N,A,N,WK,IWK)
        RETURN
        END
C...
        SUBROUTINE SOLVE2(N,A,B,X)
C.....SUBROUTINE FOR SOLVING MATRIX
```

```
C...'LINK XXX,SOLVE,IMSL/LIB'....
      DIMENSION A(N,N),B(N),X(N)
      INTEGER N
      DO 100 J=1,N
      X(J)=0.0
      DO 100 I=1,N
      X(J)=X(J)+A(J,I)*B(I)
 100  CONTINUE
      RETURN
      END
```

```
C....PROGRAM FOR SOLVING A CONDUCTION HEAT TRANSFER PROBLEM IN A
C....LIQUID DROPLET LAID ON THE SURFACE OF AN INFINITE LARGE SOLID.
C......THE BOUNDARY ELEMENT METHOD IS USED FOR THE SOLID
C......AND THE INTEGRAL CONTROL VOLUME METHOD IS USED FOR THE
C......LIQUID
C......CRANK-NICHOLSON SCHEME IS USED
C......IM: NUMBER OF POINTS IN LIQUID DROP IN VERTICAL DIRECTION
C......JM: NUMBER OF POINTS IN LIQUID DROP IN HORIZATAL DIRECTION
C......JE: NUMBER OF POINTS ON EXPOSED SOLID SURFACE
C......KNT0: NUMBER OF RECOLLECTION TIME STEPS
C......NIMSL: TOTAL GRID POINTS
      PARAMETER (IM=16,JM=11,JS=JM-1,JE=4*JS,
     $           KNT0=60,NIMSL=IM*JM+JE)
      DIMENSION TN1(IM*JM+JE),TR(IM*JM+JE),THALF(IM*JM+JE)
      DIMENSION TX(IM*JM+JE),TA(IM*JM,4),TB(IM*JM+JE,IM*JM+JE)
      DIMENSION W(JM+JE-1,JM+JE-1),FTIM(JM+JE-1,KNT0),F(JM+JE-1)
      DIMENSION W1(JM+JE-1,JM+JE-1,KNT0)
      DIMENSION RHS(JM+JE-1),CT(JM),W0(JM+JE-1,JM+JE-1)
      DIMENSION EWIS(JM),SX(JM),SX2(JM)
      DIMENSION R(IM+1,JM+1),Z(IM+1,JM+1),DZ(JM),RS0(5*JS)
      DIMENSION RO3(IM),ZO3(IM),PTT(50)
      DIMENSION IWK(NIMSL),WK(NIMSL+NIMSL*(NIMSL-1)/2)
      DIMENSION TMD(300),TPLOT((IM-1)*(JM-1)+1)
      DIMENSION TBS(JM+JE,JM+JE),TRS(JM+JE),TXS(JM+JE)
        COMMON /SUBS/TIME,DTIME,TMPAIR,TSLD0,RR,KNT,RHK
        COMMON /WORKSP/RWKSP
        COMMON /CONST/ ALFA,PI
        COMMON /GRID/ DR0,DT0,NDP,NP
        COMMON /INTG/ AT0,ERRREL,IRULE
        COMMON /SOLID/ SK,SC,SR
        COMMON /WATER/ COEFKW,CPW,RHOW
        COMMON /TSTEP/ NT
C..
        PI=4.*ATAN(1.0)
        IRULE=2
        AT0=0.001
        ERRREL=0.001
        DTIME=.1
        NTIME=500
C....CHOICE OF THE MATERIAL FOR THE SOLID SURFACE
        PRINT *,' SOLID = ?  (TEST=0, ALUMINUM=1, MACOR=2,
     $  STEEL=3,MARBLE=4,BAKELITE=5)'
        READ(5,*)LMAT
C....INITIAL SETTING THE DROPLET SIZE BY KNOWING V0 AND BETA
        PRINT *,' INITIAL VOLUME OF THE DROPLET= ?'
        READ(5,*)VO
        PRINT *,' BETA= ?'
        READ(5,*)BETA
C...RR: RADIUS OF THE WETTED AREA
C...AA: APEX OF THE DROPLET
        RR=BETA*EXP(1./3.*LOG(.75*VO/PI))
```

```
          UU=EXP(1./3.*LOG(3.*VO/PI+SQRT(RR**6+9./PI**2*VO**2)))
          AA=UU-RR**2/UU
C..
          MMD=INT(10*RR)
C.........
          VO0=VO
          AA0=AA
C....VERIFY
        VO=PI*AA/6.*(3.*RR**2+AA**2)
        PRINT *,'RR=',RR,' AA=',AA,' VO=',VO,' DT=',DTIME
C...AIR TEMP.
        TMPAIR=20.
C...INITIAL TEMPERATURE OF THE LIQUID DROP
        TEMP0=20.
C...INITIAL TEMPERATURE OF THE SOLID
        PRINT *,'INITIAL SOLID TEMPERATURE:'
        READ(5,*)TSLD0
C...ALL  TEMPERATURES  USED  HERE,  TN1  AND  TX,  ARE  DELTAT  :
U=TEMP-TMPAIR
        TAIR=TMPAIR-TMPAIR
C...SOLID CONDUCTIVITY (SK:W/MM K; SR:KG/MM^3; SC:J/KG K)
         IF(LMAT.EQ.0)THEN
         PRINT *,'SK(W/MM K), SR(KG/MM^3), SC(J/KG K)'
         READ(5,*)SK,SR,SC
         ENDIF
C.......ALUMINUM:
         IF(LMAT.EQ.1)THEN
         SK=180.E-3
         SR=2771.E-9
         SC=962.32
         ENDIF
C.......MACOR:
         IF(LMAT.EQ.2)THEN
         SK=1.297E-3
         SR=2520.E-9
         SC=888.9
         ENDIF
C.......STEEL:
         IF(LMAT.EQ.3)THEN
         SK=12.E-3
         SR=8100.E-9
         SC=460.
         ENDIF
C.......MARBLE:
         IF(LMAT.EQ.4)THEN
         SK=2.8E-3
         SR=2600.E-9
         SC=810.
         ENDIF
C.......BAKELITE:
         IF(LMAT.EQ.5)THEN
```

```
          SK=.23E-3
          SR=1300E-9
          SC=1600.
          ENDIF
C...CONVECTIVE HEAT TRANSFER COEFF. FOR LIQUID SURFACE (W/MM^2 K)
          COEFFH=(.098*TSLD0+2.79)*1.E-6
C...HEAT TRANSFER COEFF. FOR EXPOSED SOLID SURFACE
          SH=COEFFH
C...RATIO OF SOLID H AND K : H/K
         RHK=SH/SK
C...DIFFUSIVITY OF SOLID (MM^2/S)
         ALFA=SK/(SR*SC)
C...WATER DENSITY (KG/MM^3)
         RHOW=997.6E-9
C...WATER CONDUCTIVITY (W/MM K)
         COEFKW=.613E-3
C...WATER SPECIFIC HEAT(J/KG K)
         CPW=4179.
C...DIFFUSIVITY OF WATER: ALPHA=KW/(RHO*CP) (MM^2/S)
          ALPHA=COEFKW/(RHOW*CPW)
C...RATIO BETWEEN LIQUID AND SOLID CONDUCTIVITES
          RKLS=COEFKW/SK
C...AIR SPECIFIC HEAT (J/KG K)
         CA=1009.
C...AIR PRESSURE (BAR)
         PA=1.014
C..XA IS DETERMINED WHEN PJ IS EVALUATED AT AIR TEMP.
C         XA=EXP(11.7789-3876.0717/(TMPAIR+229.4483))/PA
         XA=.012
C....LAMDA (LATENT HEAT): (J/KG)
C         ALAMDA=(2509.-2.51*TJ)*1000.
         ALAMDA=2250.*1000.
         ALAMD=2500.*1000.
C..........FOR PLOT INFORMATION
         PRINT *,'HOW MANY PLOTS YOU NEED?'
         READ(5,*)NPT
         PRINT *,'AT WHAT TIME (SECOND)'
         READ(5,*)(PTT(NN),NN=1,NPT)
C...INITIAL SETTING THE DROPLET TEMP.
         DO 5 I=1,IM
         DO 5 J=1,JM
         IJ=(I-1)*JM+J
         TN1(IJ)=TEMP0-TMPAIR
  5         CONTINUE
C....CONTACT TEMPERATURE
         CALL CTEMP0(IM,JM,JE,TMPAIR,TN1,TSLD0,CT,TT0)
C....SETTING INITIAL TEMP. FOR FAKE PTS. (TN1(I=IM))
         DO 51 J=1,JM+JE
         IJ=(IM-1)*JM+J
         TN1(IJ)=TSLD0-TMPAIR
         ENDIF
```

```
  51      CONTINUE
C...MAXIMUM TEMP. LIMIT
        TLIMIT=99.5-TMPAIR
        RR0=AA
        Q0=RHOW*VO*ALAMD/(PI*RR**2)
        TE0=RR0*RHOW*CPW/COEFFH
        TFINT=0.
        TF1=0.
        TF2=0.
C....FOR AN INITIAL TEMP SETUP
          KL=0
          KKNT=0
          TIME=-0.5*DTIME
 999      IF(KKNT.EQ.0)THEN
          KNT=10
          ELSE
          KNT=KNT0
          AA=AA0
          VO=VO0
          ENDIF
          NT=0
C....
          DO 53 I=1,JM+JE-1
          RHS(I)=0.
  53      CONTINUE
C.....................................
C         DO 1 NT=1,NTIME
  1       NT=NT+1
C.....................
         TIME=TIME+DTIME
C...SET NEW GRID POINTS BASED ON NEW RR,AA
        CALL RZ90(IM,JM,RR,AA,R,Z,JS,RS0)
        CALL TRIO(IM,JM,R,Z,RO3,ZO3)
        CALL DZ0(IM,JM,R,Z,RO3,ZO3,DZ)
C.....................................................................
        IF(NT.EQ.1.AND.KKNT.EQ.0)THEN
        DTIME=.1
        TTT=DTIME*.99
        NDP=JM-1
        NP=JM+JE-1
        DT0=DTIME
        CALL WEIGHT(TTT,W0,RS0)
        ENDIF
   81       CONTINUE
C...SET 0 MATRIX
        DO 90 I=1,IM*JM+JE
        DO 90 J=1,IM*JM+JE
        TB(I,J)=0.
  90        CONTINUE
C...FOR LIQUID: INNER POINTS
        DO 100 I=2,IM-1
```

```
        DO 100 J=2,JM-1
        CALL NEWSO(IM,JM,R,Z,RO3,ZO3,
     $             I,J,RN,ZN,RE,ZE,RW,ZW,RS,ZS,RO,ZO)
        ALAB=SQRT((R(I+1,J+1)-R(I,J+1))**2+(Z(I+1,J+1)-Z(I,J+1))**2)
        ALBC=SQRT((R(I,J+1)-R(I,J))**2+(Z(I,J+1)-Z(I,J))**2)
        ALCD=SQRT((R(I,J)-R(I+1,J))**2+(Z(I,J)-Z(I+1,J))**2)
        ALDA=SQRT((R(I+1,J)-R(I+1,J+1))**2+(Z(I+1,J)-Z(I+1,J+1))**2)
        AREA=.25*(ALAB+ALCD)*(ALBC+ALDA)
        DXN=SQRT((RN-RO)**2+(ZN-ZO)**2)
        DXW=-SQRT((RO-RW)**2+(ZO-ZW)**2)
        DXS=-SQRT((RO-RS)**2+(ZO-ZS)**2)
        DXE=SQRT((RE-RO)**2+(ZE-ZO)**2)
        IJ=(I-1)*JM+J
C....
        CONST=.25*DTIME*ALPHA/(RO*AREA)
        AIM1J=CONST*ALBC*(R(I,J+1)+R(I,J))/DXN
        AIJP1=CONST*ALAB*(R(I+1,J+1)+R(I,J+1))/DXE
        AIJM1=-CONST*ALCD*(R(I,J)+R(I+1,J))/DXW
        AIP1J=-CONST*ALDA*(R(I+1,J)+R(I+1,J+1))/DXS
        AIJ=-(AIM1J+AIJM1+AIJP1+AIP1J)
C....
        TB(IJ,IJ+1)=-AIJP1
        TB(IJ,IJ+JM)=-AIP1J
        TB(IJ,IJ-JM)=-AIM1J
        TB(IJ,IJ-1)=-AIJM1
        TB(IJ,IJ)=1.-AIJ
C...
        IF(NT.EQ.1)THEN
        TA(IJ,1)=AIJP1
        TA(IJ,2)=AIP1J
        TA(IJ,3)=AIM1J
        TA(IJ,4)=AIJM1
        ENDIF
        TR(IJ)=TA(IJ,1)*TN1(IJ+1)+TA(IJ,2)*TN1(IJ+JM)
     $+TA(IJ,3)*TN1(IJ-JM)+TA(IJ,4)*TN1(IJ-1)
     $+(1.-(TA(IJ,3)+TA(IJ,4)+TA(IJ,1)+TA(IJ,2)))*TN1(IJ)
C..SAVE FOR NEXT TIME STEP
        TA(IJ,1)=AIJP1
        TA(IJ,2)=AIP1J
        TA(IJ,3)=AIM1J
        TA(IJ,4)=AIJM1
C..
  100       CONTINUE
C....FOR J=JM: EDGE POINTS, TRIANGULAR ELEMENTS
        J=JM
        DO 110 I=2,IM-1
        CALL NEWSO(IM,JM,R,Z,RO3,ZO3,
     $             I,J,RN,ZN,RE,ZE,RW,ZW,RS,ZS,RO,ZO)
        ALCA=SQRT((R(I,J+1)-R(I+1,J))**2+(Z(I,J+1)-Z(I+1,J))**2)
        ALAB=SQRT((R(I,J+1)-R(I,J))**2+(Z(I,J+1)-Z(I,J))**2)
        ALBC=SQRT((R(I+1,J)-R(I,J))**2+(Z(I+1,J)-Z(I,J))**2)
```

```
        AREA=.25*(ALCA+ALAB)*(ALBC+ALAA)
        DXN=SQRT((RN-RO)**2+(ZN-ZO)**2)
        DXW=-SQRT((RO-RW)**2+(ZO-ZW)**2)
        DXS=-SQRT((RO-RS)**2+(ZO-ZS)**2)
        IJ=(I-1)*JM+J
C....
        CONST=.25*DTIME*ALPHA/(RO*AREA)
        AIJP1=0.
        AIP1J=-CONST*ALCA*(R(I+1,J)+R(I,J+1))/DXS
        AIM1J=CONST*ALAB*(R(I,J+1)+R(I,J))/DXN
        AIJM1=-CONST*ALBC*(R(I,J)+R(I+1,J))/DXW
        AIJ=-(AIM1J+AIJM1+AIJP1+AIP1J)
C....
        TB(IJ,IJ+1)=-AIJP1
        TB(IJ,IJ+JM)=-AIP1J
        TB(IJ,IJ-JM)=-AIM1J
        TB(IJ,IJ-1)=-AIJM1
        TB(IJ,IJ)=1.-AIJ
        IF(NT.EQ.1)THEN
        TA(IJ,1)=AIJP1
        TA(IJ,2)=AIP1J
        TA(IJ,3)=AIM1J
        TA(IJ,4)=AIJM1
        ENDIF
        TR(IJ)=TA(IJ,2)*TN1(IJ+JM)

     $         +TA(IJ,3)*TN1(IJ-JM)+TA(IJ,4)*TN1(IJ-1)

     $         +(1.-(TA(IJ,3)+TA(IJ,4)+TA(IJ,1)+TA(IJ,2)))*TN1(IJ)
C..SAVE FOR NEXT TIME STEP
        TA(IJ,1)=AIJP1
        TA(IJ,2)=AIP1J
        TA(IJ,3)=AIM1J
        TA(IJ,4)=AIJM1
C..
  110       CONTINUE
C..FOR I=1: LIQUID - AIR INTERFACE
        I=1
        DO 120 J=2,JM
C...PROPERTIES BASED ON THE DROPLET SURFACE TEMP. TJ(DEGREE C)
        TJ=.5*(TN1(J)+TN1(J+JM))+TMPAIR
C....SURFACE PRESSURE (BAR).
C....10<TJ<100, OTHERWISE SX<0. AND DVDT<0.
        IF(TJ.LE.10..AND.TJ.GE.100.)PRINT *,'TJ IS OUT RANGE FOR SX'
        IF(TJ.GE.99.5)THEN
        PJ=1.
        ELSE
        PJ=EXP(11.7789-3876.0717/(TJ+229.4483))
        ENDIF
        XJ=PJ/PA
        SX(J)=(XJ-XA)/(1.-XJ)
```

```
C...LEWIS NUMBER
      EWIS(J)=6.0*(-.0005279*TJ+1.152)
C........
      IJ=J
      IF(J.EQ.JM)THEN
      RM=RO3(I)
      ZM=ZO3(I)
      RP=RO3(I+1)
      ZP=ZO3(I+1)
      ELSE
      RM=.25*(R(I,J)+R(I,J+1)+R(I+1,J+1)+R(I+1,J))
      ZM=.25*(Z(I,J)+Z(I,J+1)+Z(I+1,J+1)+Z(I+1,J))
      RP=.25*(R(I+1,J)+R(I+1,J+1)+R(I+2,J+1)+R(I+2,J))
      ZP=.25*(Z(I+1,J)+Z(I+1,J+1)+Z(I+2,J+1)+Z(I+2,J))
      ENDIF
      DZ1=SQRT((RM-RP)**2+(ZM-ZP)**2)
      TB(IJ,IJ+JM)=1.-.5*COEFFH*DZ1/COEFKW
      TB(IJ,IJ)=-1.-.5*COEFFH*DZ1/COEFKW
C...CONST1 IS FROM THE B.C.
      ALAMDA=(2509.-2.51*TJ)*1000.
      CONST1=.624*DZ1*COEFFH*ALAMDA*EWIS(J)*SX(J)/(COEFKW*CA)
C....
      TR(IJ)=CONST1-TAIR*DZ1*COEFFH/COEFKW
  120       CONTINUE
C..FOR I=IM: LIQUID - SOLID INTERFACE
C...COUPLED BOUNDARY ELEMENT AND CONTROL VOLUME METHODS
      I=IM
      PRINT *,'TIME=',TIME
C.................................................
      DO 130 J=2,JM
      IJ=(I-1)*JM+J
      DO 135 JJ=2,JM
      IJ1=(I-1)*JM+JJ
      IJ2=(I-2)*JM+JJ
      IF(IJ1.NE.IJ)THEN
      TB(IJ,IJ1)=RKLS*W0(J-1,JJ-1)/DZ(JJ)
      TB(IJ,IJ2)=-RKLS*W0(J-1,JJ-1)/DZ(JJ)
      ELSE
      TB(IJ,IJ1)=.5+RKLS*W0(J-1,J-1)/DZ(JJ)
      TB(IJ,IJ2)=.5-RKLS*W0(J-1,J-1)/DZ(JJ)
      ENDIF
  135   CONTINUE
      DO 136 JJ=JM+1,JM+JE
      IJ3=(I-1)*JM+JJ
      TB(IJ,IJ3)=RHK*W0(J-1,JJ-1)
  136   CONTINUE
      TR(IJ)=RHS(J-1)
      SWJ=0.
      DO 137 JJ=2,JM+JE
      SWJ=SWJ+W0(J-1,JJ-1)
  137 CONTINUE
```

```
      TR(IJ)=TR(IJ)+(TSLD0-TMPAIR)*(1.+RHK*SWJ)
  130      CONTINUE
C....FOR PTS ON SOLID EXPOSED SURFACE
      DO 150 J=JM+1,JM+JE
      IJ=(I-1)*JM+J
      TB(IJ,IJ)=1.+RHK*W0(J-1,J-1)
      DO 155 JJ=2,JM
      IJ1=(I-1)*JM+JJ
      IJ2=(I-2)*JM+JJ
      TB(IJ,IJ1)=RKLS*W0(J-1,JJ-1)/DZ(JJ)
      TB(IJ,IJ2)=-RKLS*W0(J-1,JJ-1)/DZ(JJ)
  155    CONTINUE
      DO 156 JJ=JM+1,JM+JE
      IJ3=(I-1)*JM+JJ
      IF(IJ3.NE.IJ)TB(IJ,IJ3)=RHK*W0(J-1,JJ-1)
  156    CONTINUE
       TR(IJ)=RHS(J-1)
      SWJ=0.
      DO 157 JJ=2,JM+JE
      SWJ=SWJ+W0(J-1,JJ-1)
  157  CONTINUE
      TR(IJ)=TR(IJ)+(TSLD0-TMPAIR)*(1.+RHK*SWJ)
  150    CONTINUE
C...FOR J=1. B.C. T(I,1)=T(I,2), SYMMETRIC TO Z-AXIS
      J=1
      DO 140 I=1,IM
      IJ=(I-1)*JM+J
      TB(IJ,IJ)=1.
      TB(IJ,IJ+1)=-1.
      TR(IJ)=0.
  140      CONTINUE
C......NORMALIZING THE MATRIX
      DO 143 I=1,IM*JM+JE
      TBM=TB(I,I)
      DO 144 J=1,IM*JM+JE
      TB(I,J)=TB(I,J)/TBM
  144      CONTINUE
      TR(I)=TR(I)/TBM
  143      CONTINUE
C...TEMPERATURE CALCULATION BY SOLVING TB*TX=TR
C....SOLVE FOR EVERY STEP AFTER PRE-SETTING A TEMP. DISTRIBU
                  IF(NT.NE.1.OR.KKNT.NE.0)THEN
C.....................................................
      CALL SOLVE(IM*JM+JE,TB,TR,TX,IWK,WK)
      KT=0
C....AVERAGE BETWEEN CURRENT AND PREVIOUS STEPS
      DO 300 IJ=1,IM*JM+JE
      THALF(IJ)=.5*(TN1(IJ)+TX(IJ))
      TN1(IJ)=TX(IJ)
  300      CONTINUE
      JU=(IM-2)*JM
```

```
        JL=(IM-1)*JM
C......MDDATA DRL=1.
        TMD(1)=.25*(THALF(JU+1)+THALF(JU+2)+THALF(JL+1)
     $             +THALF(JL+2))+TMPAIR
        DO 910 I=1,MMD
        DO 911 J=2,JM+JE-1
        IF(I.GE.RS0(J-1).AND.I.LT.RS0(J))THEN
        IF(I.LT.RR)THEN
        TMD1=.5*(THALF(JU+J)+THALF(JL+J))
        TMD2=.5*(THALF(JU+J+1)+THALF(JL+J+1))
        TMD(I+1)=(TMD2-TMD1)*(I-RS0(J-1))/
     $ (RS0(J)-RS0(J-1))+TMD1+TMPAIR
        ENDIF
        IF(I.EQ.RR)THEN
        TMD1=.5*(THALF(JU+JM)+THALF(JL+JM))
        TMD2=THALF(IM*JM+1)
        TMD(I+1)=(TMD2-TMD1)*(I-RS0(J-1))/
     $ (RS0(J)-RS0(J-1))+TMD1+TMPAIR
        ENDIF
        IF(I.GT.RR)THEN
        TMD1=THALF((IM-1)*JM+J)
        TMD2=THALF((IM-1)*JM+J+1)
        TMD(I+1)=(TMD2-TMD1)*(I-RS0(J-1))/
     $ (RS0(J)-RS0(J-1))+TMD1+TMPAIR
        ENDIF
        ENDIF
  911   CONTINUE
        TEDGE=THALF(IM*JM)+(THALF(IM*JM+1)
     $ -THALF(IM*JM))*(RR-RS0(JS))
     $       /(RS0(JS+1)-RS0(JS))+TMPAIR
        T3R=THALF(IM*JM+2.*JS)+TMPAIR
        IF(I.GE.RS0(JM+JE-1))THEN
        TMD(I+1)=TSLD0
        ENDIF
  910   CONTINUE
C......FORCING ALL TEMP. UNDER THE LIMIT
        DO 310 I=1,2
        DO 310 J=1,JM
        IJ=(I-1)*JM+J
        IF(TN1(IJ).GE.TLIMIT)TN1(IJ)=TLIMIT
  310    CONTINUE
C....CAL NEW DROPLET VOLUME AND AA
        CALL SURF(DTIME,IM,JM,RR,VO,AA,R,Z,DVDT,
     $            EWIS,COEFFH,SX,RHOW,CA)
C.....................................................................
                                ENDIF
C...   UPDATE THE FLUX MATRIX
        DO 417 KK=KNT,2,-1
        DO 417 II=1,JM+JE-1
        FTIM(II,KK)=FTIM(II,KK-1)
  417   CONTINUE
```

```
C...  COMPUTE THE FLUX AT CURRENT TIME: FTIM(II,1)
        DO 418 JJ=2,JM+JE
        J1=(IM-1)*JM+JJ
        J2=(IM-2)*JM+JJ
        I=IM
C...FLUXES
        IF(JJ.LE.JM)THEN
        FTIM(JJ-1,1)=RKLS*(TN1(J2)-TN1(J1))/DZ(JJ)
     $               +RHK*(TSLD0-TMPAIR)
        ELSE
        FTIM(JJ-1,1)=-RHK*(TN1(J1)+TMPAIR-TSLD0)
        ENDIF
 418    CONTINUE
C...FOR SOLID SURFACE POINTS
        CALL NEXTR(NT,KNT,FTIM,RHS,TIME,W,F,WF,RS0,W1)
C...DETERMINE IF THE DROPLET IS COMPLETELY EVAPORATED
        IF(DVDT*DTIME.GT.VO.OR.AA.LT..01)THEN
        DO 700 J=1,JM+JE
        IF(J.LE.JM)THEN
        TN1(J)=.5*(TN1((IM-1)*JM+J)+TN1((IM-2)*JM+J))
        ELSE
        TN1(J)=TN1((IM-1)*JM+J)
        ENDIF
  700   CONTINUE
        ETIME=TIME
        PRINT *,'THE DROPLET IS GONE AT TIME=',ETIME
        ENDIF
        IF(NT.EQ.KNT+1.AND.KKNT.EQ.0)THEN
        DO 380 KK=KNT,1,-1
        DO 380 II=1,JM+JE-1
        FTIM(II,KK)=0.
  380   CONTINUE
        KKNT=1
        TIME=0.
        DTIME=.5
        DT0=DTIME
        NTCI=0
        GO TO 999
        ENDIF
C.....
        GO TO 1
C.....
  2     STOP
        END
C...SUB. ASSIGNING THE CENTER PTS. FOR THOSE CELLS AT EDGE WHICH
C...ARE TRIANGLES.
           SUBROUTINE TRIO(IM,JM,R,Z,RO3,ZO3)
        DIMENSION R(IM+1,JM+1),Z(IM+1,JM+1)
        DIMENSION RO3(IM),ZO3(IM)
        J=JM
        DO 10 I=1,IM
```

```
      A=(.5*(Z(I,J)+Z(I,J+1))-Z(I+1,J))/
     $   (.5*(R(I,J)+R(I,J+1))-R(I+1,J))
      B=(.5*(Z(I+1,J)+Z(I,J+1))-Z(I,J))/
     $   (.5*(R(I+1,J)+R(I,J+1))-R(I,J))
      IF(ABS(A-B).GT.1.E-7)
     $ RO3(I)=(Z(I,J)-Z(I+1,J)+A*R(I+1,J)-B*R(I,J))/(A-B)
      ZO3(I)=Z(I,J)+B*(RO3(I)-R(I,J))
   10 CONTINUE
      RETURN
      END
      SUBROUTINE NEWSO(IM,JM,R,Z,RO3,ZO3,I,J,RN,ZN,RE,ZE,
     $                 RW,ZW,RS,ZS,RO,ZO)
C
C....SUBROUTINE FOR ASSIGNING THE POSITIONS AT NORTH, EAST, WEST,
C....SOUTH OF  A CELL.
C....THE LEFT UPPER CORNER IS THE POSITION R(I,J) AND Z(I,J)
      DIMENSION R(IM+1,JM+1),Z(IM+1,JM+1)
      DIMENSION RO3(IM),ZO3(IM)
      IF(J.EQ.JM)THEN
      RO=RO3(I)
      ZO=ZO3(I)
      RN=RO3(I-1)
      ZN=ZO3(I-1)
      RS=RO3(I+1)
      ZS=ZO3(I+1)
      RW=.25*(R(I,J)+R(I,J-1)+R(I+1,J-1)+R(I+1,J))
      ZW=.25*(Z(I,J)+Z(I,J-1)+Z(I+1,J-1)+Z(I+1,J))
      ELSE
      RO=.25*(R(I,J)+R(I,J+1)+R(I+1,J+1)+R(I+1,J))
      ZO=.25*(Z(I,J)+Z(I,J+1)+Z(I+1,J+1)+Z(I+1,J))
      RE=.25*(R(I,J+1)+R(I,J+2)+R(I+1,J+2)+R(I+1,J+1))
      ZE=.25*(Z(I,J+1)+Z(I,J+2)+Z(I+1,J+2)+Z(I+1,J+1))
      RN=.25*(R(I,J+1)+R(I-1,J+1)+R(I-1,J)+R(I,J))
      ZN=.25*(Z(I,J+1)+Z(I-1,J+1)+Z(I-1,J)+Z(I,J))
      RW=.25*(R(I,J)+R(I,J-1)+R(I+1,J-1)+R(I+1,J))
      ZW=.25*(Z(I,J)+Z(I,J-1)+Z(I+1,J-1)+Z(I+1,J))
      RS=.25*(R(I+1,J)+R(I+1,J+1)+R(I+2,J+1)+R(I+2,J))
      ZS=.25*(Z(I+1,J)+Z(I+1,J+1)+Z(I+2,J+1)+Z(I+2,J))
      ENDIF
      RETURN
      END
C
      SUBROUTINE RZ90(IM,JM,RR,AA,R,Z,JS,RS0)
C
C.....SUBROUTINE FOR ASSIGNING THE GRID POINTS.....
C.....R(I,J), Z(I,J): I=1,IM+1, J=1,JM+1
C.....IMAGINARY POINTS: 1) R(1,J), Z(1,J)
C                       2) R(IM+1,J), Z(IM+1,J)
C                       3) R(I,1), Z(I,1)
C.....AA: DROPLET HEIGHT; RR: DROPLET RADIUS.
      DIMENSION Z(IM+1,JM+1),R(IM+1,JM+1)
```

```
      DIMENSION RS0(5*JS)
        COMMON /CONST/ ALFA,PI
        COMMON /TSTEP/ NT
      RRR=AA/RR
C..
      DO 10 I=2,IM
      FI=1.-(I*1.-2.)/(IM*1.-2.)
      DO 10 J=2,JM
      GJ=(J*1.-2.)/(JM*1.-1.)
C..
      IF(I.EQ.IM.OR.J.EQ.2)THEN
      IF(I.EQ.IM)THEN
      R(I,J)=RR*GJ
      Z(I,J)=0.
      ENDIF
      IF(J.EQ.2)THEN
      R(I,J)=0.
      Z(I,J)=AA*FI
      ENDIF
C..
      ELSE
      FIR=1./(FI*RRR)-FI*RRR
      A=(1.+GJ**2+2.*(1.-GJ))*RR/FIR
      B=-2.*(GJ+(1.-GJ)/GJ)/FIR
      IF(FIR.GT.1.E-3)THEN
      FACTOR=1.
      ELSE
      FACTOR=1.E-6
      ENDIF
      ALFA1=(1.+B**2)*FACTOR
      BEITA=2.*(A*B-(GJ+(1.-GJ)/GJ)*RR)*FACTOR
      GAMMA=(A**2+(GJ**2+2.*(1.-GJ))*RR**2)*FACTOR
      TF=BEITA**2-4.*ALFA1*GAMMA
      IF(TF.LT.0.)TF=0.
      IF(TF.GE.0.)THEN
      R(I,J)=(-BEITA-SQRT(TF))/(2.*ALFA1)
      ELSE
      PRINT *,'TF<0.????? IT IS WRONG! I=',I,' J=',J
      ENDIF
      Z(I,J)=SQRT((1./(FI*RRR)+FI*RRR)**2/4.*RR**2-R(I,J)**2)
     $ -(1./(FI*RRR)-FI*RRR)/2.*RR
       ENDIF
 10       CONTINUE
      DO 20 I=1,IM+1
      R(I,JM+1)=RR
      Z(I,JM+1)=0.
 20       CONTINUE
C..FOR IMAGINARY POINTS
      DO 30 I=1,IM+1
      R(I,1)=-R(I,3)+2.*R(I,2)
      Z(I,1)=Z(I,3)
```

```
  30        CONTINUE
            DO 40 J=1,JM
            R(IM+1,J)=R(IM-1,J)
            Z(IM+1,J)=-Z(IM-1,J)+2.*Z(IM,J)
  40        CONTINUE
            I=1
            AA1=AA+(Z(2,2)-Z(3,2))
            RRR=AA1/RR
            FI=1.
            Z(I,2)=FI*AA1
            DO 50 J=3,JM
            GJ=(J*1.-2.)/(JM*1.-1.)
            FIR=1./(FI*RRR)-FI*RRR
            A=(1.+GJ**2+2.*(1.-GJ))*RR/FIR
            B=-2.*(GJ+(1.-GJ)/GJ)/FIR
            IF(FIR.GT.1.E-3)THEN
            FACTOR=1.
            ELSE
            FACTOR=1.E-6
            ENDIF
            ALFA1=(1.+B**2)*FACTOR
            BEITA=2.*(A*B-(GJ+(1.-GJ)/GJ)*RR)*FACTOR
            GAMMA=(A**2+(GJ**2+2.*(1.-GJ))*RR**2)*FACTOR
            TF=BEITA**2-4.*ALFA1*GAMMA
            IF(TF.LT.0.)TF=0.
            IF(TF.GE.0.)THEN
            R(I,J)=(-BEITA-SQRT(TF))/(2.*ALFA1)
            ELSE
            PRINT *,'TF<0.????? IT IS WRONG! I=',I,' J=',J
            ENDIF
            Z(I,J)=SQRT((1./(FI*RRR)+FI*RRR)**2/4.*RR**2-R(I,J)**2)
           $-(1./(FI*RRR)-FI*RRR)/2.*RR
  50        CONTINUE
C....
            R(1,1)=-R(1,3)+2.*R(1,2)
            Z(1,1)=Z(1,3)
C.....ASSIGNING POINTS ON SOLID SURFACE WHERE THE TEMPERATURES
C.....ARE CALCULATED
            IF(NT.EQ.1)THEN
            DO 60 J=1,JS
            RS0(J)=.5*(R(IM,J+1)+R(IM,J+2))
  60    CONTINUE
C...USE FINER GRID NEAR THE EDGE
            DO 61 J=JS+1,3*JS
            AJ=(1.*J-1.*JS)/(2.*JS)*PI/2.
            RS0(J)=RR*(1.+2.*(1.-COS(AJ)))
  61    CONTINUE
            DR1=RS0(3*JS)-RS0(3*JS-1)
            DO 63 J=3*JS+1,4*JS
            RS0(J)=RS0(J-1)+2.*DR1
  63    CONTINUE
```

```
      DO 64 J=4*JS+1,5*JS
      RS0(J)=RS0(J-1)+8.*DR1
   64 CONTINUE
      ENDIF
C.....
      RETURN
      END
C
      SUBROUTINE DZ0(IM,JM,R,Z,RO3,ZO3,DZ)
C
C....SUBROUTINE FOR FINDING THE DZ AT THE LIQUID AND SOLID
C....INTERFACE
      DIMENSION R(IM+1,JM+1),Z(IM+1,JM+1),DZ(JM)
      DIMENSION RO3(IM),ZO3(IM)
      I=IM
      DO 135 JJ=2,JM
      IF(JJ.EQ.JM)THEN
      RM=RO3(I)
      ZM=ZO3(I)
      RP=RO3(I-1)
      ZP=ZO3(I-1)
      ELSE
      RM=.25*(R(I,JJ)+R(I,JJ+1)+R(I+1,JJ+1)+R(I+1,JJ))
      ZM=.25*(Z(I,JJ)+Z(I,JJ+1)+Z(I+1,JJ+1)+Z(I+1,JJ))
      RP=.25*(R(I-1,JJ)+R(I-1,JJ+1)+R(I,JJ+1)+R(I,JJ))
      ZP=.25*(Z(I-1,JJ)+Z(I-1,JJ+1)+Z(I,JJ+1)+Z(I,JJ))
      ENDIF
      DZ(JJ)=SQRT((RM-RP)**2+(ZM-ZP)**2)
  135   CONTINUE
      RETURN
      END
C
      SUBROUTINE SOLVE(N,A,B,X,IWK,WK)
C
C.....SUBROUTINE FOR SOLVING MATRIX
      DIMENSION A(N,N),B(N),X(N)
      DIMENSION IWK(N),WK(N+N*(N-1)/2)
      INTEGER N
      COMMON /WORKSP/RWKSP
      CALL L2NRG(N,A,N,A,N,WK,IWK)
      DO 100 J=1,N
      X(J)=0.0
      DO 100 I=1,N
      X(J)=X(J)+A(J,I)*B(I)
  100 CONTINUE
      RETURN
      END
C
      SUBROUTINE SURF(DTIME,IM,JM,RR,VO,AA,R,Z,DVDT,
     $                EWIS,COEFFH,SX,RHOW,CA)
C
```

```
C.....SUBROUTINE FOR CALCULATING THE SIZE OF THE LIQUID DROP RR, AA
C.....WHILE RR IS A CONSTANT
         DIMENSION R(1+IM,1+JM),Z(1+IM,1+JM),EWIS(JM),SX(JM)
         COMMON /MATER/ LMAT
        PI=4.*ATAN(1.)
C....VO=PI*AA/6.*(3.*RR**2+AA**2)
        SSX=0.
        DO 10 J=2,JM
        RJ=.5*(R(2,J)+R(2,J+1))
        DRJ=SQRT((R(2,J+1)-R(2,J))**2+(Z(2,J+1)-Z(2,J))**2)
        SSX=SSX+EWIS(J)*COEFFH*SX(J)*RJ*DRJ
  10        CONTINUE
        DVDT=2.*PI*.624/(RHOW*CA)*SSX
        VO=VO-DVDT*DTIME
C...SOLVING CUBE EQ. AA**3+3.*RR*82*AA-6./PI*VO=0.
        U=EXP(1./3.*LOG(3.*VO/PI+SQRT(RR**6+9./PI**2*VO**2)))
        AA=U-RR**2/U
        RETURN
        END
C
          SUBROUTINE NEXTR(NT,KT,FTIM,R,TIME,W,F,WF,RS0,W1)
          DIMENSION W(NP,NP),F(NP),FTIM(NP,KT),W1(NP,NP,KT)
          DIMENSION WF(NP),R(NP),RS0(NP)
          COMMON /CONST/ ALFA,PI
          COMMON /GRID/ DR0,DT0,NDP,NP
          COMMON /INTG/ AT0,ERRREL,IRULE
          COMMON /MATER/ LMAT
          DO 149 II=1,NP
          R(II)=0.
  149      CONTINUE
          IF(NT.LE.KT)THEN
          KKT=NT
          ELSE
          KKT=KT
          ENDIF
          DO 150 IT=1,KKT
C   SELECT PROPER WEIGHTS
          T0=IT*DT0
C..GET W FROM THE PREVIOUS CALCULATION
          IF(IT.LE.KKT-1.OR.KKT.EQ.KT)THEN
          DO 151 I=1,NP
          DO 151 J=1,NP
          W(I,J)=W1(I,J,IT)
  151     CONTINUE
          ELSE
C...CAL. THE WEIGHT FOR CURRENT TIME STEP
          CALL WEIGHT(T0,W,RS0)
C...SAVE FOR LATER STEPS
          DO 152 I=1,NP
          DO 152 J=1,NP
          W1(I,J,IT)=W(I,J)
```

```
  152     CONTINUE
          ENDIF
C   PICK UP CORRESPONDING FLUX
          DO 100 I=1,NP
          F(I)=FTIM(I,IT)
  100     CONTINUE
C   SUMMATION IN SPACE
          CALL MULT(NP,NP,W,F,WF)
C   SUMMATION IN TIME
          CALL ADD(NP,WF,R)
  150     CONTINUE
          RETURN
          END
C
          SUBROUTINE MULT(M,N,W,F,WF)
          REAL W(M,N),F(N),WF(N)
C
          DO 50 I=1,M
          WF(I)=0.0
          DO 50 K=1,N
          WF(I)=WF(I)+W(I,K)*F(K)
  50      CONTINUE
          RETURN
          END
C
          SUBROUTINE ADD(NP,WF,R)
          REAL WF(NP),R(NP)
C
          DO 50 I=1,NP
          R(I)=R(I)+WF(I)
  50      CONTINUE
          RETURN
          END
C
          SUBROUTINE WEIGHT(T0,W,RS0)
          REAL W(NP,NP),RS0(NP)
          REAL QDAG,BSI0E,ERF
          EXTERNAL F1
C
          COMMON /CONST/ ALFA,PI
          COMMON /GRID/ DR0,DT0,NDP,NP
          COMMON /INTG/ AT0,ERRREL,IRULE
          COMMON /RR0/ R,R0
          COMMON /MATER/ LMAT
C
          DO 50 I=1,NP
          DO 50 J=1,NP
          IF(J.EQ.1)THEN
          DR0=2.*RS0(J)
          ELSE
          IF(J.EQ.NP)THEN
```

```
            DR0=DR0
            ELSE
            DR0=.5*(RS0(J+1)-RS0(J-1))
            ENDIF
            ENDIF
            R=RS0(I)
            R0=RS0(J)
C    SET UP (W) FOR T0 < DT0
            ERRABS=0.0
            IF(T0.LT.DT0)THEN
            W(I,J)=QDAG(F1,AT0,.5,ERRABS,ERRREL,IRULE,RESULT,ERREST)
            W(I,J)=RESULT
            END IF
C    SET UP (W) FOR T0 > DT0
            IF(T0.GE.DT0)THEN
            ARG1=DR0/SQRT(16*ALFA*T0)
            ARG3=(R-R0)**2/(4*ALFA*T0)
            ARG4=0.5*R*R0/(ALFA*T0)
            IF(I.NE.J)THEN
            W(I,J)=(1.0/SQRT(4.0*PI*ALFA))*R0*(T0**(-1.5))*
     &           BSI0E(ARG4)*EXP(-ARG3)*DR0*DT0
            ELSE
            W(I,J)=(R/T0)*BSI0E(ARG4)*ERF(ARG1)*DT0
            END IF
            END IF
   50       CONTINUE
            RETURN
            END
C
            FUNCTION F1(T0)
            REAL BSI0E,ERF
            COMMON /CONST/ ALFA,PI
            COMMON /GRID/ DR0,DT0,NP
            COMMON /RR0/ R,R0
C
            ARG1=DR0/SQRT(16*ALFA*T0)
            ARG3=(R-R0)**2/(4*ALFA*T0)
            ARG4=0.5*R*R0/(ALFA*T0)
            E=0.0
            IF(ARG3.LE.100.0)E=EXP(-ARG3)
            IF(R.NE.R0)THEN
            F1=(1.0/SQRT(4.0*PI*ALFA))*R0*(T0**(-1.5))*
     &      BSI0E(ARG4)*E*DR0
            ELSE
            F1=(R/T0)*BSI0E(ARG4)*ERF(ARG1)
            END IF
            RETURN
            END
C
          SUBROUTINE CTEMP0(IM,JM,JE,TREF,TWATER,TSOLID,CT,TT0)
C...SUBROUTINE CALCULATING THE CONTACT TEMPERATURE TO BE USED AT
```

```
C...THE SOLID-LIQUID INTERFACE
      DIMENSION TWATER(IM*JM+JE),CT(JM)
      COMMON /SOLID/ SK,SC,SR
      COMMON /WATER/ COEFKW,CPW,RHOW
C......
      SQRCKW=SQRT(RHOW*CPW*COEFKW)
      SQRCKA=SQRT(SR*SC*SK)
C....
      DO 10 J=1,JM
      CT(J)=(SQRCKW*(TWATER((IM-2)*JM+J)+TREF)
     $                    +SQRCKA*TSOLID)/(SQRCKW+SQRCKA)
      TT=((SQRCKW+SQRCKA)*100.-SQRCKW*(TWATER((IM-2)*JM+J)
     $                    +TREF))/SQRCKA
C..DIMENSIONLESS TEMP.
      TT0=(TSOLID-TREF)/(TT-TREF)
C..
      IF(CT(1).GE.100.)THEN
      PRINT *,'THE CONTACT TEMP. IS GREATER THAN 100C!'
      PRINT *,' *** TRY AGAIN ***'
      PRINT *,'ENTER ANY NUMBER TO CONTINUE OR CTRL-C TO STOP'
      READ(5,*)NCT
      ENDIF
  10  CONTINUE
      PRINT *,'CONTACT TEMPERATURE=',CT(1)
      PRINT *,'DIMENSIONLESS TEMP: (TS-TAMB)/(TREF-TAMB)=',TT0
      RETURN
      END
```

NIST-114
(REV. 9-92)
ADMAN 4.09

U.S. DEPARTMENT OF COMMERCE
NATIONAL INSTITUTE OF STANDARDS AND TECHNOLOGY

MANUSCRIPT REVIEW AND APPROVAL

(ERB USE ONLY)
ERB CONTROL NUMBER | DIVISION
PUBLICATION REPORT NUMBER: NIST-GCR-93-623 | CATEGORY CODE

INSTRUCTIONS: ATTACH ORIGINAL OF THIS FORM TO ONE (1) COPY OF MANUSCRIPT AND SEND TO: THE SECRETARY, APPROPRIATE EDITORIAL REVIEW BOARD.

PUBLICATION DATE: April 1993 | NUMBER PRINTED PAGES

TITLE AND SUBTITLE (CITE IN FULL)

TRANSIENT COOLING OF A HOT SURFACE BY DROPLETS EVAPORATION

CONTRACT OR GRANT NUMBER: GRANT NO. 70NANB8H0840

TYPE OF REPORT AND/OR PERIOD COVERED: Final Report, November 1991

AUTHOR(S) (LAST NAME, FIRST INITIAL, SECOND INITIAL)
P. Tartarini, Y. Liao, C. Kidder, M. di Marzo
University of Maryland
Mechanical Engineering Department
College Park, MD 20742

PERFORMING ORGANIZATION (CHECK (X) ONE BOX)
[ ] NIST/GAITHERSBURG
[ ] NIST/BOULDER
[ ] JILA/BOULDER

LABORATORY AND DIVISION NAMES (FIRST NIST AUTHOR ONLY)

SPONSORING ORGANIZATION NAME AND COMPLETE ADDRESS (STREET, CITY, STATE, ZIP)
U.S. Department of Commerce
National Institute of Standards and Technology
Gaithersburg, MD 20899

RECOMMENDED FOR NIST PUBLICATION

[ ] JOURNAL OF RESEARCH (NIST JRES)	[ ] MONOGRAPH (NIST MN)	[ ] LETTER CIRCULAR
[ ] J. PHYS. & CHEM. REF. DATA (JPCRD)	[ ] NATL. STD. REF. DATA SERIES (NIST NSRDS)	[ ] BUILDING SCIENCE SERIES
[ ] HANDBOOK (NIST HB)	[ ] FEDERAL INF. PROCESS. STDS. (NIST FIPS)	[ ] PRODUCT STANDARDS
[ ] SPECIAL PUBLICATION (NIST SP)	[ ] LIST OF PUBLICATIONS (NIST LP)	[X] OTHER NIST-GCR
[ ] TECHNICAL NOTE (NIST TN)	[ ] NIST INTERAGENCY/INTERNAL REPORT (NISTIR)	

RECOMMENDED FOR NON-NIST PUBLICATION (CITE FULLY) [ ] U.S. [ ] FOREIGN

PUBLISHING MEDIUM
[X] PAPER [ ] CD-ROM
[ ] DISKETTE (SPECIFY)
[ ] OTHER (SPECIFY)

SUPPLEMENTARY NOTES

ABSTRACT (A 1500-CHARACTER OR LESS FACTUAL SUMMARY OF MOST SIGNIFICANT INFORMATION. IF DOCUMENT INCLUDES A SIGNIFICANT BIBLIOGRAPHY OR LITERATURE SURVEY, CITE IT HERE. SPELL OUT ACRONYMS ON FIRST REFERENCE.) (CONTINUE ON SEPARATE PAGE, IF NECESSARY.)

This report describes the research performed during the period July 1990 - July 1991 under a joint research program between the Mechanical Engineering Department of the University of Maryland and the Building and Fire Research Laboratory of the National Institute of Standards and Technology. The research is conducted by Graduate Research Assistants of the ME Department under the joint supervision of Dr. di Marzo (UMCP) and Dr. Evans (CFR - NIST). This joint research program was initiated in January 1985. The long term objective of the study of droplet-solid interaction is to obtain information applicable to the extinguishment of fire throug a droplet array (e.g. spray). The solids of concern include low thermal conductivity materials, typical of fire applications. Several important results were obtained in the first years of research. In particular, the modelling of the boundary condition at the liquid-vapor interface (at the droplet exposed surface) was validated with the data collected for water droplets evaporating on an aluminum block (diMarzo 1986a, 1986b, 1988).

KEY WORDS (MAXIMUM 9 KEY WORDS; 28 CHARACTERS AND SPACES EACH; ALPHABETICAL ORDER; CAPITALIZE ONLY PROPER NAMES)
computer programs; cooling; droplets; evaporation; solid surfaces; water

AVAILABILITY
[X] UNLIMITED [ ] FOR OFFICIAL DISTRIBUTION. DO NOT RELEASE TO NTIS.
[ ] ORDER FROM SUPERINTENDENT OF DOCUMENTS, U.S. GPO, WASHINGTON, D.C. 20402
[X] ORDER FROM NTIS, SPRINGFIELD, VA 22161

NOTE TO AUTHOR(S) IF YOU DO NOT WISH THIS MANUSCRIPT ANNOUNCED BEFORE PUBLICATION, PLEASE CHECK HERE. [ ]

ELECTRONIC FORM